AUTO REGRESSIVE MOVING AVERAGE SIMULATION OF RANDOM WAVE FORCES ON OFFSHORE STRUCTURES

by Kamyab Samii

Abstract

A new method is presented for numerical simulation of wave kinematics at any place on an offshore structure and at any time. The random wave particle kinematics are modelled by an auto-regressive moving average process which generates a time history using Gaussian white noise as input. For each desired wave spectrum, a small number of ARMA coefficients are required. The method for computing these coefficients is described. From the origin of coordinates, the waves are propagated horizontally and vertically throughout the water column to each node of a finite element model of an offshore structure. The stretched linear approximation is incorporated into the method to model finite amplitude effects. Spectral directionality is incorporated to take into account the effects of wave energy spreading. In all examples the deep water wave dispersion relation is assumed. In the case of shallow waters or intermediate depths, the same methodology applies: only the dispersion relation is different. Once the wave kinematics are simulated at each grid-point or node, it is a simple step then to compute wave forces, using the Morison equation.

The strong points of this method are its accuracy, its numerical efficiency, the inclusion of finite wave amplitude effects and the means for accounting for the effects of wave spreading. In contrast to the discrete spikes which result when one sums sinusoids, the ARMA spectrum is smooth and continuous, properly modelling the non-linearities which depend on difference frequencies, as in the case of slowly varying drift forces. When compared to summing sinusoids, this method is more efficient in terms of calculations, memory storage, and input/output memory transfer because it is based on a series of recursive algorithms. Moreover, by dividing the wave propagation problem into a horizontal one and a vertical one, the wave spreading and directionality problem is easily solved. The finite amplitude non-linearities are modelled by implementing the stretched linear approximation. For both deepwater and shallow waters, the same methodology yields a numerically efficient random wave force time history simulation, modelling wave dispersion, spreading, and finite amplitudes.

Thesis Supervisor: Professor J. Kim Vandiver
Title: Associate Professor of Ocean Engineering

ACKNOWLEDGEMENTS

This research was made possible through the support of the Minerals Management Service, Department of the Interior.

I am indebted to my thesis committee chairman, Prof. J. Kim Vandiver, whose encouragement and friendship throughout my work have allowed me to pursue my ideas and goals.

For their contributions during the course of the research, I express my appreciation to the members of my thesis committee: Prof. A.B. Baggeroer, Prof. M. Triantafyllou and Prof. Shyam Sunder.

Finally, I express my gratitude to my parents and my brothers for their continuous support and interest.

TABLE OF CONTENTS

		PAGE
Abstract		2
Acknowledgements		3
Table of Contents		4
Nomenclature		6
List of Figures		11
Chapter 1:	Introduction	13
Chapter 2:	The ARMA Model	21
	2.1 Introduction	21
	2.2 Linear Filtering: A Review	24
	2.2.1 Time Series of a Random Process	24
	2.2.2 Linear Theory	25
	2.3 Modelling of Time Series	28
	2.3.1 The Auto-Regressive Model	29
	2.3.2 The Moving Average Model	32
	2.3.3 The Auto-Regressive Moving Average Model	33
	2.4 The ARMA Approximation	35
	2.4.1 A General Overview	35
	2.4.2 Summary of the Steps in Computing the ARMA Coefficients	36
	2.5 Errors Associated with the ARMA Approximations of H_s and F_o	41
Chapter 3:	The Hydrodynamic Model	45
	3.1 Wave Spectrum and Autocorrelation	47
	3.2 Simulation of Wave Kinematics by Sum of Sinusoids	48
	3.3 Wave Forces	53
	3.4 The ARMA Simulation of Wave Kinematics	55
	3.5 Vertical and Horizontal Propagation of Wave Kinematics	59
	3.5.1 Vertical Propagation	60
	3.5.2 Horizontal Propagation	61
	3.6 Impulse Response for Horizontal Propagation	65
	3.7 Impulse Response for Vertical Convolutions	72

TABLE OF CONTENTS

		PAGE
3.8	Comparison of the Numerical Efficiency of the ARMA Method With the Sum of Sinusoids	76
	3.8.1 Number of Multiplications or Additions	79
	3.8.2 Number of Memory Storages	80
	3.8.3 Example and Comparison	82
Chapter 4:	Applications and Results	86
4.1	ARMA Modelling of Sea Spectra	88
4.2	Vertical Wave Propagation	93
4.3	Finite Amplitude Effects and Stretched Linear Approximation	99
	4.3.1 Stretched Linear Application	99
	4.3.2 Calculation of Base Shear and Overturning Moment	103
4.4	Horizontal Wave Propagation	114
4.5	The Wave Spreading Problem and Directional Spectra	119
4.6	Hilbert Transforms and Differentiation	124
4.7	Wave Kinematics for Intermediate Depths and Shallow Waters	125
4.8	Statistics of ARMA Wave Forces - Comparison to Real Data and to the Crandall and Moe Model	137
Chapter 5:	Conclusion	143
Appendix 1:	Characteristics of the Velocity Spectrum	147
Bibliography		152

NOMENCLATURE

WAVE CHARACTERISTICS

T	wave period (sec)
$\Omega=2\pi/T$	wave frequency (rad/sec)
f	wave frequency (cycle/sec)
L	wave length (meter)
$k=2\pi/L$	wave number (wave/meter)
H	wave height (meter)
C_d	drag coefficient
C_m	mass coefficient
g	gravity field (meter/sec^2)
D	structural member dimension (meter)
V	vertical wave velocity (meter/sec)
U	horizontal wave velocity (meter/sec)
$A_v=\dot{V}$	vertical wave acceleration (meter/sec^2)
$A_h=\dot{U}$	horizontal wave acceleration (meter/sec^2)
η	wave elevations (meter)
$S_x(f)$	wave amplitude spectrum (meter^2-sec)
$R_x(\tau)$	wave elevations autocorrelation (meter^2)
H_s	significant wave height (meter)
F_o	peak frequency of the wave amplitude spectrum (Hz)
M_o	area under the wave amplitude spectrum (meter^2)
M_2	second moment of the wave amplitude spectrum (meter^2/sec^2)

A_i	root mean square of the wave elevation for each frequency component $A_i=\sqrt{2S_x(\Omega)\Delta\Omega}$ (meter)
ϕ_i	random phase of each frequency component, uniformly distributed between 0 and 2

ARMA SIMULATION

F_c	cutoff frequency
$F_s=1/Dt$	sampling frequency
Dt	sampling time
$\omega=2\pi fDt$	normalized frequency,
$z^{-1}=\exp(-j\omega)$	unit-sample delay used in digital Fourier transform
V(n)	output of the ARMA simulation, vertical wave velocity
W(n)	input of the ARMA simulation, Gaussian white noise
H=B/A	ARMA transfer function modelling the given spectrum or autocorrelation sequence
$S=\|H\|^2$	ARMA spectral estimate modelling the given spectrum or autocorrelation sequence
A(z)	denominator of the ARMA model, a polynomial of the powers of z, roots of A(z)=0 give the poles of the ARMA model
B(z)	numerator of the ARMA model, a polynomial of the powers of z, roots of B(z)=0 give the zeros of the ARMA model

$\left\{a_n\right\}_N$	ARMA coefficients defining A(z)
$\left\{b_m\right\}_M$	ARMA coefficients defining B(z)
$S_{a.r.}$	AR (or MEM) spectral estimate of the given spectrum
$H_{a.r.}$	AR (or MEM) estimate of order $N_1(>N)$ of the transfer function of the given spectrum
h	AR (or MEM) estimate of order $N_1(>N)$ of the impulse response of the $H_{a.r.}$ transfer function
$\{a^*_n\}_{N_1}$	AR (or MEM) coefficients defining the AR (auto regressive) filter
PE	prediction error of the AR filter
$\left[R_x^{\cdot}\right](a^*)=-(R_x^{\cdot})$	YULE-WALKER matrix equation, solving for the vector (a*), AR coefficients. This equation finds a least square estimate of such a coefficients that can extrapolate the autocorrelation function by using a recursive algorithm.
$S_x^{\cdot}(f)$	wave velocity spectrum
$R_x^{\cdot}$	wave velocity autocorrelation function
$S_x^{\cdot\cdot}(f)$	wave acceleration spectrum

HORIZONTAL PROPAGATION

Dx	horizontal distance of propagation
$H_{hor}(f,Dx)$	transfer function for any wave particle kinematics or elevations between two points separated by a horizontal distance Dx

$\|H\|_{hor} = 1$	magnitude of the transfer function, an even function of frequency
$\varphi_{hor}=\|k\|Dx$	phase of the horizontal transfer function, an odd function of frequency. For deepwater waves, the phase is a quadratic function of frequency.
L_c	wave length corresponding to the cutoff frequency
N_{hor}	number of samples, and order of the FIR filter modelling the transfer function Hhor
$Df=F_s/N_{hor}$	frequency sampling interval of H_{hor}
$\Delta\varphi_{max}= \pi/4$	the maximum phase difference corresponding to the frequency interval at the cutoff frequency, $\Delta\varphi_{max}= \varphi(Fc)-\varphi(Fc-Df)$. $\Delta\varphi_{max}$ is set inferior to $\pi/4$
$\alpha = Dx/L$	number of wave lengths that one wants to be able to propagate horizontally the wave kinematics
$R= F_s/2F_c$	ratio of the bandwidth (Fs/2) to the cutoff frequency Fc; $R\geq 1$, and R=1 corresponds to the Nyquist sampling rate.
$h_{hor}(t,Dx)$	impulse response corresponding to $H_{hor}(f,Dx)$

VERTICAL PROPAGATION

Dz	vertical distance of propagation
$\alpha_z = Dz/L_c$	number of wavelengths that one wants to be able to propagate the wave kinematics vertically

G(f,Dz)	transfer function for any wave particle kinematics or elevations between two points separated by a vertical distance Dz
g(t,Dz)	impulse response corresponding to G(f,Dz)
N_{vert}	number of samples, order of the vertical propagation filter
σ_f	parameter defining the G(f,Dz), which has a Gaussian magnitude (bell shape) for deepwater waves
σ_t	parameter defining the g(t,Dz), which has also a Gaussian magnitude for deepwater waves

DIFFERENTIATION and HILBERT TRANSFORM

I(z)	integrator used to obtain free surface amplitudes from velocities
N_{intg}	order of the integration filter
D(z)	differentiator to obtain accelerations from velocities
N_{dif}	order of the differentiation filter
$H_{hilb}(f)$, $h_{hilb}(t)$	Hilbert transform performing a 90-degree shift on the vertical kinematics in order to obtain deepwater wave horizontal kinematics.
N_{hilb}	order of the Hilbert transform filter

LIST OF FIGURES

FIGURE		PAGE
1	ARMA Coefficients	91
2	ARMA (21,21) Compared to the Bretschneider Velocity Spectrum Frequency Range From 0 to 6F	92
3	Wave Kinematics (Velocity) at the Origin Input to the Vertical Convolution (Calm Sea)	95
4	Simulation Result Compared with Theoretical (Shift of One DT Between Both Graphs) (Calm Sea)	96
5	Wave Kinematics (Velocity) at the Origin Input to the Vertical Convolution (Storm Sea)	97
6	Simulation Result Compared With Theoretical (Shift of One DT Between Both Graphs) - Wave Kinematics (Storm Sea) At -20 Meters Vertically	98
7	Free Surface Amplitude Used for the Stretched Linear Approximation	104
8	Vertical Velocity at the Stretched Free Surface Input to the Vertical Convolution	105
9	Comparison of Sums of Sines and Convolution For the Stretched Linear at -25M Deep	106
10	MEM Spectral Estimate of Gaussian White Noise	111
11	MEM Spectrum of Vertical Velocity	112
12	Comparison of Linear and Stretched Linear Spectra of Forces	113
13	Impulse Response Function	116
14	Input to the Convolution (Vertical Velocities at the Origin of Coordinates - Moderate Seas	117
15	Simulation at 100 Meters Horizontally Compared to the Theoretical Kinematics	118
16	Vertical Velocity Used as Input to the Hilbert Filter	126
17	Horizontal Velocity Calculated by Hilbert Filter from Vertical Velocity as Input	127

LIST OF FIGURES

		PAGE
18	Theoretical Horizontal Velocity (90 Degree Shift)	128
19	Velocity Input to the Differentiator	129
20	Acceleration Obtained from Velocity Using a Central Difference Differentiator	130
21	Theoretical Acceleration (68 Samples, DT = .25)	131
22	Wave Forces Histogram at MWL	141
23	Histogram of Peak Wave Forces for Linear Wave at MWL	142

CHAPTER 1

INTRODUCTION

The design of platforms in deepwater requires the investigation of their dynamic behavior. This thesis presents a new method for time domain wave force simulation, which is important for the dynamic analysis of offshore structures. The dynamic analysis may emphasize either a deterministic or a random wave process. Deterministic analysis of the response to a single design wave is generally done in the time domain and may include non-linear wave theories. This will not be discussed further in this manuscript. The emphasis here is on the modelling of random wave excitation on offshore structures. The response to random wave excitation is important in the estimation of fatigue life.

Two approaches are commonly available. The first approach is the frequency domain. A linear transfer function is required, in which the response spectrum is proportional to the input wave amplitude spectrum. Use of this approach generally prevents the inclusion of nonlinear wave mechanisms, but is otherwise numerically very efficient. The time domain approach[7 and 12] allows the

use of nonlinear wave force models but has the disadvantage that long time histories are required to obtain accurate estimates of response statistics. Present techniques of generating long wave force time histories are numerically very inefficient and often sufficiently expensive in computer time that the designer is forced to do without adequate simulation. A principal contribution of this research is a substantial increase in the efficiency of time domain wave force simulations.

In order to simulate wave forces on an offshore structure, wave particle velocities and accelerations are needed. In the new procedure presented in this thesis, wave kinematics are generated in the time domain by using an Auto Regressive Moving Average model (ARMA). The ARMA model[15 and 23] has a transfer function whose magnitude squared approximates a target spectrum. In this thesis, the ARMA model time series for the wave velocity is generated first and then differentiated to obtain wave acceleration. The target spectrum is the velocity spectrum $S_x^{\bullet}(f)$ and is mathematically related to the wave amplitude spectrum $S_x(f)$. The ARMA wave kinematics are propagated throughout the water column. The horizontal and vertical wave propagation problems are solved by implementing time convolutions which are based on three non-dimensional parameters. A set of simple and rational criteria are derived for implementing

the convolutions. A systematic use of techniques in digital signal processing and statistics allows the modelling of several difficult features of random wave forces in a range of shallow to deep waters. One such characteristic is wave energy spreading[4 and 5]; time simulation of directional seas are currently expensive on computers. However, with the ARMA model, the method for simulating random, directional wave kinematics and forces has been dramatically simplified and made numerically very efficient. Another difficult characteristic of random wave force modelling is that of nonlinear finite wave amplitude effects. Typically, the stretched linear approximation[12], which is a nonlinear approximation for deep water waves, is incorporated to take the finite amplitude effects into consideration. The new procedure presented in this thesis provides a systematic method to model the stretched linear random wave force on an offshore structure. The advantages of the ARMA method are that its procedures are numerically efficient in terms of calculations, memory storages, and input/output memory transfers and it models accurately any target wave spectrum with a continuous and smooth spectrum.

The state-of-the-art for simulating wave kinematics is to superpose sinusoids at discrete frequencies[4]. The amplitudes of these sinusoids are deduced from the magnitude of the desired spectrum around each selected frequency

component. This method yields a discrete approximation to the desired spectrum. A disadvantage is that all phenomena sensitive to sum and difference frequencies between components may be inaccurately modelled since the spectrum will not be a smooth one. Moreover, the calculations are very expensive in terms of both memory transfers and storage, and in the number of computations. In contrast, an intrinsic characteristic of an ARMA model is that future values of wave kinematics are computed from a simple recursion relation. This reduces drastically the computer simulation cost and makes therefore the ARMA wave force simulation method very advantageous.

Before going into the description of an ARMA wave kinematics model, it is useful to review[22] how the sea is modelled as a weakly stationary, and ergodic random process. First, it is a weakly stationary process, if at an arbitrary position in time and space, the wave elevation has constant mean and mean square values and the autocorrelation function reduces to a function of time intervals. Second, it is an ergodic random process if both temporal and spatial averages and statistical expectations yield the same results for the mean, the mean square, and the autocorrelation statistics. The autocorrelation and the power spectrum are a Fourier transform pair that are very useful in most applications. Several spectra have been introduced to model developing or

fully developed seas. The two most common parameters for classification of wave spectra are the significant wave height and the zero-crossing period.

The forces that waves induce on floating and fixed offshore structures are of great importance in design. The wave forces are commonly assumed to be the sum of an inertial and a drag force as expressed by the Morison formula:

$$F = \rho \forall C_m \dot{U} + \frac{1}{2} \rho C_D D U|U| \quad (1.4)$$

where F is the wave force vector, C_m the mass coefficient, C_D the drag coefficient, ρ the water density, $\forall$ the displaced volume, D the projected area of the tubular members at the grid point level. This formulation is not appropriate when wave diffraction is significant or when vortex excited motions are present.

The input to the ARMA model is Gaussian white noise, W. The output is the desired random wave the velocity. In this thesis, random wave velocities are simulated numerically by an ARMA model of a given wave velocity spectrum $S_x^{\cdot}$ deduced from the wave amplitude spectrum S_x by the following relation:

$$S_x^{\cdot}(f) = (2\pi f)^2 S_x(f) = |H|^2$$

The ARMA spectrum must approximate the target velocity spectrum $S_{\dot{x}}$ and minimize an error integral in a least square sense. The ARMA model time series for the wave velocity is generated first and then differentiated or integrated to obtain respectively the wave acceleration or elevation.

In order to propagate the wave particle velocities and accelerations spatially, two fundamental transfer functions are required.

The first transfer function, H(f,Dx) is used for horizontal propagation and relates any wave component between two points separated by a horizontal distance Dx. The second transfer function, G(f,Dz) is used for vertical wave propagation and relates any wave component between two points separated by a vertical distance Dz. In this thesis, these transfer functions' impulse responses are used to implement numerical time domain convolutions. The convolutions allow for obtaining time series of random wave kinematics and forces throughout the water column using the ARMA time series as input.

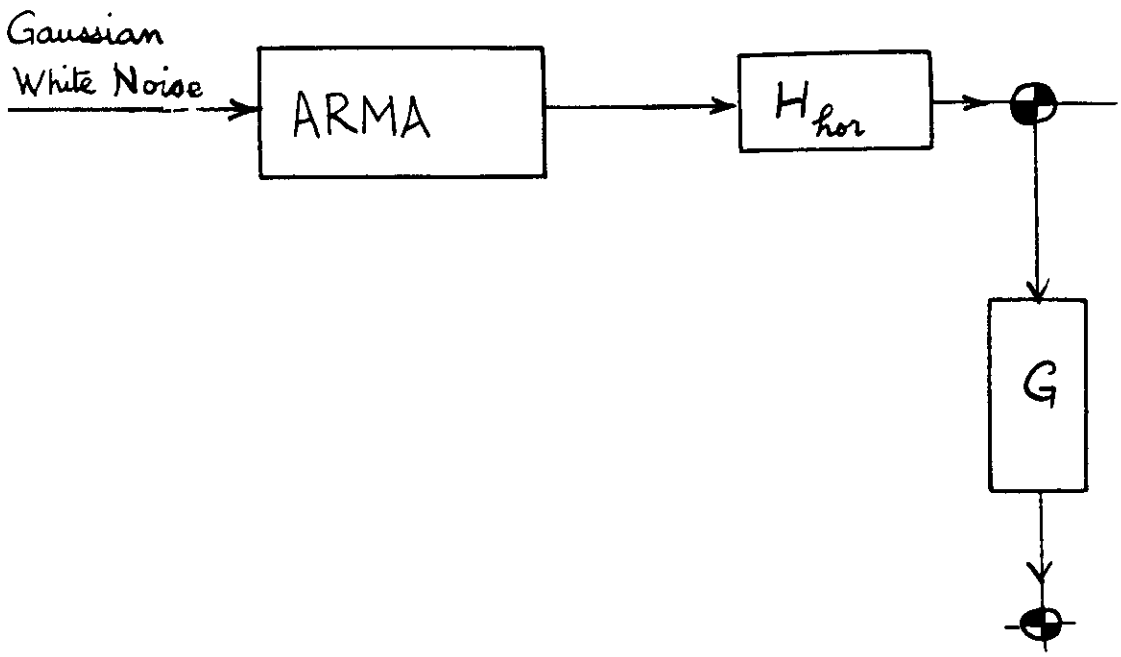

A summary of each chapter is presented below.

Chapter 2 explains the characteristics of an ARMA model as they pertain to the simulation of wave kinematics of a target wave spectrum, or from a given autocorrelation sequence. It offers an error criterion for the ARMA model based on two important parameters of the wave spectrum, i.e. the significant wave height and the peak frequency of the target spectrum.

Chapter 3 explains the wave kinematics simulation problem for offshore structures. Linear wave theory and the deepwater dispersion relation are initially assumed. The water column is divided into a grid of points that correspond to the nodes of a finite element model of an offshore structure. The relation between the wave kinematics at two separate locations is modelled by a set of linear transfer functions, derived from deepwater linear

wave theory. The procedure for generation of all necessary kinematics at each grid point throughout the water column is explained. Since each wave force component, horizontal and vertical, depends on the acceleration and the velocity, it is then a simple step to compute nodal wave forces on the offshore structure. This chapter closes with a comparison of this method, in terms of numerical efficiency, to the present state-of-the-art, i.e. the superposition of sinusoids.

Chapter 4 shows the methods used, and the results obtained from the simulation of two sea states, one representing storm conditions and another with moderate wave heights. Three examples that are very useful for offshore engineering applications are presented in Chapter 4. They are:

1) the effect of finite amplitude waves and implementation of the stretched linear approximation. An example calculation of base shear and overturning moment on a single pile structure are presented,
2) the effect of wave spreading or directionality of the wave spectrum, and
3) the effect of shallow water.

Chapter 5 contains the conclusions of this thesis and suggestions for future research in this field.

CHAPTER 2

THE A.R.M.A. MODEL

2.1 Introduction

This chapter explains the characteristics of an Auto Regressive Moving Average model, as they pertain to the simulation of wave kinematics from a target spectrum or a given autocorrelation sequence. The input to the ARMA model is Gaussian white noise, W. The output is the vertical wave particle velocity V. The target spectrum is, for purposes of example the velocity spectrum $S_x^*(f)$ derived from a Bretschneider wave amplitude spectrum. It depends on the two wave spectral parameters frequently used in offshore engineering, i.e. H_s, the significant wave height and F_o, the peak frequency of the wave amplitude spectrum. The choice of such a target spectrum is arbitrary: any other spectrum can easily be handled by an ARMA model[17,18]. The Bretschneider spectrum applies for developing seas, fully developed and decaying seas, while the Pierson-Moskowitz applies for a fully developed seas only. The JONSWAP spectrum applies for fetch limited conditions. The author recognizes that such an idealization is not necessarily realistic, but for the purpose of an example simulation of wave kinematics, finds it useful. Moreover, the

Bretschneider spectrum in terms of H_s and T_z is accepted by many codes including API, DnV, etc., in lieu of more accurate information[27].

$S_x^*(f)$, the wave velocity spectrum is considered to be equal to the magnitude squared of the transfer function H(f) of the ARMA model:

$$S_x^*(f) = |H(f)|^2$$

Instead of the frequency f, the following normalized frequency is introduced $\omega = 2\pi fDt = 2\pi f/Fs$ ($|\omega| \leq \pi$) where Dt is the sampling time and F_s, the sampling frequency. The variable, $z = \exp(j\omega)$, is a function of the frequency f and is often used to describe the frequency dependence of digital filters. The digital functions H(z) and h(n) correspond to the analog filter H(f) and its impulse response h(t). Similarly, the continuous spectrum $S_x^*(f)$ and the autocorrelation $R_x^*(t)$ are sampled and their discrete representations are the symbols $S_x^*(z) = |H(z)|^2$ and $R_x^*(n)$.

The ARMA approximation problem that is solved later in this chapter, is to find an ARMA model, B/A, a rational transfer function, that approximates the target spectrum, $S_x^* = |H|^2$ and its autocorrelation function R_x^*. The problem is stated as follows[15]: given the data h(0),...,h(M) and $R_x^*(0),\ldots,R_x^*(N)$, find the lowest order recursive filter which matches the data. This problem is called a "second order interpolation" problem in the spectral analysis

literature. Thus, one starts with the autocorrelation function for wave velocities. This function can either come from observed data or from an idealized wave amplitude spectrum.

In this chapter, background is provided on modelling a random process, e.g., wave kinematics, by linear filters, such as the functions H(z) and h(n). Then, Auto Regressive, 1/A(z), and Moving Average, B(z), models are introduced and their characteristics are presented. The ARMA model B(z)/A(z) is a combination of both models and its particular properties are presented. The algorithm needed to estimate the ARMA model is explained. This rational filter B(z)/A(z) is determined when the coefficients $\{b_m\}_M$ and $\{a_n\}_N$ that define the polynomials B(z) and A(z) are calculated by the algorithm. The order (M,N) of an ARMA filter corresponds to the number of $\{b_m\}$ and $\{a_n\}$ coefficients. Since the ARMA filter is a recursive filter, the sampled time history of wave particle velocities is easily obtained by the following relation:

$$V(t) = -\sum_{n=1}^{N} a_n \, V(t-nDt) + \sum_{m=0}^{M} b_m \, W(t-mDt) \qquad (2.1)$$

where W is Gaussian white noise; V, vertical velocities; $\{a_n\}_N$ and $\{b_m\}_M$, the ARMA coeficients. This time simulation is compatible with the target spectrum S_x^* and the

autocorrelation R_x. Since for a given spectrum, there exists no unique time series matching the spectral shape, the order of the ARMA model may be varied until satisfactory accuracy is achieved. At the end of the chapter, an error calculation is presented that computes the relative errors on two parameters of wave spectra, i.e. the significant wave height, H_s, and the peak frequency F_o.

2.2 Linear Filtering- A Review

2.2.1 Time Series of a Random Process

A time series consists of a set of observations made sequentially in time. Let V(n) denote such a set of observations made at equal time intervals. If future values of the series can be described only in terms of a probability distribution, such a time series represents one particular realization of a random process. In most applications, wide-sense stationarity is assumed, meaning that the second order statistical moments of any set of observations are unaffected by shifting all the times of observations forward or backwards in time. The second order statistical moments depend only on time differences not on the time origin. In this case, the mean $M_x(n)$ (the first order moment) and the autocorrelation $R_x(m,n)$ (the second order moment) of such a process for time origin n and m time lags can be written:

1) $M_x(n) = E(V(n)) = \text{constant}$ for all n (2.2)

2) $R_x(m,n) = R_x(m) = E(V(n+m) V(n))$

for all n where E is the expectation operator.

The wave velocity autocorrelation function $R_x(\tau)$ relates the value of the velocity V(t) at time t to its value at a later time $t+\tau$, and so provides an indication of the correlation of the signal with itself for various time lags. The autocorrelation function is a real and even function of the time lags.

2.2.2 Linear Theory

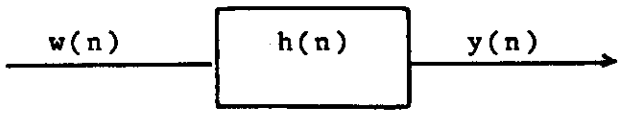

Considering a time series w(n) of length N applied to a linear filter of impulse response h(n) of length M. The resulting response of the filter denoted by y(n) is given by the convolution-sum:

$$y(n) = \sum_{k=0}^{M-1} h(k)w(n-k) \qquad 0 \leq n \leq M+N \tag{2.3}$$

Therefore, the processing of a time series is easily accomplished by means of a linear filter. One can describe the input-output relation of a linear filter by transforming the time domain description into the frequency domain. Any linear shift-invariant system is completely characterized by

its impulse-response h(n). The steady-state response to a sinusoidal input is sinusoidal at the same frequency as the input, with phase and amplitude determined by the system. This property makes Fourier representation of signals in terms of sinusoids and complex exponentials very useful.

A special case of particular importance for the ARMA simulation method, is when the input is Gaussian white noise, w(t). The output y(t) of the linear system h(t) is also Gaussian. In order for y(t) to be one realization of the velocity at a point, the wave velocities are modelled as a random, stationary, ergodic and Gaussian process with an autocorrelation function R_x and a spectrum S_x. As a result of linear systems theory, it can be shown that this wave velocity spectrum is modelled by the output spectrum $S_y(f)$ when white noise is used as input.

$$S_x(f) = S_y(f) = |H(f)|^2 \quad S_w = |H(f)|^2 S_o \qquad (2.4)$$

since the spectrum of Gaussian white noise is a constant $S_o = S_w$.

For discrete-time systems[16], the input, output, and the response sequence are defined as a superposition (integral) of exponential signals with complex amplitudes. The Fourier transform of these sequences are expressed in the form of Fourier series where the Fourier coefficients correspond to the sampled sequence. The Fourier transform pairs are:

$$\text{input:}\quad w(n)=\int_{-\pi}^{\pi} W(e^{j\omega})e^{j\omega}\,d\omega/2\pi \qquad W(e^{j\omega})=\sum_{n=-\infty}^{+\infty} w(n)e^{-j\omega n}$$

$$\text{output:}\quad y(n)=\int_{-\pi}^{\pi} Y(e^{j\omega})e^{j\omega}\,d\omega/2\pi \qquad Y(e^{j\omega})=\sum_{n=-\infty}^{+\infty} y(n)e^{-j\omega n}$$

$$\text{system:}\quad h(n)=\int_{-\pi}^{\pi} H(e^{j\omega})e^{j\omega}\,d\omega/2\pi \qquad H(e^{j\omega})=\sum_{n=-\infty}^{+\infty} h(n)e^{-j\omega n} \qquad (2.5)$$

where $\omega=2\pi f Dt$ is the normalized frequency $|\omega|\leq\pi$, Dt is the sampling time and $j^2=-1$. The output response y(n) can be determined either from its own Fourier transform

$$Y(e^{j\omega}) = H(e^{j\omega})W(e^{j\omega}) \qquad (2.6)$$

or from the convolution-sum

$$y(n) = \sum_{k=0}^{M-1} h(k)\, w(n-k) \quad 0\leq n\leq N+M \qquad (2.3)$$

The variable $z^{-1} = Fe^{-jw}$ is called the unit delay operator:

$$z^{-1}w(n) = w(n-1) \qquad (2.7)$$

In this thesis, the input w(t) is often taken to be Gaussian white noise.

2.3 Modelling the Time Series

A stochastic process like sea wave kinematics may be modelled by the output of a linear filter produced by a white noise input of zero mean. The idea is that a time series can be generated from a series of independent impulses drawn from a fixed distribution usually assumed Gaussian having a zero mean and a constant variance per unit frequency. One must estimate the coloring filter, or transfer function B/A, that generates wave kinematics from Gaussian white noise[17,18,19]. This transfer function B/A becomes very important in the development of this chapter because it must approximate a target spectrum. A least-square error minimization[15] is used to fit the transfer function to the desired spectrum as shown in the following expression:

$$\text{Min } E^2 = \int df \left| HA - B \right|^2 \qquad (2.8)$$

The transfer function B/A is a rational polynomial including both poles and zeros, which represents both a pure deterministic regression and an average of pure random inputs. The A.R.M.A. model is a combination of a A.R. or Auto Regressive - and a M.A. or Moving Average model.

The transfer function B(z)/A(z) is a digital filter, represented by a finite number of coefficients. It is desirable in practice to employ the smallest number of

filter parameters which results in an adequate representation of the transfer function of the process.

2.3.1 The Auto Regressive Model

In this model, the present value V(n) of the vertical velocity time series is expressed as a finite linear combination of N_1 previous values of the time series and the current innovation w(n). An auto regressive time series of order N_1 is represented mathematically by[10,11]:

$$V(n)+ a^*_1 V(n-1)+\ldots+ a^*_{N_1} V(n-N_1) = w(n) \quad (2.9)$$

This is a linear model relating a dependent variable V(n) to a set of independent variables $V(n-1),\ldots,V(n-N_1)$ plus an error term w(n), or, equivalently, the variable x(n) is regressed on previous values of itself. The A.R. operator has a Z-transform:

$$A(z) = 1+ a^*_1 z^{-1} +\ldots+ a^*_{N_1} z^{-N_1} \quad (2.10)$$

The Auto Regressive model provides a means of extrapolating N_1 samples of a known autocorrelation function by the following recursion relation:

$$R_{\hat{x}}(k)= -a^*_1 R_{\hat{x}}(k-1) - \ldots -a^*_{N_1} R_{\hat{x}}(k-N_1) \text{ for } k>0 \quad (2.11)$$

where the autocorrelation function is given or calculated for at least N_1 lags. This autocorrelation function is given when one selects an idealized target spectrum and computes its Inverse Fourier Transform, or is calculated when real wave data has been processed to yield an estimate of the following integral sum:

$$R_x^*(t) = \lim_{T\to\infty}\left\{\frac{1}{T}\int_{-T/2}^{T/2} V(u)V(u+t)\ du\right\} \qquad (2.12)$$

In practice for real wave data, the period T, used to obtain the temporal average, is of course finite but sufficiently large so as to ensure that acceptable variance in the estimate of R_x^* is obtained. The wave velocity spectrum is the Discrete Fourier Transform of its autocorrelation function. To overcome the effects of the truncation (after N_1 lags) of the estimate of the autocorrelation, the Maximum Entropy method of spectral analysis uses an auto regressive model to achieve an extrapolation by satisfying the two following criteria:

1) the spectral estimate agrees with the N_1+1 known values of the autocorrelation function.
2) the extrapolation is based on the fewest possible assumptions about the autocorrelation function beyond N lags (maximizing the entropy).

In the results shown in Chapter 4, a Bretschneider spectrum has been selected. From real wave data, the measured autocorrelation can be used to find an Auto Regressive model. However one must be warned that stability problems may be encountered with AR models of high order. The parameters $\{a^*_n\}_{N_1}$ that define an Auto Regressive model are obtained as the solution of the Yule-Walker equation resulting from minimizing the mean-square error between the observed random process and that predicted by the AR model. The Yule-Walker equation is expressed in a matrix form by:

$$\begin{bmatrix} R_{\dot{x}}(0) & \cdots & R_{\dot{x}}(N_1-1) \\ \vdots & \ddots & \vdots \\ R_{\dot{x}}(N_1-1) & \cdots & R_{\dot{x}}(0) \end{bmatrix} \begin{Bmatrix} a^*_1 \\ \vdots \\ a^*_{N_1} \end{Bmatrix} = -\begin{Bmatrix} R_{\dot{x}}(1) \\ \vdots \\ R_{\dot{x}}(N_1) \end{Bmatrix} \qquad (2.13)$$

or

$$(R^{\cdot}_{\dot{x}})(a^*) = -(R^{\cdot}_{\dot{x}}) \qquad (2.14)$$

This matrix equation is solved for the $\{a^*_n\}_{N_1}$ coefficients. An efficient technique for solving the Yule-Walker equation has been developed by Levinson and simplified by Durbin[8]: it takes advantage of the special diagonal symmetry of the autocorrelation matrix $(R^{\cdot}_{\dot{x}})$.

For the ARMA model that is calculated in this thesis, the AR model serves as a first approximation in the calculation of the ARMA parameters. While the AR model is best suited for a pole dominant spectrum, one finds numerical difficulties in approximating a wave velocity spectrum of the form

$$S_x^{\cdot}(f) = \exp(-B/f^4)\ A/f^3$$

because it possesses a zero of infinite order at f=0. The exponential function will tend to zero as the frequency tends to zero in a stronger manner than any power of f.

$$\lim_{f \to 0} f^p \exp(-B/f^4) = 0 \text{ for any } p$$

This means that the spectrum possesses a zero of infinite order at the origin f=0 and therefore the AR model is not best suited to describe this spectrum. Of critical importance is the selection of the sampling time for the autocorrelation function and the order N_1, of filter in order to avoid ill conditioning of the Yule-Walker equations.

2.3.2 The Moving Average Model

Here, the time series V(n) is linearly dependent on a finite number M of previous innovations:

$$V(n) = w(n) + b_1 w(n-1) + b_2 w(n-2) + \ldots + b_m w(n-M) \qquad (2.15)$$

The name moving average is misleading because the weights $1, b_1, \ldots, b_m$ multiply the innovations w(n). These MA coefficients need not be positive and need not sum to one as would be implied by the term moving average. The Moving Average operator has a Z-transform:

$$B(z) = 1 + b_1 z^{-1} + \ldots + b_M z^{-M} \qquad (2.16)$$

2.3.3 The Auto Regressive Moving Average Model

A.R.M.A output : V(n) = A.R. + M.A. components

= aa(n) + bb(n)

The advantage of an A.R.M.A model is flexibility, and the small number of parameters needed in fitting most physical time series. Assuming that the aa(n) and the bb(n) are each stationary time series and mutually uncorrelated, then the following properties describe each time series:

1) the A.R. component aa(n) is deterministic: this means that aa(n+k) can be predicted for any k from its past values with full accuracy. Therefore, it is equivalent to a completely predictable series

feedback.

2) the M.A. component bb(n) is non-deterministic, completely random and unpredictable. Gaussian white noise W is chosen as input to the moving average component. This input innovation series yields a stationary output as long as the ARMA system is stable. Stability of an ARMA system is assured when the polynomial A(z) has no zeros outside or on the unit circle.

$$V(z) = (B(z) \,/\, A(z)\,)\, W(z) \qquad (2.17)$$

$$\frac{V(z)}{W(z)} = \frac{1 + b_1 z^{-1} + b_2 z^{-2} + \ldots + b_M z^{-M}}{1 + a_1 z^{-1} + a_2 z^{-2} + \ldots + a_N z^{-N}} \qquad (2.18)$$

Another interpretation is to consider the rational transfer function (ARMA): H(z) = B(z)/A(z) as a system characterized by a set of poles and zeros. Given a set of initial conditions, the poles correspond to frequencies that can appear in the output even when the input is nil:

$$A(z)V(z) = 0 \longrightarrow A(z)=0 \qquad (2.19)$$

The poles graphically correspond to peaks. As to the zeros, they correspond to frequencies at which the input can be absorbed in order to yield a nil output:

$$B(z)W(z) = 0 \longrightarrow B(z)=0 \qquad (2.20)$$

Graphically, the zeros correspond to a trough annihilating the energy of the spectrum.

2.4 The ARMA Approximation

2.4.1 A General Overview

In the context of this section, the three following concepts have a particular importance:

First, the ARMA rational transfer function, B/A, is used to generate a wave kinematics simulation using Gaussian white noise as input. The ARMA spectrum $|B/A|^2$ approximates a target wave velocity spectrum $S_{\dot{x}} = |H|^2$. In the time domain, the sampled impulse response h(n) is the Discrete Inverse Fourier Transform of H(z).

Second, one must recognize that if an arbitrary wave amplitude spectrum like Bretschneider's is chosen, the idealization is not necessarily realistic. Nonetheless, one may find it useful to work with such idealizations[6]. In the method presented hereafter, one starts with a specified autocorrelation sequence for wave velocities. This autocorrelation may come from an idealized spectrum or from real sea data. In either case, the same procedure is used to obtain the ARMA coefficients. In working with real wave data one may encounter numerical stability problems: the uncertainty in the spectral estimate would, therefore,

restrict the order of the ARMA model[17,18].

Third, the Yule-Walker equation mentioned in the paragraph about pure Auto-Regressive models, is an important step in the procedure because an AR model is used to find estimates of the above mentioned impulse response h(n). The Yule-Walker equation is used to solve for the AR coefficients $\{a_n^*\}_{N_1}$.

$$[R_x^*]\ (a^*) = -(R_x^*) \qquad (2.14)$$

2.4.2 Summary of Steps in Computing the ARMA Coefficients

The ARMA approximation of the velocity spectrum and the time simulation of the wave particle kinematics are obtained with the following steps[15,23]:

1) Given a target wave velocity spectrum S_x^*, the autocorrelation function R_x^* is computed by performing an inverse Fourier transform of S_x^*.

2) Using this autocorrelation function, a high order A.R. model is found which satisfies the Yule-Walker equation (2.14).

3) The AR model is used to obtain an approximation of the first M+i values of the impulse response h(m): h(0),..., h(M).

An Auto Regressive model of high order is found that matches the autocorrelation function's first N_1 points. This is done by finding an M.E.M. filter of order N_1:

$$V(n) = -\sum_{k=1}^{N_1} a^*_k \, V(n-k) + PE \; W(n) \qquad (2.21)$$

or

$$V(z) = (PE/A^*(z)) \; W(z) \qquad (2.22)$$

where the prediction error PE^2 is given by

$$PE^2 = Dt^2 (R_{\dot{x}}(0) - \sum_{k=1}^{N_1} a^*_k R_{\dot{x}}(k)) \qquad (2.23)$$

These $\{a^*_n\}$ parameters satisfy the Yule-Walker equation or

$$\left[R_{\dot{x}} \right] (a^*) = -(R_{\dot{x}}) \qquad (2.14)$$

The $\{a^*_n\}$ coefficients extrapolate the autocorrelation sequence as in equation (2.11). Here $R_{\dot{x}}(n)$: $R_{\dot{x}}(0),\ldots,R_{\dot{x}}(N_1)$, the autocorrelation sequence of N_1+1 lags, is deduced for the wave kinematics either by performing an Inverse Fourier Transform of the corresponding target spectrum or by directly computing them from a sea data record.

This AR(N_1) model is used to obtain an approximation of the first M+1 values of the impulse response h(m): h(0),..., h(M). Having solved the equation (2.13) by

Levinson's algorithm, we obtain these $\{a^*_n\}_{N_1}$ parameters that will estimate the impulse response h(k) by the following regression:

$$h_{ar}(k) = 0 \qquad k < 0 \qquad (2.24)$$

$$h_{ar}(k) = (PE)\delta(k)+\sum_{j=1}^{N_1} a^*_j \, R_x(k-j) \text{ otherwise}$$

Usually, the first N (or M) impulse response samples match the true impulse response:

$$H = H_{ar} \qquad (2.25)$$

4) The following second order interpolation problem is solved by the Mullis and Roberts algorithm. This problem is stated as follows: given the data h(0),..., h(M) and $R_x(0),\ldots,R_x(N)$, find the lowest order recursive filter which matches the data by using a least square error integral. Minimize the following error integral by finding a rational transfer function R/A that matches the data

$$\text{Min } E^2 = \int_{-F_s/2}^{+F_s/2} \frac{df}{F_s} \left| HA - B \right|^2 \qquad (2.26)$$

The solvability of the second order interpolation depends on whether or not the impulse response data $h(0),\ldots,h(M)$ is consistent with the autocorrelation data $R_x^*(0),\ldots,R_x^*(N)$. Therefore, one can calculate the matrix $(K(M,N))$, a $(N+1)x(N+1)$ symmetric matrix:

$$\left[K(M,N)_{i,j}\right] = \left(R_x^*(|i-j|) - \sum_{k=0}^{M} h(k)\, h(k+|i-j|)\right) \tag{2.27}$$

where $i,j = 0,1,\ldots,N$.

If $[K(M,N)]$ is positive definite or positive semidefinite, the data is consistent and the interpolation problem is solvable. If $[K(M,N)]$ is positive semidefinite and $\det(K(M,N))=0$, there exists one recursive filter, ARMA(M,N), that matches the data. The ARMA filter is indeed a recursive digital filter that is a rational function B/A. There are M+1 coefficients, $\{b_m\}_M$, that define the numerator B and N+1 coefficients, $\{a_n\}_N$, that define the denominator A. The resulting expression is henceforth denoted by ARMA(M,N).

The coefficients $\{a_n\}_N$ are solved first. An $(N+1)x(N+1)$ matrix, $[K(M,N)]$, is created from a combination of the data given, h and R_x^*. In order to solve the least square error integral (2.21) for the $\{a_n\}_N$ coefficients, this equation (2.21) can be rewritten in terms of the matrix $[K(M,N)]$ and the a coefficients:

$$E^2 = (a_N, \ldots, a_o) \left[K(M,N)\right] \begin{Bmatrix} a_N \\ \vdots \\ a_o \end{Bmatrix} \qquad (2.28)$$

and the minimization of the error integral (2.28) with respect to the $\{a_n\}_N$ coefficients yields the following equation:

$$\left[K(M,N)\right] \begin{Bmatrix} a_N \\ \vdots \\ a_1 \\ a_o \end{Bmatrix} = \alpha_{M,N} \begin{Bmatrix} 0 \\ \vdots \\ 0 \\ 1 \end{Bmatrix} \quad ; a_o = 1 \qquad (2.29)$$

and Mullis and Roberts show that the $\{b_m\}_M$ coefficients are the solution of the following recursion equation:

$$b_m = \sum_{k=0}^{N} a_k \; h(m-k) \qquad m = 0, \ldots, M \qquad (2.30)$$

5) The ARMA filter coefficients are normalized so that the ARMA spectral estimate $|B/A|^2$ has the same peak frequency and the same peak value as the original spectrum.

6) An ARMA time history of wave particle vertical velocties, V, is simulated, using Gaussian white noise, W, as input:

$$V(t) = -\sum_{n=1}^{N} a_n \; V(t-n\Delta t) + \sum_{m=0}^{M} b_m \; W(t-m\Delta t) \qquad (2.1)$$

2.5 Errors on the ARMA Spectrum Approximation

For a given spectrum, there exists no unique time series matching the spectral shape. Therefore, the smallest numbers N and M are selected that give in the frequency domain an acceptable error between the ARMA model and the given spectrum.

There exists no criterion that allows us to find the optimal ARMA spectrum. However by normalizing the ARMA spectrum at the peak frequency at least the relative error on the zeroth and second moment will become negligible. This characteristics stems from the fact that a non-dimensional spectral shape exists for both the Pierson-Moskowitz and the Bretschneider spectra that depends on the two parameters, the peak frequency F_o and the spectral value, $S_x(F_o)$, at the peak.

We present here the error measurements on the two parameters of most sea spectra H_s and F_o, the significant wave height and the peak frequency, respectively. Since we normalize the ARMA velocity spectrum $S_x^*(f)$ so that at $f=F_1$, the peak value:

$$S_x^*(F_1) = \text{ARMA spectrum at } f=F_1 \qquad (2.31)$$

the relative errors on the zeroth and second moments of the Bretschnéider wave elevation spectrum are set equal to zero.

This implies that the relative errors on H_s and F_o become equal and nil.

$$M_o \doteq H_s \doteq S_x(F_1)/\ F_1 \qquad (2.32)$$

$$M_2 \doteq H_s\ F_o \doteq S_x(F_1)\ F_1 \qquad (2.33)$$

where $\doteq$ means "proportional to", H_s is the significant wave height, F_o is the peak frequency of the wave elevation spectrum, F_1 is the theoretical peak frequency of the velocity spectrum $S_{\dot{x}}(F_1)$.

For a wave amplitude spectrum of the form

$$\frac{S_x(f)}{S_x(F_o)} = (F_o/f)^5 \exp(-\frac{5}{4}(F_o/f)^4)\ e^{5/4} \qquad (2.34)$$

and a wave velocity spectrum

$$\frac{S_{\dot{x}}(f)}{S_{\dot{x}}(F_1)} = (F_1/f)^3 \exp(-\frac{3}{4}(F_1/f)^4)\ e^{3/4} \qquad (2.35)$$

the peak of the velocity spectrum, F_1, is proportional to the peak frequency of the wave elevation spectrum F_o, therefore the relative errors on F_o and on F_1 are equal (see the appendix for details).

$$F_o/F_1 = \sqrt[4]{3/5} \qquad (2.36)$$

Since the normalization procedure becomes so important, an outline is given on how to find the peak frequency of an ARMA spectrum from its coefficients $\{a_n\}_N$ and $\{b_m\}_M$ in the appendix.

The maximum of the ARMA spectrum is a solution to :

$$\text{Extremum } \frac{d}{df} S_{\dot{x}} = 0 \qquad \sum_{l=1}^{N} \left(\frac{\alpha_l}{\alpha_o} - \frac{\beta_l}{\beta_o}\right) l \sin(2\pi \hat{F} \Delta t\, l) = 0 \Rightarrow \hat{F} = F_1 \qquad (2.37)$$

$$\text{Maximum } \frac{d^2}{df^2} S_{\dot{x}} < 0 \qquad \sum_{l=1}^{N} \left(\frac{\alpha_l}{\alpha_o} - \frac{\beta_l}{\beta_o}\right) l^2 \cos(2\pi \hat{F} \Delta t\, l) < 0 \qquad (2.38)$$

where

$$\alpha_l = \sum_{k=0}^{N-l} a_k\, a_{k+l} \qquad (2.39)$$

$$\beta_l = \begin{cases} \sum_{k=0}^{M-l} b_k\, b_{k+l} & 0 \le l \le M \\ 0 & M < l \le N \end{cases} \qquad (2.40)$$

Then, the theoretical peak frequency F_1 is set equal to the solution of (2.37) and (2.38). Since the shape of the given spectrum depends on the non-dimensional ratio f/F_1, one can normalize the abscissa of the spectral shape to the given F_1 frequency and the ordinate to the value $S_{\dot{x}}(F_1)$.

This scaling affects the sampling time and frequency since the velocity spectrum cutoff frequency is a function of F_1.

For 20 dB down from the peak on the velocity spectrum:

$$\text{cutoff} = F_c = 6.\ F_1 \qquad (2.41)$$

This gives a minimum sampling frequency of $12F_1$ for the velocity spectrum. The ordinate $S_x^{\cdot}(F_1)$ whose theoretical value is known, gives the scaling factor of the ARMA spectrum. The ARMA coefficients however are scaled by $\sqrt{S_x^{\cdot}(F_1)}$ and the sampling time Dt=1./Fs.

CHAPTER 3

THE HYDRODYNAMIC MODEL

Chapter 3 describes the wave kinematics simulation problem for offshore sructures. The water column is modelled by a set of linear transfer functions, which assume linear wave theory and the deepwater dispersion relationship. Since each wave force component, horizontal and vertical, depends on the acceleration and the square of the velocity, it is a simple step to compute wave forces from wave kinematics and to use them as inputs to the nodes of a finite element model of an offshore structure. It will be explained in this chapter how all necessary wave kinematics can be generated at each grid point throughout the water column.

This method will be compared to the present method of summing sinusoids. An example of the number calculations, of the required memory storage, and of input/output memory transfers required for one hour of data at 10x10(=100), and at 100x100(=10,000) grid points will demonstrate that the ARMA model is both accurate in describing the target sea spectrum and numerically efficient when compared to current techniques.

First, a review will be made of the state-of-the-art and the current assumptions in wave kinematics simulation, and in the study of the dynamic behavior of offshore structures.

In the design of an offshore structure, a variety of options for wave force simulation are available. The first method is to perform a static analysis: one rule of thumb is that this is acceptable for structural systems with fundamental periods smaller than two seconds. In many cases however, a static analysis is just a preliminary in the design to be followed by a thorough study of the dynamic behavior of the structure.

The dynamic analysis may emphasize either a deterministic or a random wave process. Deterministic analyses of, for example, the response to a single design wave are generally done in the time domain and may include non-linear wave theories. These will not be discussed further. The emphasis here is on the modelling of random wave excitation on offshore structures. The response to random wave excitation is important in the estimation of fatigue life.

Two approaches are commonly available. The first is the frequency domain. A linear transfer function approach is required, in which the response spectrum is proportional to the input wave amplitude spectrum. Use of this approach

generally prevents the inclusion of nonlinear wave force mechanisms, but is otherwise numerically very efficient.

The time domain alternative allows the use of non-linear wave force models but has the disadvantage that long time histories are required to obtain accurate estimates of response statistics. Present techniques of generating long wave force time histories are numerically very inefficient and often sufficiently expensive in computer time that the designer is forced to do without adequate simulation. A principal contribution of this research is a substantial increase in the efficiency of wave force simulations.

3.1 Wave Spectrum and Autocorrelation

A prevailing view in marine hydrodynamics is to consider the waves as a random process that is weakly stationary and ergodic. This allows one to define the mean, and the covariance and the autocorrelation functions, and to devise ways to obtain these functions from wave amplitude records. Moreover, a Fourier transform pair can be conceived as building bridges between the time domain autocorrelation and the frequency domain power spectrum[23].

Many wave spectra models exist. The Bretschneider spectrum is a convenient spectral model suggested in the literature. It applies to developing, fully developed, and

decaying seas depending on the value of its peak frequency. It is used in examples in this thesis. The Pierson-Moskowitz spectrum applies to fully developed seas. This means that the wind acting on the ocean's surface has had the time "to fetch over a large enough area for a large enough time." In fact, the wind generates, first, high frequency wavelets and as it continues to blow for a long time the other frequency components appear in the spectrum. When the Bretschneider spectrum is expressed in terms of H_s and T_z, the significant wave height and zero crossing period, fully developed seas are not assumed.

3.2 Simulation of Wave Kinematics by Sum of Sinusoids

The state-of-the-art[4] for more than a quarter of a century is to superpose sinusoids at discrete frequencies. The amplitude of a sea wave in a frequency band around $_i$ is given by:

$$A_i = \sqrt{2S_x(\Omega_i)\Delta\Omega} \qquad (3.1)$$

where $S_x(\Omega)$ is the wave amplitude spectrum. Such a wave has a random phase and linear wave theory is assumed. The sea elevation at a point may be expressed mathematically by:

$$\eta(t,0,0) = \int \sqrt{2S_x(\Omega)\, d\Omega} \quad \sin(\Omega t + \varphi(\Omega)) \qquad (3.2)$$

The phase ϕ of all such components are assumed to be uniformly distributed on the $(0,2\pi)$ interval. Assuming the deepwater dispersion relation, the wave elevation at another location somewhere within the water column, designated by horizontal and vertical translations Dx and Dz, are given by:

$$\eta(t,Dx,Dz) = \int \sqrt{2S_x(\Omega)\, d\Omega}\; e^{-\frac{\Omega^2 Dz}{g}} \sin\left(\Omega t + \varphi(\Omega) - \Omega^2 \frac{Dx}{g}\right) \qquad (3.3)$$

where the deepwater wave dispersion relationship is given by:

$$gk = \Omega^2 \qquad (3.4)$$

Similarly, the water particle kinematics are derived from their spectral properties:

$$S_{\dot{x}} = \Omega^2 S_x(\Omega) \qquad (3.5)$$

$$S_{\ddot{x}} = \Omega^4 S_x(\Omega) \qquad (3.6)$$

The vertical velocity V and acceleration A_v throughout the water column are given by:

$$V(t,Dx,Dz) = \int \Omega \sqrt{2d\Omega\, S_x(\Omega)}\; e^{-\frac{\Omega^2 Dz}{g}} \cos\left(\Omega t + \varphi - \Omega^2 \frac{Dx}{g}\right) \qquad (3.7)$$

$$\dot{V} = A_v = -\int \Omega^2 \sqrt{2d\Omega\, S_x(\Omega)}\; e^{-\frac{\Omega^2 Dz}{g}} \sin\left(\Omega t + \varphi - \Omega^2 \frac{Dx}{g}\right) \qquad (3.8)$$

and the horizontal velocity U and acceleration A_h by:

$$U(t,Dx,Dz) = \int \Omega \sqrt{2 d\Omega \, S_x(\Omega)} \; e^{-\Omega^2 \frac{Dz}{g}} \sin\left(\Omega t + \varphi - \Omega^2 \frac{Dx}{g}\right) \qquad (3.9)$$

$$\dot{U} = A_h = \int \Omega^2 \sqrt{2 d\Omega \, S_x(\Omega)} \; e^{-\Omega^2 \frac{Dz}{g}} \cos\left(\Omega t + \varphi - \Omega^2 \frac{Dx}{g}\right) \qquad (3.10)$$

In practice, the integrals in these equations are discretized both in terms of frequency components and of time samples in order to obtain a time history. Thus, the wave kinematics are simulated by summing sinusoids at discrete frequencies: the sea spectrum becomes then a set of discrete impulses rather than a continuum.

A large number of spectral samples (NSpec) are then needed in order to model accurately the non-linearities which depend on the difference frequencies as in the case of slowly varying forces; such forces are important on structures such as tension leg platforms. This large number of spectral samples (NSpec) must be calculated at each structural mode or grid point throughout the water column, and at each time step the whole procedure must be repeated. Since there is no recursion in the state-of-the-art algorithm, the number of input/output transfers can be very large. Moreover, a well-known fact of the Fourier analysis is that if one starts with a superposition of N sinusoids in

order to describe the wave elevations, the first and second derivatives - wave velocity and acceleration - will require many more sinusoidal components (4N and 16N) in order to describe the wave kinematics with the same level of accuracy as the wave elevations. This increases the number of spectral samples NSpec to an even higher magnitude if one wants to have smooth and accurate sea spectra for wave kinematics.

Suppose the vertical and horizontal wave kinematic velocities V, U ,and the corresponding accelerations A_v and A_h must be obtained at a grid of points. There are KL number of points under consideration: K vertical rows and L horizontal lines defining a grid throughout the water column. Let the following equations be computed at each grid-point defined by its coordinates (Dx, Dz).

$$V=\sum^{NSpec} \Omega_i \sqrt{2\, S_x(\Omega_i)\Delta\Omega}\; e^{-\Omega_i^2 \frac{Dz}{g}} \cos\left(\Omega_i t+\varphi_i-\Omega_i^2\frac{Dx}{g}\right) \qquad (3.11)$$

$$U=\sum^{NSpec} \Omega_i \sqrt{2\, S_x(\Omega_i)\Delta\Omega}\; e^{-\Omega_i^2 \frac{Dz}{g}} \sin\left(\Omega_i t+\varphi_i-\Omega_i^2\frac{Dx}{g}\right) \qquad (3.12)$$

$$\dot{V}=A_v=-\sum^{NSpec} \Omega_i^2 \sqrt{2\, S_x(\Omega_i)\Delta\Omega}\; e^{-\Omega_i^2 \frac{Dz}{g}} \sin\left(\Omega_i t+\varphi_i-\Omega_i^2\frac{Dx}{g}\right) \qquad (3.13)$$

$$\dot{U} = A_h = \sum_{i}^{NSpec} \Omega_i^2 \sqrt{2 S_x(\Omega_i) \Delta\Omega}\; e^{-\Omega_i^2 \frac{D_z}{g}} \cos\left(\Omega_i t + \varphi_i - \Omega_i^2 \frac{D_x}{g}\right) \quad (3.14)$$

The total number of operations for the four wave kinematics at all grid-points is equal to 8 NSpec KL because at least two multiplications (or two additions) are needed for each of the four wave kinematic components. The total number of memory storage locations required for all the grid-points is equal to 3 NSpec KL because at least the NSpec spectral samples of $S_x(\Omega_i)$, the frequency samples Ω_i, and the random phases ϕ_i must be stored for each grid-point. The total number of input/output memory transfers is at least equal to NSpec KL because the time t must be changed in the equations for each frequency component. Thus, not only the number of memory input/output transfers is large at each time step, but the number of operations (additions and multiplications) and the number of memory storages becomes gigantic when one must simulate a time domain fatigue analysis of an offshore structure subjected to each of the sea states of a wave scatter diagram in order to obtain fatigue life estimates. A comparison of the state-of-the-art with the ARMA wave kinematics simulation for offshore structures will be presented at the end of this chapter.

A significant advantage of an Auto Regressive Moving Average A.R.M.A. model of a given target spectrum is that it uses a recursive algorithm with a small number of fixed parameters. Thus, the number of memory input/ouput transfers is dramatically reduced and the number of required operations (additions and multiplications) and of memory storages is much less.

Another advantage of the ARMA wave simulation method is that it provides the designer with a continuous and smooth spectrum. This feature is specific to ARMA models and is important because it properly models the non-linearities which depend on the difference frequencies as is the case for slowly varying drift forces; such forces are important on structures such as tension leg platforms.

3.3 Wave Forces

Forces on structures are functions of the relative dimension of the structural member, D, compared to the wave height, H, and length, L[22].

First, when H is greater than approximately L/7, the deep-water wave breaks.

Second, if the structure is large, then wave diffraction is important: this occurs when L is typically smaller than 5D. For columns and other small volume structures, the inertia and the drag forces may be computed

using the Morison equation.

The Morison equation tells us that the horizontal force on a strip of vertical circular cylinder is the sum of drag and inertial forces. The equation of motion of the structure takes the form:

$$(M+\rho C_a \forall)\ddot{X} + C\dot{X} + KX = \rho \forall C_m \dot{U} + \frac{1}{2}\rho C_d D(U-\dot{X})|U-\dot{X}| \quad (3.15)$$

where $M+\rho C_a \forall$ is the structural mass and added mass; C, the structural damping; K, the structural stiffness; $\ddot{X}$, $\dot{X}$, X are respectively the structural acceleration, velocity and displacements; $C_a = C_m - 1$; C_m is the mass coeficient; C_d, the drag coefficient; $\forall$, the displaced volume; D, the diameter of the structural member; ρ, the fluid density.

Assuming that C_m and C_d are approximately constant with depth, the drag force is more concentrated in the free-surface zone. The drag and the inertia forces decay exponentially with the depth z respectively as exp(-2 kz) and as exp(-kz).

It has been experimentally shown that the drag force is a viscous force approximately proportional to the square of the fluid's velocity. By assuming linear wave theory, the relation between wave kinematics at different points throughout the water column may be described by transfer

functions. However, because of the non-linear drag term, the relation between wave forces at different grid-points can not be described by linear transfer functions.

When the drag force is small compared to the inertial force, the Morison equation can be linearized. Defining the relative velocity $V_r = U - \dot{X}$, one writes the quadratic term as:

$$V_r \mid V_r \mid = A_f \, V_r$$

If the excitation is assumed to be a zero mean ergodic Gaussian process, A_f becomes a constant proportional to the root-mean-square of the relative velocity:

$$A_f = \sigma_{v_r} \sqrt{8/\pi}$$

The modified Morison equation is given by:

$$(M+\rho C_a \forall)\ddot{X}+(C+\tfrac{1}{2}\rho C_d A_f D)\dot{X}+KX = \rho \forall C_m + \tfrac{1}{2}\rho C_d A_f U \qquad (3.16)$$

The values of C_m and C_d depend on the Reynolds and the Keulegan Carpenter numbers. Either form of the Morison equation may be used with ARMA simulations of acceleration and velocity.

3.4 The ARMA Simulation of Wave Kinematics

One starts by selecting a target vertical velocity spectrum and models it by an ARMA approximation. With a and b as the two sets of parameters defining the ARMA model, the

following recursion formula simulates the wave velocity V using past consecutive values of V and Gaussian white noise W.

$$V(n) = -\sum_{j=1}^{N} a_j \, V(n-j) + \sum_{k=0}^{M} b_k \, W(n-k) \qquad (3.17)$$

where the current time t is sampled t= nDt.

Accelerations are just the derivative of the velocity time history: the differentiator filter D(z) is used.

$$D(z) = (z - z^{-1}) / 2Dt \qquad (3.18)$$

Simultaneously then, the time histories of vertical velocities and accelerations may be obtained:

(3.17)

(3.18)

where W(z) is Gaussian white noise, V the vertical velocity and A_v the vertical acceleration.

For the horizontal kinematics, velocity and acceleration, the Hilbert filter $H_{hilb}(z)$[16] is used at each grid-point: it is a non-causal filter. The Hilbert filter has a frequency response with unit magnitude, a phase angle of $+\pi/2$ for positive frequencies, and a phase angle of $-\pi/2$ for negative frequencies. Such a system is often

referred to as a 90-degree phase shifter or Hilbert transform.

$$H_{hilb}(\omega) = \begin{cases} -j & 0 > \omega \geq -\pi \\ j & \pi \geq \omega > 0 \end{cases} \tag{3.19}$$

$$H_{hilb}(t=nDt) = \begin{cases} 0 & n=0 \\ 2\sin(nDt\pi/2)/nDt\pi & n \neq 0 \end{cases} \tag{3.20}$$

where $j^2 = -1$ and Dt is the sampling time, ω is the normalized frequency $\omega = 2\pi f Dt$ and $|\omega| \leq \pi$.

Thus the ideal Hilbert transform or 90-degree phase shifter corresponds to the transformation one has to perform to obtain horizontal linear wave kinematics from vertical kinematics. According to deepwater linear wave theory, vertical and horizontal kinematic components have the same magnitude but only a phase shift of 90-degrees. Approximations to the ideal Hilbert transform can, of course, be obtained. In the case of finite-duration approximations,[21] the standard technique of windowing, frequency sampling, and equiripple approximation can be applied in approximating the ideal characteristics (see Chapter 4 for results).

In summary, the method for obtaining the vertical velocities V is by the ARMA time simulation recursive algorithm (3.17); the vertical accelerations are obtained by differentiating V to obtain A_v (3.18); the horizontal velocity U is the Hilbert Transform (3.19) of the vertical velocity V; and finally, the horizontal acceleration A_h is the result of a differentiation (3.18) of the horizontal velocity U.

For generating wave forces near the free-surface, the sea profile must be known. The wave forces should be calculated with respect to the actual location of the free surface and not at the mean-water line. To know the sea profile, one has to integrate the vertical velocity V at the mean water line with a filter, I(z). In the examples discussed here, the vertical velocity time series is integrated using the trapezoidal rule, and then is passed through a low pass filter to get rid of very low frequency components that blow up numerically in the integration filter[27]. In engineering applications, the effect of a wave's finite amplitude is used to modify the wave force calculations. Results for the application of the so-called "stretched linear approximation" are presented in Chapter 4.

3.5 Vertical and Horizontal Propagation of Wave Kinematics

Two sea states, one storm and one moderate sea in the Gulf of Mexico, are considered. The ARMA approximations of Bretschneider spectra are modelled to simulate each of the two sea-states under study. The ARMA simulated waves are propagated horizontally and vertically throughout the water column so that wave kinematics are obtained at each grid-point throughout the structure.

In the system studied, the waves are numerically simulated by an ARMA model at the origin of coordinates. Each additional point of interest is defined by rectangular coordinates: the vertical axis z is directed positively upwards with z=-d as the sea bottom. The deepwater wave dispersion relation is assumed for linear waves. The method may be modified to account for shallow water effects. This is discussed later. The horizontal axis x is directed positive to the right in the direction of wave travel. A sketch of typical grid of points follows.

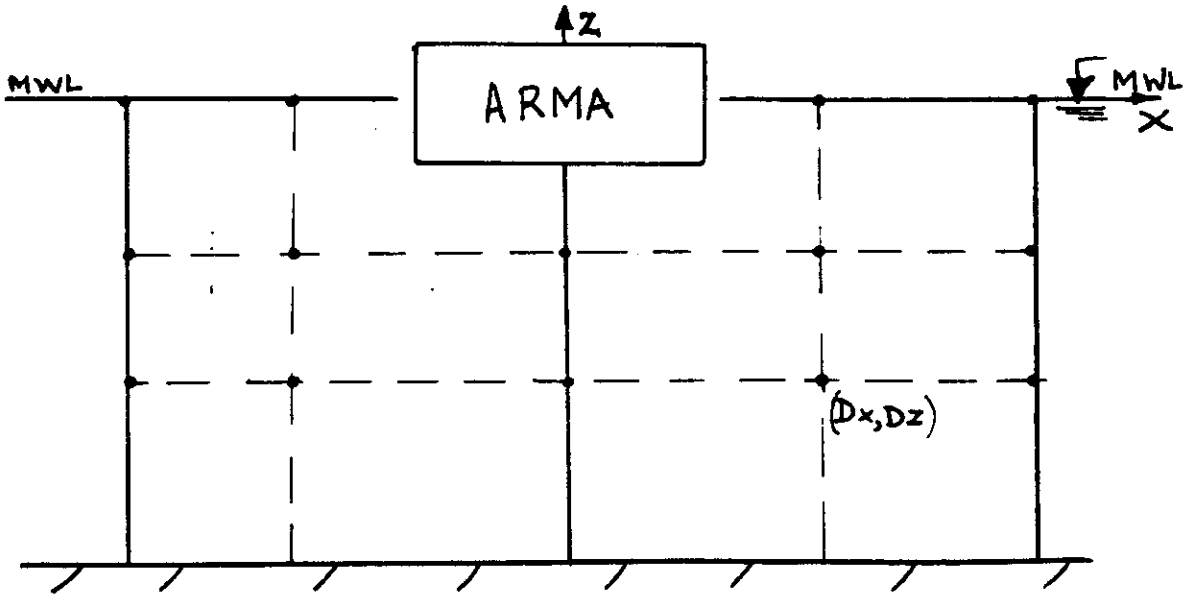

3.5.1 Vertical Propagation

The manner in which the waves change at different depths, is called the vertical propagation problem. For linear deepwater waves, the dispersion relation is $k= \Omega^2/g$ where the wave number k is related to the wave frequency. At a given frequency, the linear wave decays exponentially in amplitude throughout the water column. If the wave height at a depth Z_o from the free surface is given by

$$\eta(t;X;Z_o)=A \exp(-k\ Z_o)\ \exp(j\Omega t) \qquad (3.23)$$

then at a depth Z_i

$$\eta(t;X;Z_i)= \eta\ (t;X;Z_o)\exp(-k\ Dz/g) \qquad (3.24)$$

where $Dz=(Z_i - Z_o)$ is the vertical distance in depth between the free surface and the grid point at depth Z_i.

The transfer function characterizing the vertical propagation of a given wave profile is defined by the ratio of the transforms of the output at a depth Z_i and of the input at a depth Z_o. At any point along the line x=constant

$$G(f,Dz) = \frac{Y(X;Z_i;f)}{Y(X;Z_o;f)} = \exp(-kDz) = \exp(-(2\pi f)^2 Dz/g) \qquad (3.25)$$

where Y can be either the wave elevation, the wave velocity or the wave acceleration, and the deepwater dispersion relation $kg = (2\pi f)^2$ holds. This last relation gives a Gaussian shape to the transfer function: it is a low-pass filter. As the depth Dz increases, the high frequency components are attenuated more rapidly. All components attenuate exponentially. Since the transfer function depends only on the vertical distance, the reference of vertical coordinates for the vertical propagation can be the mean water line or the actual free surface elevation (as is used to model finite amplitude effects)

3.5.2 Horizontal Propagation

The waves disperse when they travel horizontally along the x axis. For linear deepwater waves, the phase shift varies as the product of the horizontal distance $Dx=(X_i-X_o)$ by the wave number k. This is a frequency dependent phase shift. For a wave of a given frequency, the phase shift difference between a wave profile at X_i and the original wave profile at X_o is given by

$$\Phi = kDx = \Omega^2 Dx/g$$

For grid points lying along the direction of propagation the transfer function is:

$$H(f;Dx) = \frac{Y(X_i;Z;f)}{Y(X_0;Z;f)} = \exp(j|k|Dx) \tag{3.27}$$

$$= |H| \exp(-j\phi) = \exp(-j(2\pi f)^2 \text{sign}(f) Dx/g)$$

This transfer function gives a non-causal impulse response.

If a grid-point is in the direction opposite to the wave propagation, then the transfer function can be rewritten as:

$$H(f,-Dx) = \exp(j|k|Dx)$$

and the impulse response is the symmetric image of the other.

Graphically, this is illustrated by the following:

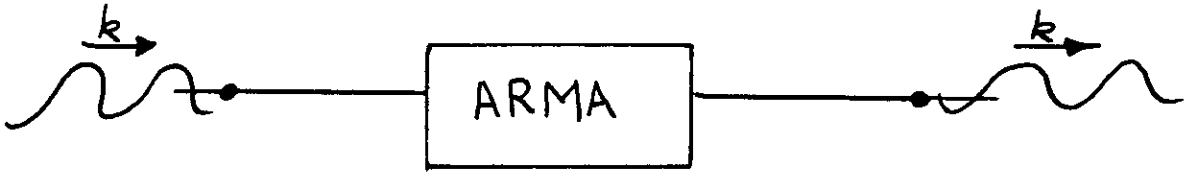

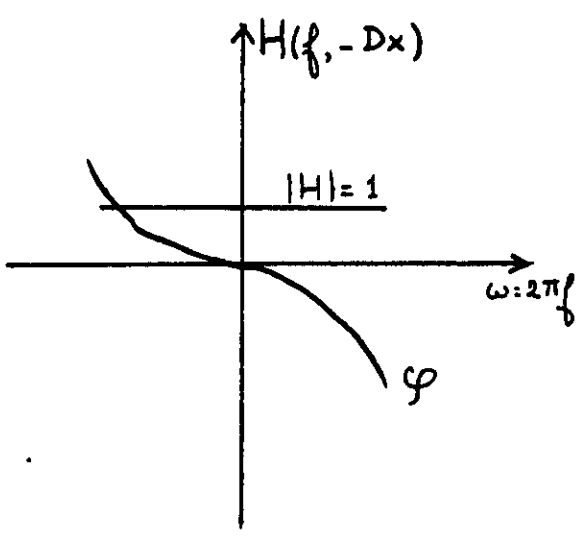

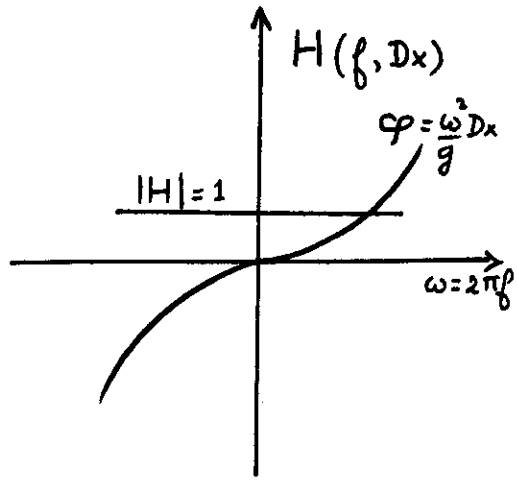

Similarly, the transfer function characterizing the horizontal wave propagation is defined by the ratio of the transforms of the output signal at a horizontal coordinate X_i and the input signal at X_o.

At any point along the axis z=constant, the phase is equal to the scalar product of two vectors:

$$\phi = \vec{k}.\vec{Dx} = |\vec{k}||\vec{Dx}|\cos(\vec{k};\vec{Dx}) \qquad (3.26)$$

where the argument of the cosine in the expression cos(k;Dx) refers to the angle between the vectors, the wave number is in the direction of wave propagation and $\vec{Dx}$ is the position vector defining where the grid-point is located. This formula defines the phase in all generality and takes care of oblique waves. However in this section, the problem is restricted to considering a simple unidirectional spectrum. This implies that if the wave propagates towards the grid-point located on the mean water line at a distance Dx, the phase is equal to

$$\varphi = k\ Dx$$

Similarly, if the grid-point is located in the direction diametrically opposite to the wave's propagation, the phase is equal to $-|k|Dx$, i.e. the antisymmetric function of k (and therefore the frequency f).

The absolute sign of the wave number k and the frequency f in equation (3.27) indicates that the phase shift is an odd function of k and therefore of the frequency f. This is consistent with the fact that the above transfer function must correspond to a real impulse response h(t). This implies that the magnitude of $H_{hor}(f)$ should be an even function of frequency and an odd function of the phase.

$$H_{hor}(f,Dx)\begin{cases} \text{phase} = (2\pi f)^2 \text{sign}(f) Dx/g & \text{-odd} \\ \text{magnitude} = 1. & \text{-even} \end{cases}$$

Analytically, the impulse response of such a transfer function is given by:

$$h_{hor}(t,Dx) = \int_{-F_c}^{+F_c} H_{hor}(f,Dx)\, e^{j2\pi ft}\, df = 2\int_{0}^{F_c} df\, \cos\left(2\pi ft - \frac{Dx}{g}(2\pi f)^2\right)$$

where F_c is the cutoff frequency.

The bandlimited Inverse Fourier Transform of $H_{hor}(f,Dx)$ is analytically defined in terms of Fresnel Integral functions S and C:

$$S(y) = \int_0^y \sin\frac{\pi}{2}u^2\,du \qquad \text{and} \qquad C(y) = \int_0^y \cos\frac{\pi}{2}u^2\,du$$

$$h_{hor}(t,Dx) = \sqrt{\frac{g}{2\pi Dx}}\left[\left(S\left(2\sqrt{\alpha}-\frac{F_c t}{\sqrt{\alpha}}\right)+S\left(\frac{F_c t}{\sqrt{\alpha}}\right)\right)\sin\frac{\pi}{2\alpha}(F_c t)^2 + \left(C\left(2\sqrt{\alpha}-\frac{F_c t}{\sqrt{\alpha}}\right)+C\left(\frac{F_c t}{\sqrt{\alpha}}\right)\right)\cos\frac{\pi}{2\alpha}(F_c t)^2\right]$$

This impulse response depends on the non-dimensional parameter, α, defined as the ratio of the horizontal distance Dx and the wave length, L_c, corresponding to the cutoff frequency, F_c. In other words, α is the number of wave lengths one wants to propagate horizontally.

A time history of wave kinematics at each point in the grid is obtained by convolving the original ARMA simulated wave with the transfer functions for horizontal and vertical propagation.

3.6 Impulse Response for Horizontal Propagation

The transfer function is a complex function: its phase is parabolic and an odd function of frequency; its magnitude is constant and an even function of frequency. Therefore, its impulse response is a real function of time.

$$H = |H| \exp(-j\varphi) \quad \begin{cases} \text{phase} = (2\pi f)^2 \operatorname{sign}(f) \frac{Dx}{g} W(f) \\ \text{magnitude} = W(f) \end{cases} \qquad (3.28)$$

where $j^2 = -1$ and W(f) is a frequency window.

Here is a graph of the bandlimited transfer function

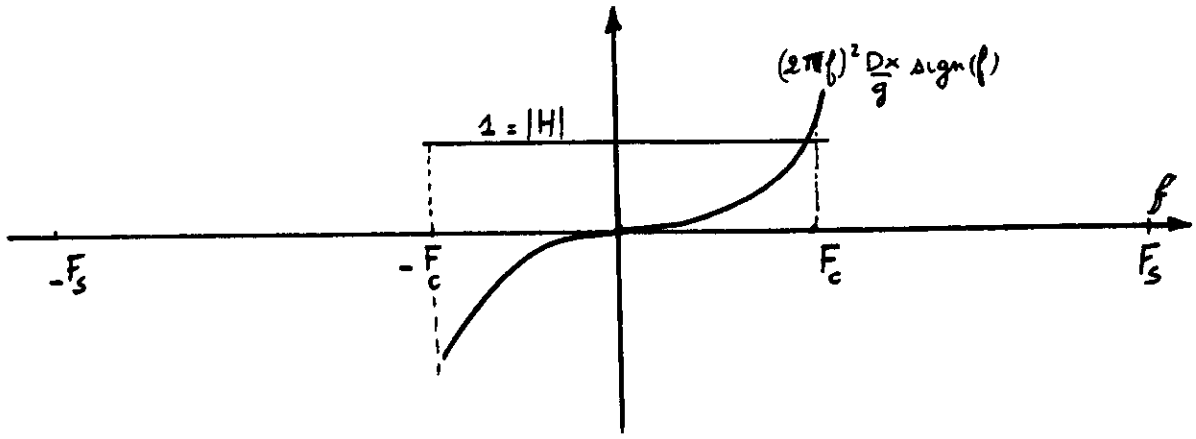

The frequency window W(f) is a rectangular block equal to unity over the sea spectral bandwidth.

The sampled transfer function is defined by:

- Dx the range of horizontal propagation,
- F_c the bandwidth frequency,
- N the number of samples.
- R, the ratio of the sampling frequency F_s to twice the cutoff frequency F_c: $R = F_s/(2F_c)$.

The impulse response is sampled every Dt where Dt, the sampling time is the inverse of the sampling frequency:

$$Dt\ F_c \leq 1/2$$

$$1 \leq R = F_s/(2F_c)$$

One can select for R either the Nyquist rate (R=1) or a higher sampling rate (R>1).

Since the theoretical transfer function is known, a sampling rate is chosen such that the largest increment in phase at the cutoff frequency would be less or equal to $\pi/4$: that is two frequency components separated by Df would have a maximum phase difference less or equal to 1/8th of a wave length. This last condition is graphically represented as follows:

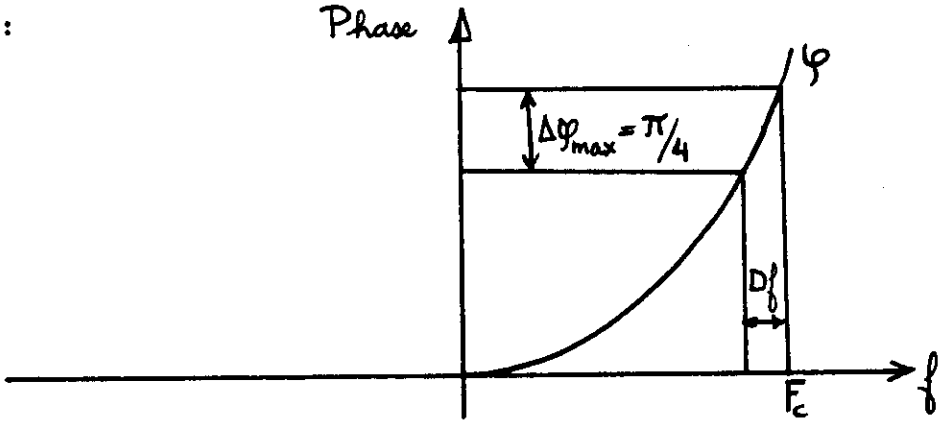

The Inverse Fourier Transform of the theoretical transfer function yields an impulse response shown in Figure 13 that may be parametrized in order to achieve high accuracy in the time convolution which is performed at each grid-point of the water column.

For the four parameters Dx, F_c, N, and R, there exists thus one relation: this leaves us with three independent parameters. One convenient way to measure the effect of these is to create a set of non-dimensional parameters.

1) The first parameter in the horizontal propagation problem is the ratio of the distance Dx to the minimum wave length L_c (corresponding to the cutoff frequency). This definition may be used for both deep and shallow water waves. This parameter, α ,combines the distance Dx and the bandwidth frequency in the following relation for the deepwater wave case:

$$\alpha = Dx/L_c = 2\pi\, Dx\, F_c^2/g \qquad (3.29)$$

where g is the gravity field.

2) The second non-dimensional parameter is N, the number of samples specifying the transfer function. One tries to use the lowest number of samples N so as to implement the convolution-sum with the fewest number of operations. If Df is the sample frequency increment, the sampling frequency Fs must equal NDf. Similarly, the total time length T_t of the impulse response is NDt and the following relations then hold:

$$F_s = NDf = N/T_t = 1/Dt$$

3) The last parameter is R, the ratio of the sampling frequency to the double of the cutoff frequency. R equals one for the Nyquist criterion:

$$R = F_s/(2F_c) \geq 1 \qquad (3.30)$$

The maximum phase shift between sample intervals is located at the bandwidth frequency:

$$\Delta\varphi_{max} = \varphi(F_c) - \varphi(F_c - Df) = 2\pi\alpha R(2N-R)/N^2 \qquad (3.31)$$

To first order approximation, the maximum phase shift between sample points is equal to

$$\Delta\varphi_{max} = \Delta k Dx = \frac{2\pi\Delta f}{C_g} Dx = \frac{2\pi F_c}{C_g}\frac{R}{N}Dx = 4\pi\alpha R/N \qquad (3.32)$$

Although it seems more complicated to use the group velocity C_g for the deepwater case, the same parameters and the same maximum phase at cutoff criterion can be used in order to describe the finite depth horizontal wave propagation. This is explained further in Chapter 4.

At cutoff F_c, the maximum phase shift, $\Delta\varphi_{max}$, is imposed to be less or equal to 1/8th of a wave length. This means that for good frequency resolution:

$$\Delta\varphi_{max} \leq \pi/4$$

This implies that

$$\frac{N^2}{g\alpha} - 2NR + R^2 \geq 0 \qquad \text{or } N/R \geq 16\alpha \qquad (3.33)$$

The result of this non-dimensional parametrization is to see the effect of each parameter on the phase and the magnitude errors. If the parametrization is correctly performed, the main source of error would be only caused by the FFT algorithm used to obtain the impulse response.

The phase error is a function of frequency and increases to a maximum at the cutoff frequency. The phase error, is defined as the difference between the theoretical phase of the transfer function at the cutoff frequency and the phase estimate of the Fourier transform of the impulse response used for the time convolution.

Phase Error= $|\varphi - \hat{\varphi}|$

The magnitude error is a function of frequency and increases to a maximum at the cutoff frequency. Theoretically, the transfer function's magnitude is equal to unity in the bandwidth interval. The relative magnitude error is defined by the ratio of the magnitude absolute error and the theoretical magnitude both considered at the bandwidth frequency.

Magnitude Error= $|H - \hat{H}|/|H| = |H - \hat{H}|$ since $|H| = 1$

These error functions are a function of the non-dimensional parameters N, R, and α. Because of the relation between these three parameters (3.33), only two of them are independent. The cutoff frequency F_c is imposed by the desired spectrum and the ARMA simulation. Therefore, the parameter is a linear function of Dx alone as appears in equations (3.29) and (3.30).

As a result of computing the maximum error at cutoff frequency as a function of increasing α, one finds that the relative errors on the impulse response's phase and

magnitude are of the order of 10^{-6}. Of course, R is then an independent parameter. The phase error functions are decreasing with an increase in the ratio R because simultaneously the number of samples N will increase ($N=16\alpha R$ and α is a constant). The value of R is fixed, however, by the ARMA velocities simulation method because the differentiation requires a ratio R larger than that required by the Nyquist rate (R=1): R usually equals 2 in the simulation results shown in Chapter 4. The number of samples, N, for the transfer function and the impulse response is given by the relation:

$$N = 16\,\alpha\,R \qquad (3.33)$$

In summary, one chooses the following quantities:

1) Select F_c from the sea spectrum and the distance Dx where the grid-point is located.
2) The value of R is selected to provide a correct simulation of velocities and accelerations usually 2 or greater
3) The number of samples 2N takes into consideration N points for the non-causal part of the impulse response and N for the causal part. This number is given by

$$2N = 32\alpha R.$$

3.7 Impulse Response for Vertical Convolution

The vertical propagation of wave kinematics is modelled after the exponential magnitude decay of wave component in deep water. The analog transfer function between two points separated by a vertical distance Dz is given by

$$G_a(f,Dz) = e^{-kDz} = \exp(-(2\pi f)^2 Dz/g) \qquad (3.25)$$

The subscript stands for analog.

The analog impulse response is

$$g_a(t) = \exp(-gt^2/4Dz)\sqrt{g/4\pi Dz}.$$

This is a pair of Fourier Transforms of particular interest. They both have a Gaussian bell shape as a function of frequency and time. The standard derivations of these bell-curves respectively σ_f and σ_t are defined by

$$\sigma_f = \sqrt{g/8\pi Dz} \qquad \sigma_t = \sqrt{2Dz/g}$$

and the pair of Gaussian magnitude curves correspond to low-pass filter

$$G_a(f,Dz) = \exp(-f^2/2\sigma_f^2) \text{ and}$$

$$g_a(t,Dz) = \exp(-t^2/2\sigma_t^2)\sqrt{g/4\pi Dz}.$$

The total time duration T_t of the impulse response g is chosen to be three times the standard derivation σ_t of the bell-shaped impulse response. The frequency cutoff of the transfer function G will, as a consequence of this choice, be even higher than three times the standard derivation σ_f of the bell-shaped transfer function. This stems from the

$$N \geq 6R\sqrt{a_z/\pi} \tag{3.39}$$

The total number of samples, 2N, includes N points for the causal part of the impulse response and N points for the non-causal part.

$$2N \geq 12R\sqrt{a_z/\pi}$$

And the impulse response in equation (3.36) can be rewritten:

$$g(n) = \exp(-\pi^2 n^2/8a_z R^2)/\sqrt{8a_z R^2} \tag{3.40}$$

3.8 Comparison of the Numerical Effficiency of the ARMA Method With the Sum of Sinusoids

The water column is divided into a grid of points. At the origin of coordinates, the Auto Regressive Moving Average wave kinematics for vertical velocity is generated by the following algorithm:

$$V(n) = -\sum_{k=1}^{N} a_k \, V(n-k) + \sum_{m=0}^{M} b_m \, W(n-m)$$

where $\{a_k\}_N$ and $\{b_m\}_M$ are the coefficient parameters of the ARMA model and V(n) and W(n) represent respectively the wave particle velocity and the Gaussian white noise time histories.

Each grid point throughout the water column is defined by its coordinates (Dx,Dz): Dx is the horizontal distance and Dz is the depth where the node of a finite element model of the offshore structure is located. Through a series of convolutions, the wave kinematics throughout the grid are generated.

First, the wave is propagated horizontally and then, vertically. From a theoretical point of view, the order of the horizontal and the vertical propagations are

A_v, A_h that are being simulated, are used in the Morison equation. The wave forces, then, are the input to the finite element model.

3.8.1 Number of Multiplications or Additions

In the ARMA wave simulation method, one propagates first horizontally and then vertically the wave particle kinematics. The number of computations is given below.

1) At the origin of coordinates, where the ARMA(M,N) wave simulation is generated, there are:

   N + M operations at each time step.

2) From the origin to each of the K-1 other grid-points on the mean water line, a horizontal propagation filter (impulse response function) $H_{hor}(t,Dx)$ is used. The total number of operations to implement all the K-1 convolutions is:

   (K-1) N_{hor}, where N_{hor} is the order of the impulse response for horizontal propagation.

3) Propagating down vertically from the K grid-points on the mean water line to (L-1) depth levels throughout the water column requires a total number of operations equal to:

   K(L-1) N_{vert}, where N_{vert} is the order of the vertical impulse response function.

4) At each of the KL grid-ponts, the total number of operations involved in computing the horizontal components and the vertical accelerations is equal to:

$KL(N_{dif}+2N_{hilb})$, where N_{dif} and N_{hilb} are the order of the differentiation and Hilbert filters.

All these operations sum up to a total of

$$Total = KL(N_{vert}+N_{dif}+2N_{hilb})+ K(N_{hor}-N_{vert})+ (N+M-N_{hor})$$

In comparison, the sum of sines method can be used to generate the four wave particle kinematics (V,U,A_v,A_h) and the number of operations involved is equal to:

8 NSpec KL

where NSpec is the number of samples of the wave spectrum.

3.8.2 Number of Memory Storages

The impulse responses needed for horizontal and vertical propagation must be stored permanently. These functions are non-dimensional and depend on non-dimensional parameters. The two parameters that depend on the location of the grid-points are α and α_z. The impulse response curves used for the wave propagation vary with these parameters α and α_z. For the horizontal propagation, one needs to determine K-1 functions because there are K-1 destination points on the mean water line. For the vertical

propagation, one needs to store L-1 impulse response functions because there are L-1 depth levels or lines in the grid. Finally, the Hilbert filter that is used to compute horizontal velocities from horizontal ones, must be stored once because it is independent of the location of the grid-point. Thus, the total number of permanent storages is:

Total: $(K-1)\, N_{hor} + (L-1)\, N_{vert} + N_{hilb}$

At each time step, the total memory storage necessary to carry out all the convolutions, must include the wave kinematics time histories that follow:

1) At each of the K grid-points on the mean water line, one must store N_{vert} past consecutive values of the wave particle vertical velocity in order to implement the necessary convolutions propagating vertically throughout the water column. The total number of memory storage for vertical propagation adds up to:

   KN_{vert}

2) At each grid-point throughout the water column, one needs to store enough wave kinematics past consecutive values in order to implement a Hilbert transform and a differentiation. The total amount of memory storage required is equal to:

$KL(N_{dif} + N_{hilb})$

3) At the origin of coordinates, one must store the past M values of the Gaussian white noise and N_{hor} past values of the vertical velocity in order to implement the original horizontal propagation. This leads to a total of permanent storages equal to:

$$\text{Total} = KL\,(N_{dif}+N_{hilb}) + (K+L)\,N_{vert} + K\,N_{hor} + N_{hilb} + M - N_{vert}$$

In the comparison, the sum of sines method requires a total number of storages of (3NSpec)KL.

3.8.3 Number of Input/Output Memory Transfers

At each time step, the recursion algorithm requires only one memory I/O transfer per grid point, this totals the number of I/O to KL.

The sum of sines method requires at least KL Nspec I/O transfers at each time step.

3.8.4 Example and Comparison

Suppose one hour of data is needed and DT=.5sec, 7200 time samples must be generated. The following data is a given to illustrate the comparison:

in the ARMA simulation N=22, M=22, N_{dif}=2, N_{hilb}=29, N_{hor}=256, N_{vert}=32.

in the state-of-the-art simulation method: N_{Spec}=256

Let us first take 100 grid-points K=10, L=10 .

	ARMA (1)	Sum of sines (2)	Ratio(2)/(1)
number of addition	8,649	204,800	24
number of memory storage	2,297	76,800	33
number of I/O transfer	100	25 600	256

Let us now take a 10000 grid-points K=100, L=100

	ARMA (1)	Sum of sines(2)	Ratio(2)/(1)
number of addition	662,185	20,480,000	31
number of memory storage	5,177	7,680,000	1,484
number of I/O transfer	10,000	2,560,000	256

As a result of this comparison, the numerical efficiency of the use of recursive impulse responses is demonstrated. The advantage of the proposed methods increases rapidly with the number of equivalent sinusoidal components. The advantage is even more pronounced when simulations of directionally spread seas are desired.

CHAPTER 4

APPLICATIONS AND RESULTS

First, an example of the ARMA simulation of deepwater wave kinematics is presented. The ARMA model matches a given spectral shape representing a storm sea (period between zero upcrossings T_z = 12 sec, significant wave height H_s = 40 ft), and a moderate sea (T_z=6 sec, H_s=4 ft). The wave kinematics are propagated horizontally, vertically, and, at each grid-point throughout the water column, a differentiation and/or a Hilbert transform are performed in order to obtain the acceleration from the velocity and/or the horizontal component from the vertical. The advantages of the convolution method are that it works on random sea data and that it is numerically more efficient as demonstrated at the end of Chapter 3. As a base case to demonstrate that the impulse response designs are accurate, a sum of 50 sines is selected to model sea amplitude and water particle kinematic time histories. Each of the 50 frequency components has a random phase φ_i. The wave kinematics are determined at a horizontal distance of 100 meters from the origin and at a depth of 20 meters down from the mean water line using the superposition of deterministic

sine waves. They are, then, compared to the results of the numerical convolutions. Similarly, the theoretical values of wave accelerations and the horizontal wave components are compared to the output of the numerical model for differentiation and Hilbert transform. Also, the author demonstrates that with this numerical methods wave spreading is easily incorporated. Results are shown to demonstrate that the vertical propagation impulse response can be modified to model the finite amplitude effects of linear waves by using the stretched linear approximation. Both the effects of directionality and of finite amplitude are usually taken into consideration when a time simulation of wave forces is calculated.

At the end of this chapter, the effect of shallow waters and finite depths is considered. The transfer functions that are required for a time domain simulation of wave kinematics are presented. The impulse responses necessary for the implementation of the convolution-sums are designed by the standard technique of windowing, frequency sampling and finite impulse response (FIR) digital filter design.

4.1 ARMA Modelling of Sea Waves

The Bretschneider spectral shape for wave particle velocity is selected as a target spectrum for illustrating the method. In a non-dimensional representation, the magnitude is normalized by its peak value ,and the frequency normalized by the peak frequency of the velocity spectrum. The wave amplitude spectrum[6] under consideration is:

$$\frac{S_x(f)}{S_x(F_o)} = e^{5/4}\left(\frac{F_o}{f}\right)^5 \exp\left(-\frac{5}{4}\left(\frac{F_o}{f}\right)^4\right) \text{ and } S_x(F_o) = \frac{5}{16F_o}H_s^2$$

where H_s is the significant wave height, and F_o, the peak frequency of the wave amplitude spectrum. A Bretschneider spectrum has several properties, and the following relations hold: $T_z = .710/F_o = \sqrt{M_o/M_2}$;

$M_o = H^2_s/16$; $M_2 = \sqrt{5\pi}\, H^2_s/32F_o$

where M_o and M_2 are respectively the zeroth and second order moments of the Bretschneider wave amplitude spectrum.

The velocity spectrum's maximum F_1 is a function of F_o:

$$F_1^4 = \frac{5}{3}F_o^4$$

i.e, F_o and F_1 are proportional and the zero crossing period T_z is related to the velocity spectrum peak frequency F_1

$$T_z = \frac{.710}{F_1} \times \sqrt[4]{\frac{5}{3}}$$

T_z and H_s can be expressed in terms of the peak value $S_x^{\bullet}(F_1)$ and the peak frequency of the velocity spectrum F_1.

Two sea states have been selected for the simulation of wave kinematics: a storm sea in the Gulf of Mexico: H_s = 40 ft and T_z= 12 sec. and a moderate sea: H_s = 4 ft and T_z= 6 sec. For Bretschneider spectra, the non-dimensional spectral shape remains unchanged for any value of H_s, and F_o (or T_z). Therefore, once an ARMA spectrum has been selected that matches the target spectrum, it can be normalized and scaled to represent any peak frequency F_1 and any corresponding spectral peak value $S_x^{\bullet}(F_1)$. One interesting characteristic of the Bretschneider spectrum is precisely the fact that in non-dimensional form, its spectral shape is independent of the actual values of the peak value F_1 and the spectral peak value $S_x^{\bullet}(F_1)$. Once one ARMA approximation has been found, it remains valid for the whole family of Bretschneider spectra: this means for the whole range of significant wave heights H_s and of peak periods F_o. The time sampling alone depends on the cutoff frequency and therefore on the value of the peak frequency F_o.

The cutoff frequency is expressed as a ratio to the peak frequency of the velocity spectrum. At $6F_1$, the spectrum is 20 dB below the peak spectral value of the velocity spectrum, while $3F_1$ corresponds to 20 dB below the peak spectral value of the wave elevation spectrum. Because

of the normalizing and scaling process, the relative errors on the two parameters H_s and F_o become negligible. One must check however that the -20 dB attenuation threshold is reached at the cutoff frequency, and that at 0.53 F_1, the lower frequencies reach the -20 dB attenuation threshold.

On Figures 1 and 2, the ARMA model's coefficients and the corresponding ARMA spectrum is shown. This ARMA(21,21) model has 21 poles and 21 zeros and approximates the velocity spectum from 0 to $6F_1$.

The ARMA velocity spectrum $|B/A|^2$ using these ARMA coefficients (Figure 1) has a unit peak magnitude, that is:

$$S_x^{\cdot}(F_1) = |B/A|^2 = 1$$

and the sampling frequency $F_s = 24F_1$. These ARMA coefficients when used in the ARMA time domain velocity simulation:

$$V(n) = -\sum_{k=1}^{N} a_k V(n-k) + \sum_{m=0}^{M} b_m W(n-m)$$

yield a velocity time series V(n) sampled at $Dt = 1/24F_1$ and the $\{b^m\}_M$ coefficients of Figure 1 should be multiplied by the scaling factor $\sqrt{S_x^{\cdot}(F_1)}$. Indeed the time simulation is performed to model a given sea state defined in terms of H_s and T_z or equivalently in terms of $S_x^{\cdot}(F_1)$ and F_1, with such a scaling factor $\sqrt{S_x^{\cdot}(F_1)}$ the peak magnitude of the velocity spectrum is correctly assigned:

FIGURE 1

ARMA COEFFICIENTS

a coefficients (denominator)	b coefficients (numerator)
A_0 = 1.000000	B_0 = 8.8021774E-01
A_1 = -2.417805	B_1 = -1.600297E-01
A_2 = 2.020816	B_2 = 2.4413279E-02
A_3 = -0.6861026	B_3 = 3.5095071E-02
A_4 = 0.1000194	B_4 = 6.0932731E-03
A_5 = 7.2162442E-02	B_5 = 2.0972779E-02
A_6 = -0.1582499	B_6 = -5.8377825E-03
A_7 = 0.2111652	B_7 = 1.2602669E-02
A_8 = -0.2363975	B_8 = -1.2525232E-02
A_9 = 0.2600787	B_9 = 8.3236791E-03
A_{10} = -0.2687707	B_{10} = -1.5151329E-02
A_{11} = 0.2738586	B_{11} = 6.5852175E-03
A_{12} = -0.2733125	B_{12} = -1.4452929E-02
A_{13} = 0.2560819	B_{13} = 5.7981272E-03
A_{14} = -0.2404137	B_{14} = -1.0514684E-02
A_{15} = 0.1908552	B_{15} = 4.0679654E-03
A_{16} = -0.1381382	B_{16} = -2.3783268E-03
A_{17} = 4.6476267E-02	B_{17} = -7.4141774E-04
A_{18} = 8.0833592E-02	B_{18} = 1.1307076E-02
A_{19} = -6.6951260E-02	B_{19} = 2.1633136E-03
A_{20} = -8.6666532E-02	B_{20} = -2.5663370E-03
A_{21} = 1.4706483E-02	B_{21} = -9.0960273E-04

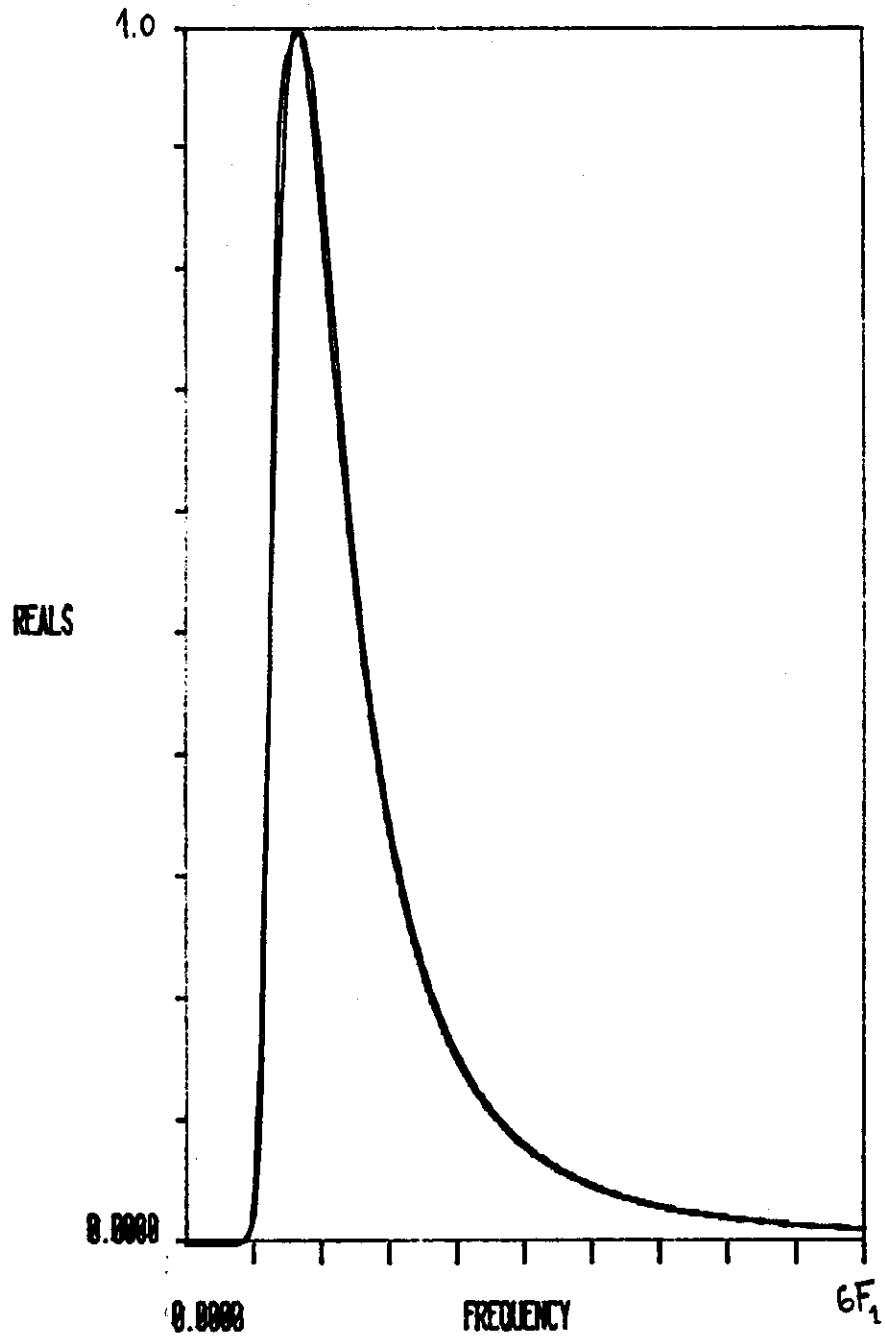

ARMA(21,21) COMPARED TO THE BRETSCHNEIDER VELOCITY SPECT
FREQUENCY RANGE FROM 0 TO 6 F_1

FIGURE 2

$$\text{at } f = F_1, \quad \left|\frac{B}{A}\right|^2 \left(\sqrt{S_{\dot{x}}(F_1)}\right)^2 = 1 \cdot S_{\dot{x}}(F_1) = S(f = F_1)$$

4.2 Vertical Wave Propagation

The proposed impulse response for deepwater linear waves has a Gaussian (bell) shape:

$$g(n) = \exp(-n^2\pi/8a_z R^2)/\sqrt{8a_z R^2}$$

or

$$g(n) = \exp(-n^2/2\sigma_t^2)/\sqrt{2\pi\sigma_t^2}$$

and $\sigma_t^2 = 4a_z R^2/\pi = 2Dz/gDt^2$

where n= 1,...,N and a_z is a non-dimensional parameter $a_z = 2\pi Dz F_c^2/g$; R is equal to the following ratio $R = F_s/2F_c$; F_s is the sampling frequency; Dt, the sampling time $Dt = 1/F_s$; F_c the cutoff frequency; Dz the vertical distance from the m.w.l. to the grid-point; g the gravity field. Note that the impulse response is a non-dimensional function that depends on a non-dimensional parameter a_z and is directly proportional to the distance Dz:

$$a_z = \frac{2\pi}{g} D_z F_c^2$$

If one stores only one impulse response function, one would have to trade-off different depths Dz for different sampling times Dt in order to keep this parameter constant. Alternatively, one can calculate a whole set of impulse responses with varying parameter a_z, and then interpolate the impulse responses for any value of a_z. In the vertical

propagation case, the impulse response is analytically simple for deepwater waves, and it may not always be necessary to do what has been suggested. Nonetheless, one may store or interpolate a set of impulse responses for various parameters.

The convolution that yields the desired wave kinematics, uses the mean water kinematics as input. Suppose that one wants to compute wave velocities at a fixed point where there is occasionally no fluid. One would perform the convolution only if this grid-point is submerged. This is logical and is easily implemented on the computer: let η be the free-surface elevation at the instant t and V_m, ,the mean water line vertical velocity:

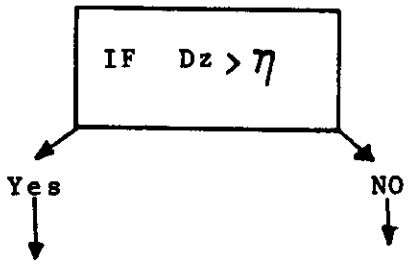

$V(t,Dx,Dz) = V_m(t,Dx,0)*g(t)$ $\qquad$ $V(t,Dx,Dz) = 0$

or

$$V(n,Dx,Dz) = \sum_k V_m(n-k)\ g(k)$$

This time convolution is performed numerically by the above sum, and V_m is the mean-water-line vertical velocity.

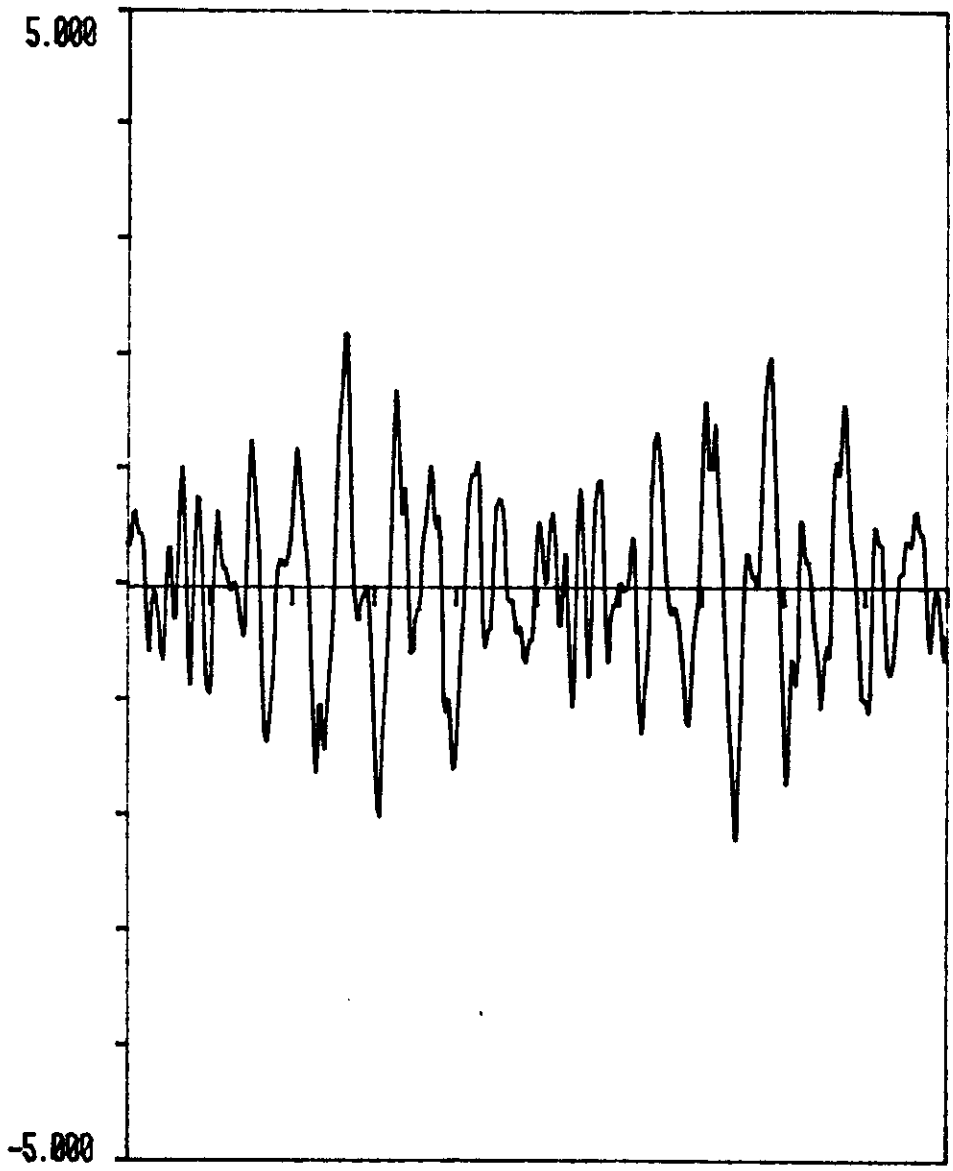

WAVE KINEMATICS (VELOCITY) AT THE ORIGIN

INPUT TO THE VERTICAL CONVOLUTION

FIGURE 3

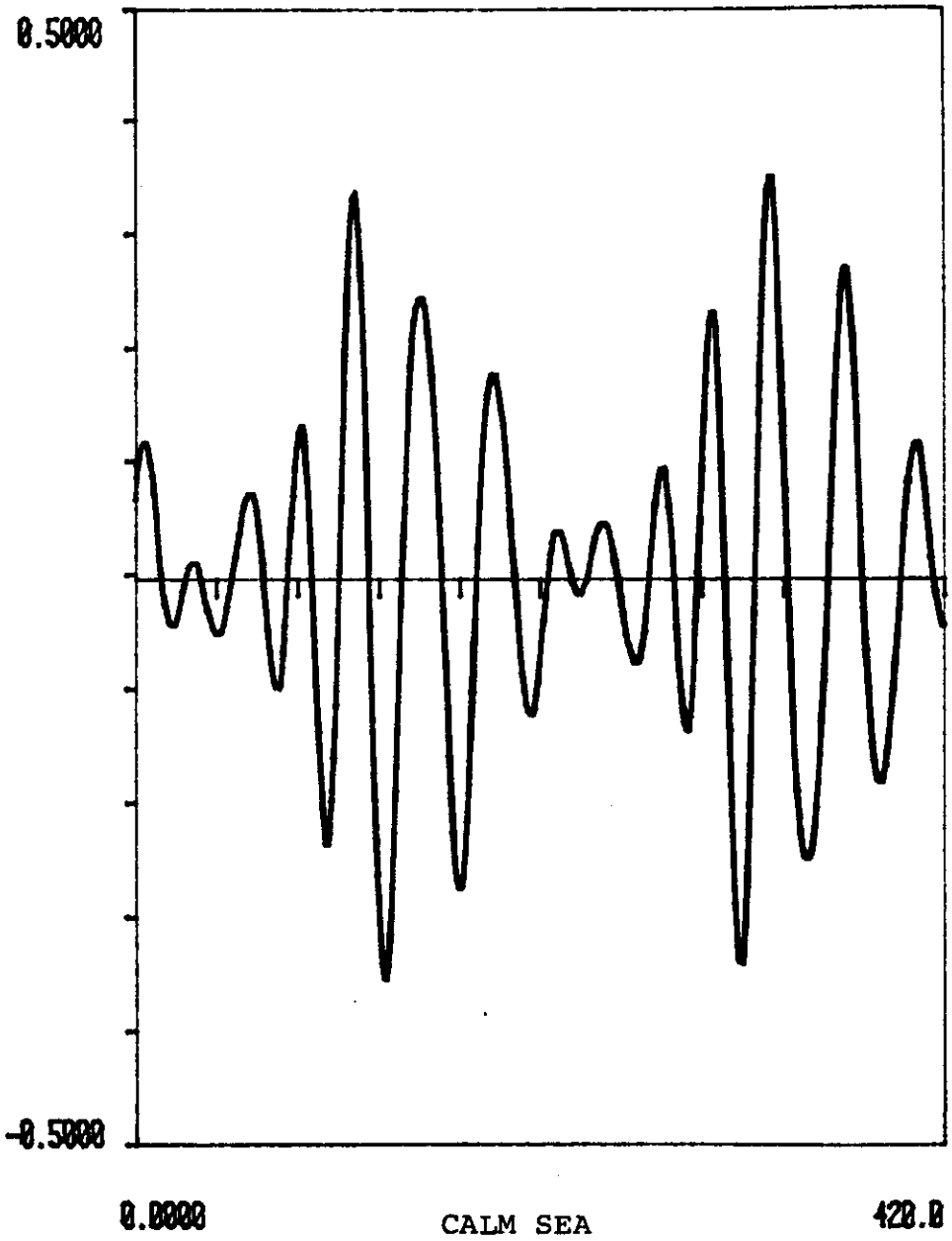

SIMULATION RESULT COMPARED WITH THEORETICAL
(SHIFT OF ONE DT BETWEEN BOTH GRAPHS)
AT -20 METERS VERTICALLY

FIGURE 4

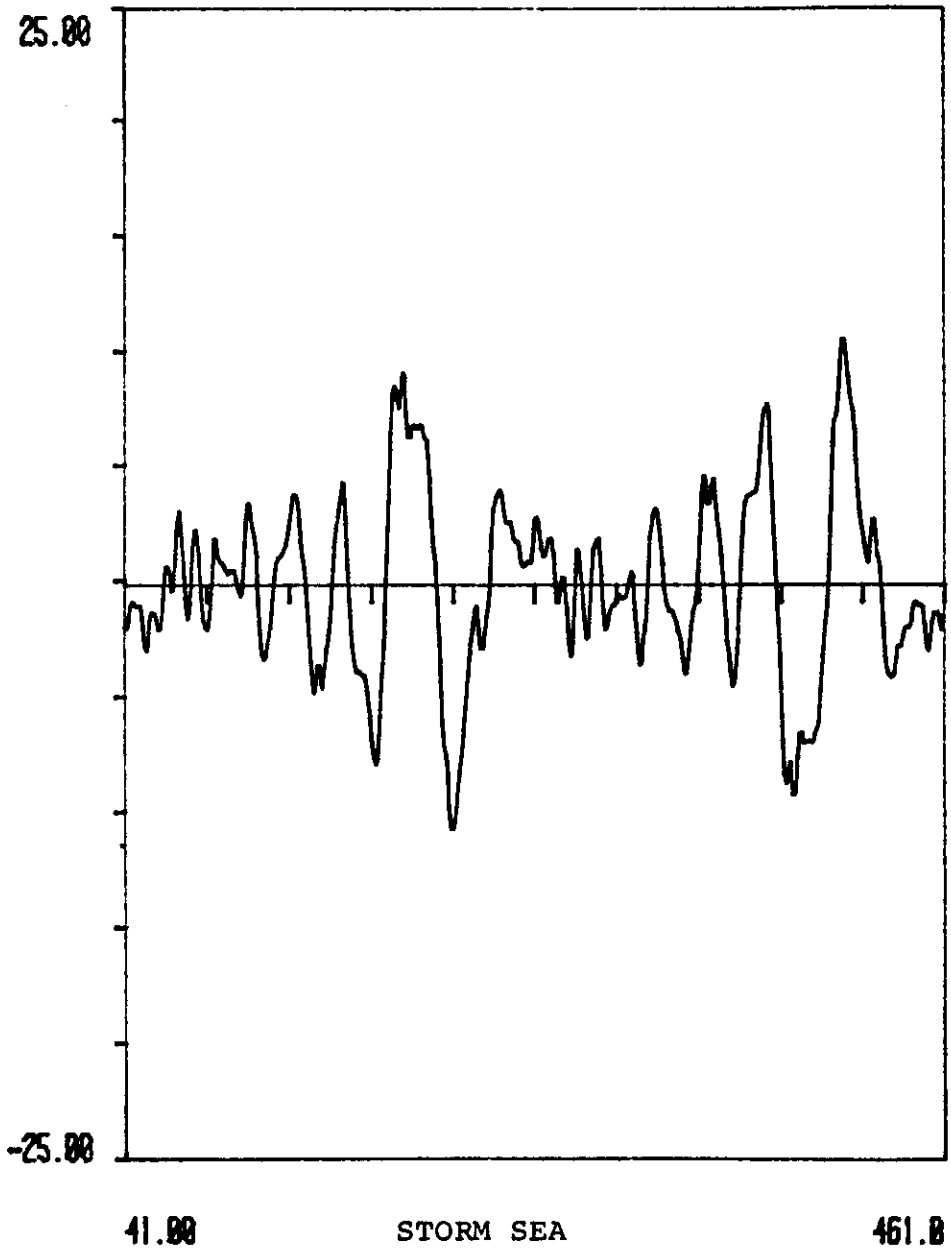

WAVE KINEMATICS (VELOCITY) AT THE ORIGIN

INPUT TO THE VERTICAL CONVOLUTION

FIGURE 5

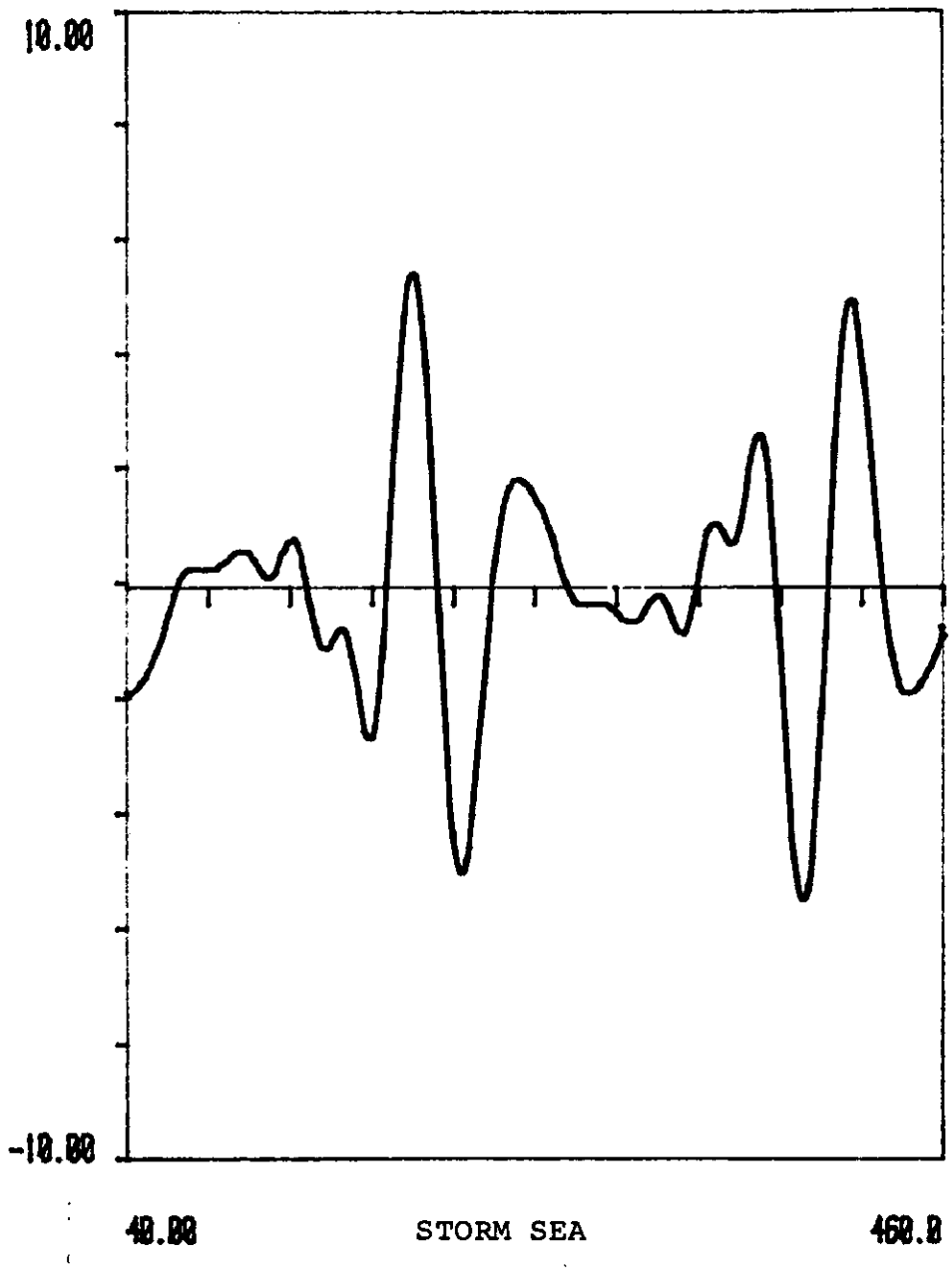

SIMULATION RESULT COMPARED WITH THEORETICAL
(SHIFT OF ONE DT BETWEEN BOTH GRAPHS)

WAVE KINEMATICS AT -20 METERS VERTICALLY

FIGURE 6

The results in Figures 3 to 6 show how the theoretical vertical velocity (sum of sines) at a depth of -20 meters compares with the output of the convolution for two cases: a calm sea (Figures 3 and 4) and a Gulf of Mexico storm (Figures 5 and 6).

4.3 Stretched Linear Approximation For Finite Amplitude Effects

4.3.1 Stretched Linear Application

In the context of wave force calculations, it is of practical importance to have an accurate knowledge of particle velocities and accelerations in steep, near-breaking waves. However, it appears that comprehensive comparisons with experiments under such extreme conditions are not commonly available. Thus in spite of the sophistication of wave theories that may be employed, uncertainties remain in the prediction model of particle kinematics for very steep waves. Linear theory is found to be fairly realistic even when there are major departures from the small wave height assumption.

The stretched linear approximation takes into account some finite amplitude effects. The mean-water-line velocity is transfered from the mean-water-line (referred hereafter as the m.w.l.) up to the elevation η. This means that the values at the m.w.l. are "stretched" and assigned to the

actual points where wave elevations are. Suppose that at a distance Dx from the origin the m.w.l. vertical velocity $V_m(t,Dx,z=o)$ is known and that the wave elevation η is known at that instant too. In the stretched linear approximation, this vertical velocity is now assigned at the point $z=\eta$ and $x=Dx$:

$$V(t,Dx,z=\eta) = V_m(t,Dx,0)$$

Another feature of the stretched linear approximation is associated with the vertical decay of wave magnitudes with depth. The starting point for the vertical decay is changed: instead of the m.w.l., it starts from the actual wave elevation position. Thus at each grid-point (Dx,Z_i) on the vertical line Dx= constant, the decay starts, at each time step, from the location of the wave elevation. At each time step, the exponential decay starts from n to the destination point at a depth level Dz+n calculated from the free-surface instead of the m.w.l. These particular characteristics of the stretched linear approximation require a lot of memory storages and input/output transfers when the "sum of sines" model is used. However, the convolution method handles the vertical propagation model in an accurate and numerically efficient manner.

Suppose that the wave particle velocity must be obtained at a fixed grid-point (Dx,Dz). First, the m.w.l. vertical velocity at a distance Dx is obtained by the

horizontal propagation convolution-sum:

$$V_m(t,Dx,z=o) = V_m(t,x=o,z=0) * h_{hor}(t,Dx)$$

$$V_m(n,Dx,z=0) = \sum_{i=-N_{hor}}^{N_{hor}} V_m(n-i,x=o,z=o)\ h_{hor}(i,Dx)$$

For the grid-point (Dx,Dz), one must compare, at each time step, Dz with the wave elevation η. If the grid-point is not submerged, the velocity is set equal to zero. If the grid-point is submerged, the velocity at (Dx,Dz) is the output of the m.w.l. velocity $V_m(Dx,z=o)$ with the "stretched linear" transfer function G.

This transfer function G and its impulse impulse response g are presented here:

$$G(f,Dz+\eta) = \exp(-(2\pi f)^2(Dz+\eta)/g)$$

$$g(t,Dz+\eta) = \exp(-gt^2/4(Dz+\eta))\sqrt{g/4(Dz+\eta)\pi}$$

where η is the free-surface wave elevation at the x=Dx. The wave kinematics magnitudes decay exponentially from the free-surface η to the grid-point located at a fixed depth Dz. At each instant, the total depth of the grid-point is exactly $Dz+\eta$ and not Dz. All these impulse responses are still a function of the parameter α_z:

$$a_z = 2\pi(Dz+\eta)F_c^2/g$$

If the impulse responses are stored and interpolated for any value of a_z there is no problem in obtaining the proper impulse response at each time step. If not, to recompute the impulse response at each time step is easy because it is given by a simple analytical formula, and because η is known at each time step.

An outline for what must be done in the stretched linear approximation for finite amplitude effects follows:

1) Obtain the m.w.l. vertical velocity $V_m(Dx,z=o)$ at a grid-point $(Dx,z=o)$ by convolving the ARMA m.w.l. velocity at the origin $(x=o,z=o)$ with the horizontal propagation transfer function.

2) Assign this m.w.l. velocity $V_m(Dx,z=o)$ to the actual position of the wave free-surface elevation rather than to the m.w.l.

3) The grid-point (Dx,Dz) can be above or below the m.w.l., and the velocity there is calculated by following these steps:

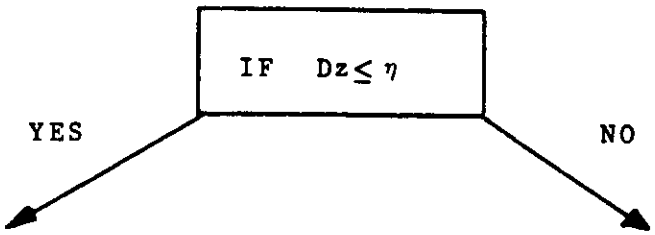

$V(Dx,Dz,t) = V_m(Dx,t) * g(t,Dz+\eta)$

this convolution is digitalized and performed in the time-domain;

$V(Dx,Dz,t) = 0$

The point (Dx,Dz) is not submerged at time t;

Note that $g(t,Dz+\eta)$ has a Gaussian magnitude (bell shape) and at each time step, a new impulse response function is used. However, this poses no problem because at each time step η is a given constant.

Figures 7 to 9 present the results of using this method on a storm sea state. The depth considered is -25 meters from the m.w.l. This convolution method is simple and still numerically more efficient than "summing deterministic sines". Moreover, it can be used on random as well as deterministic wave kinematics simulations.

4.3.2 Calculation of Base Shear and Overturning Moment on a Single Pile

A single pile of one meter diameter and one hundred meters long, representing a vertical leg of a steel jacket offshore structure, is subjected to a storm sea with seven meter significant wave height and a zero crossing period T_z of 9.94 sec. From Wiegel's formula[34]:

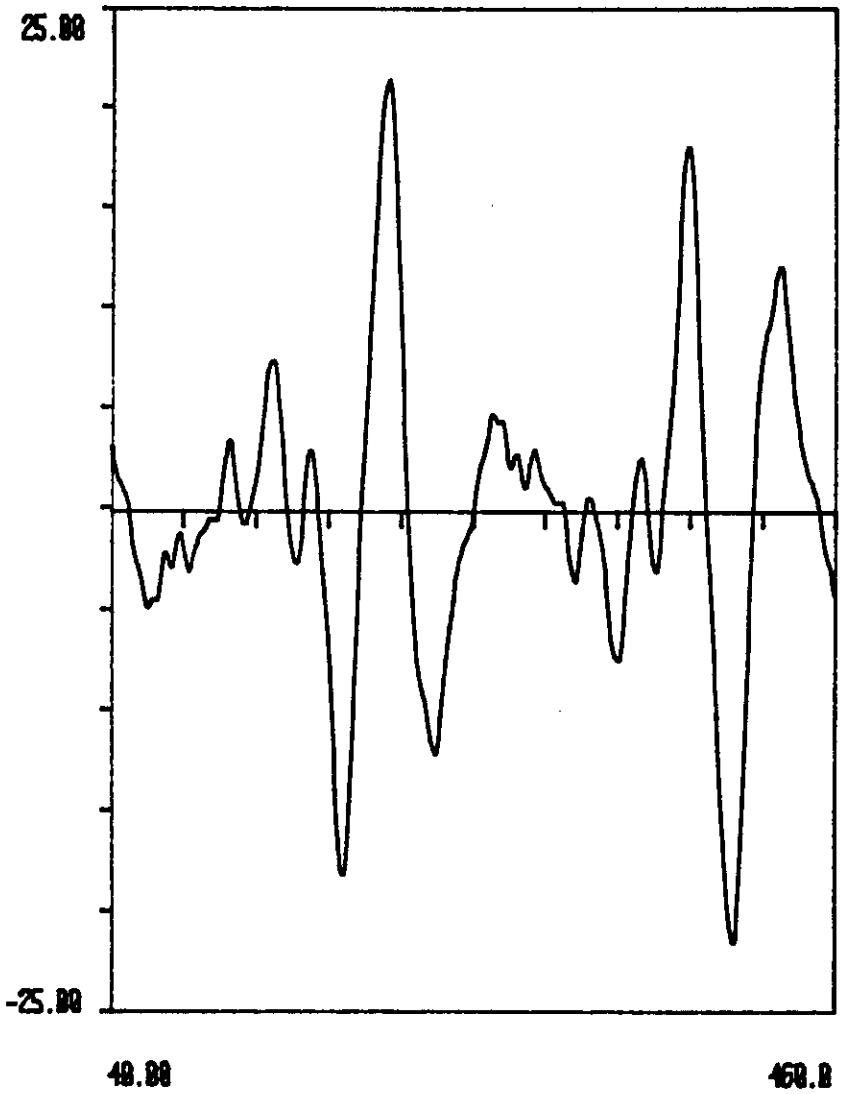
25.00
-25.00
40.00
460.0
FREE SURFACE AMPLITUDE USED FOR THE STRETCHED LINEAR APP.

FIGURE 7

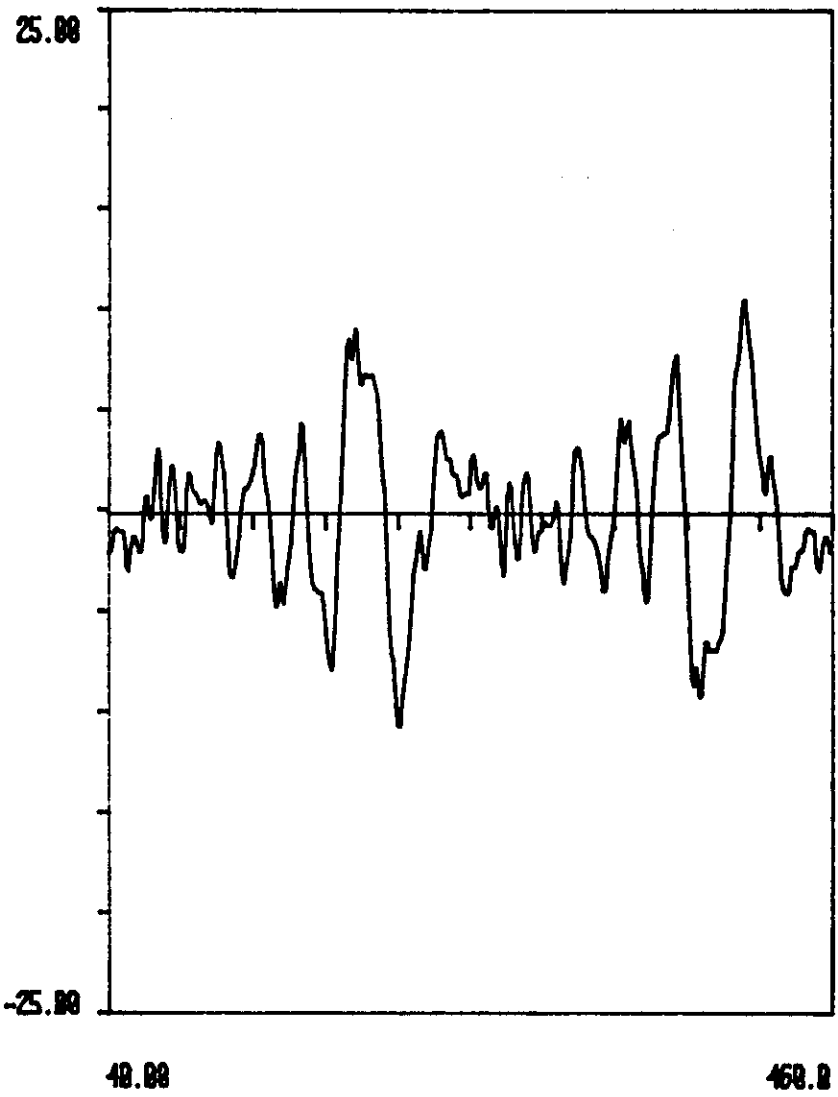

VERTICAL VELOCITY AT THE STRETCHED FREE SURFACE
INPUT TO THE VERTICAL CONVOLUTION

FIGURE 8

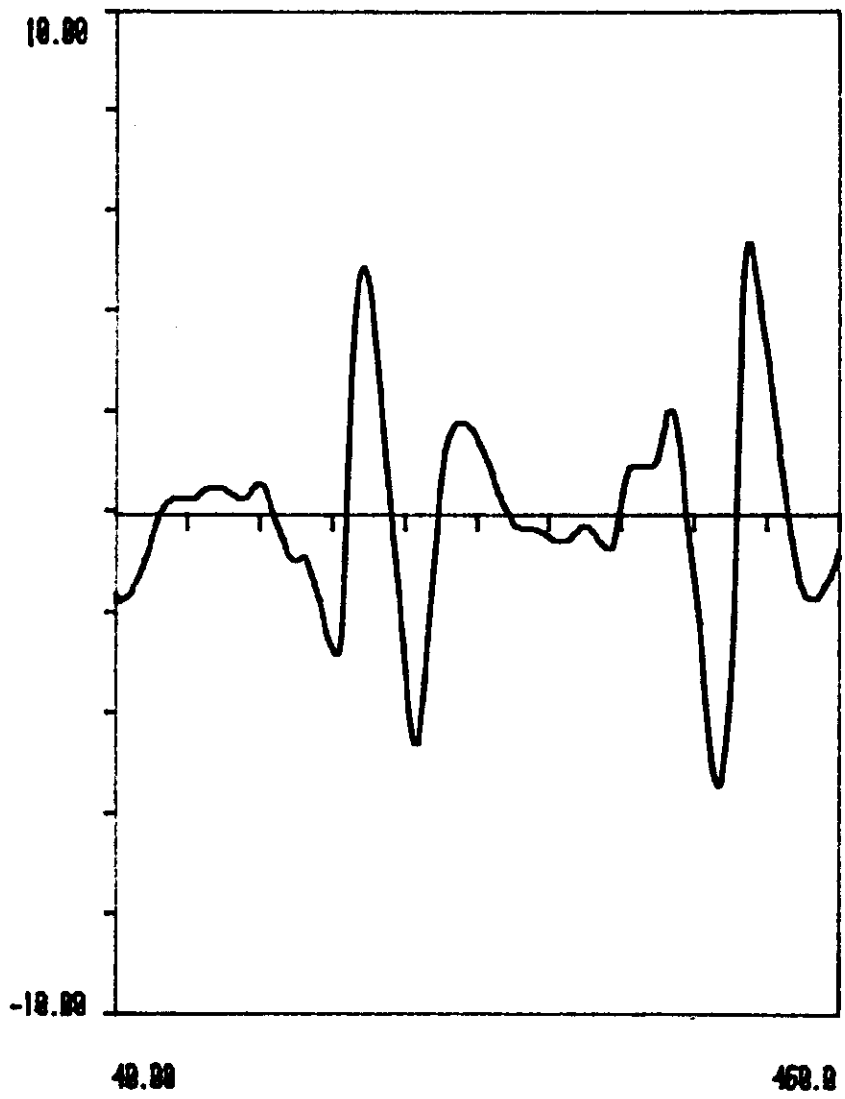

COMPARISON OF SUMS OF SINES AND CONVOLUTION

FOR THE STRETCHED LINEAR AT -25M DEEP

FIGURE 9

H_s=7m, H_s=.378$T_z^{1.788}$ T_z=9.94 sec.

The peak frequency of the wave amplitude spectrum F_o is deduced from the zero crossing period T_z by Bretschneider's formula(22):

F_o=.710/T_z = .0714Hz

The peak frequency of the velocity spectrum F_o is deduced from F_o

$$F_1 = \sqrt[4]{5/3}\, F_o = .0811\,Hz$$

Thus, the two parameters that define the ARMA velocity spectrum, F_1 the peak frequency and $S_{\dot{x}}(F_1)$ are determined and the simulation of ARMA velocities is carried out at a sampling time $Dt=1/24F_1$ and with a scaling factor $\sqrt{S_{\dot{x}}(F_1)}$

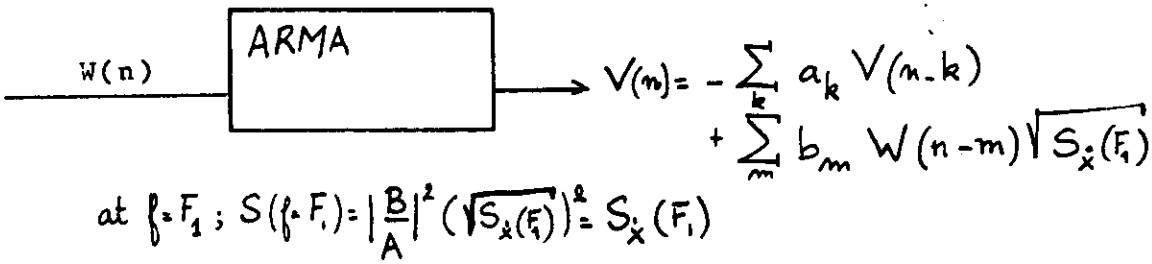

The spectrum of the Gaussian white noise input and of the ARMA simulation of the vertical velocity at m.w.l. level are obtained using Maximum Entropy Method spectral analysis and are shown in Figures 10 and 11. They are calculated by averaging the spectral estimate of 6 time series of 512 data points. The white noise spectrum is constant as expected over the range up to the sampling frequency F_s and the velocity spectrum is as obtained from a short time record

as the record. If the record length were increased to infinity, the velocity spectrum would converge to the target spectrum, Figure 2.

For calculating base shear and overturning moment, one needs the horizontal wave forces along the pile. The horizontal velocities and accelerations must be first generated from the ARMA vertical velocities at the m.w.l. Thus, a Hilbert Transform is performed on the vertical velocities time histories to obtain horizontal velocities and then the central difference differentiation formula gives the horizontal acceleration time series from the horizontal velocities.

In order to use the stretched linear theory, the actual wave elevations time series $\eta(t)$ is needed, too.

The ARMA vertical velocity is integrated by using the trapezoidal rule and is high pass filtered to avoid the numerical blowup at low frequency. Thus, knowing horizontal velocities U and accelerations A_h and the wave elevation η (t), all derived from the ARMA vertical velocities time history V, the random wave force calculation can start. Here, Morison's equation can be adequately used because the forces are drag dominated[29] (H/D=12.6, L/D=300). The force at each node is given by

$$F_n = \rho \forall C_m \ell_n \dot{U}_n + \frac{1}{2} \rho C_d \ell_n U_n |U_n|$$

The one hundred meter tall pile is divided into the following structural nodes n, and each of area 1_n.

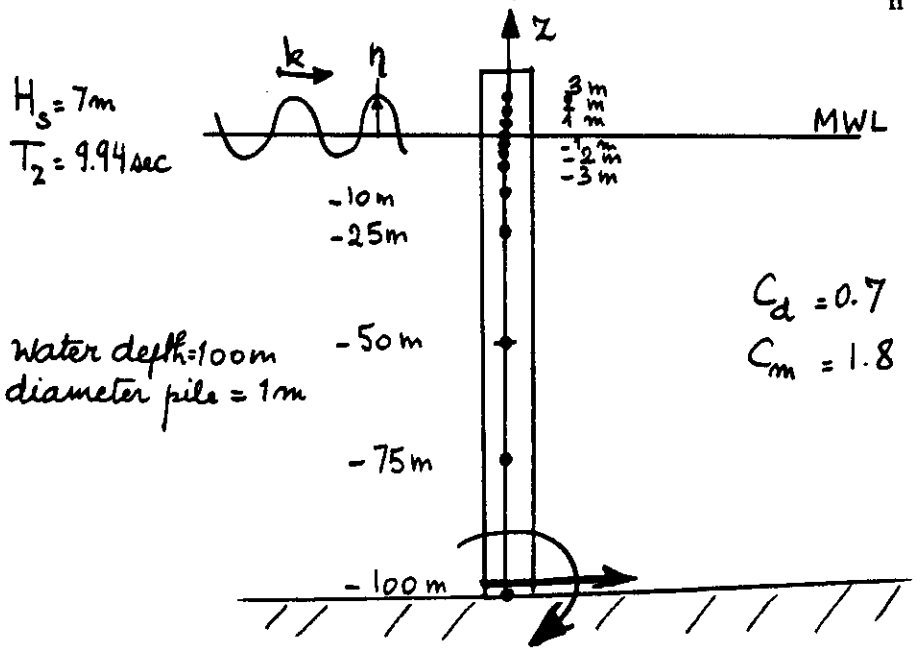

node #	coordinates	total area ℓ_n
1	3m	1.0
2	2	1.0
3	1	1.0
4	0	.5 m^2
5	-1	1.0
6	-2	1.0
7	-3	4.0
8	-10	11.0
9	-25	20.0
10	-50	25.0
11	-75	25.0
12	-100	12.5

Thus, the total shear is the sum of all the horizontal nodal forces:

$$\text{Shear Force} = \sum_{\text{nodes}} F_n$$

In the linear wave force calculation, the first node is n=4, the m.w.l. node and its area is strictly below the m.w.l. The wave kinematics are exponentially decaying from the m.w.l. In the stretched linear wave force calculations, the first node is the first inundated nodal area and it varies with the wave elevation time series $\eta(t)$. The vertical propagation decays the wave kinematics from the wave elevationn coordinate $z=\eta(t)$ up to the nodal coordinates z. The z axis starts at the m.w.l. and is directed positively downwards to the water depth. The overturning moment is defined as the sum of the moment of all nodal forces F_n with respect to the base of the pile at z=100m. The overturning moment and the base shear are higher in magnitude when stretched linear theory is used because the finite wave amplitude above the m.w.l. creates new nodal forces and moments. Moreover, the interruption of wave force in the stretched linear force calculation when a node is not inundated, creates higher wave force spectrum that would not exist if linear wave theory was used. Some reservations should be emphasized because Morison's equation is not made to account for such effects. This is important in the design of offshore platforms because it

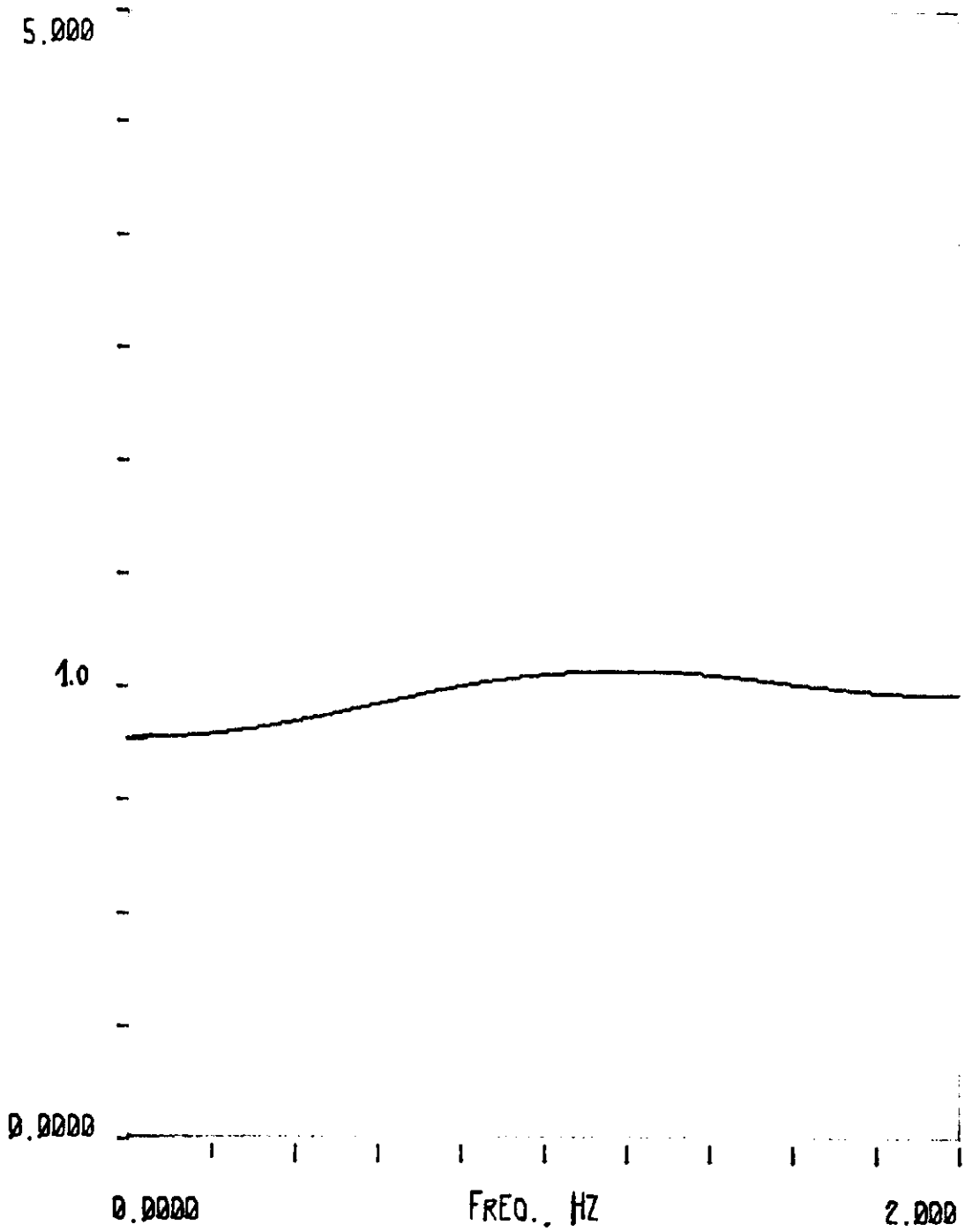

MEM SPECTRAL ESTIMATE of Gaussian White Noise

FIGURE 10

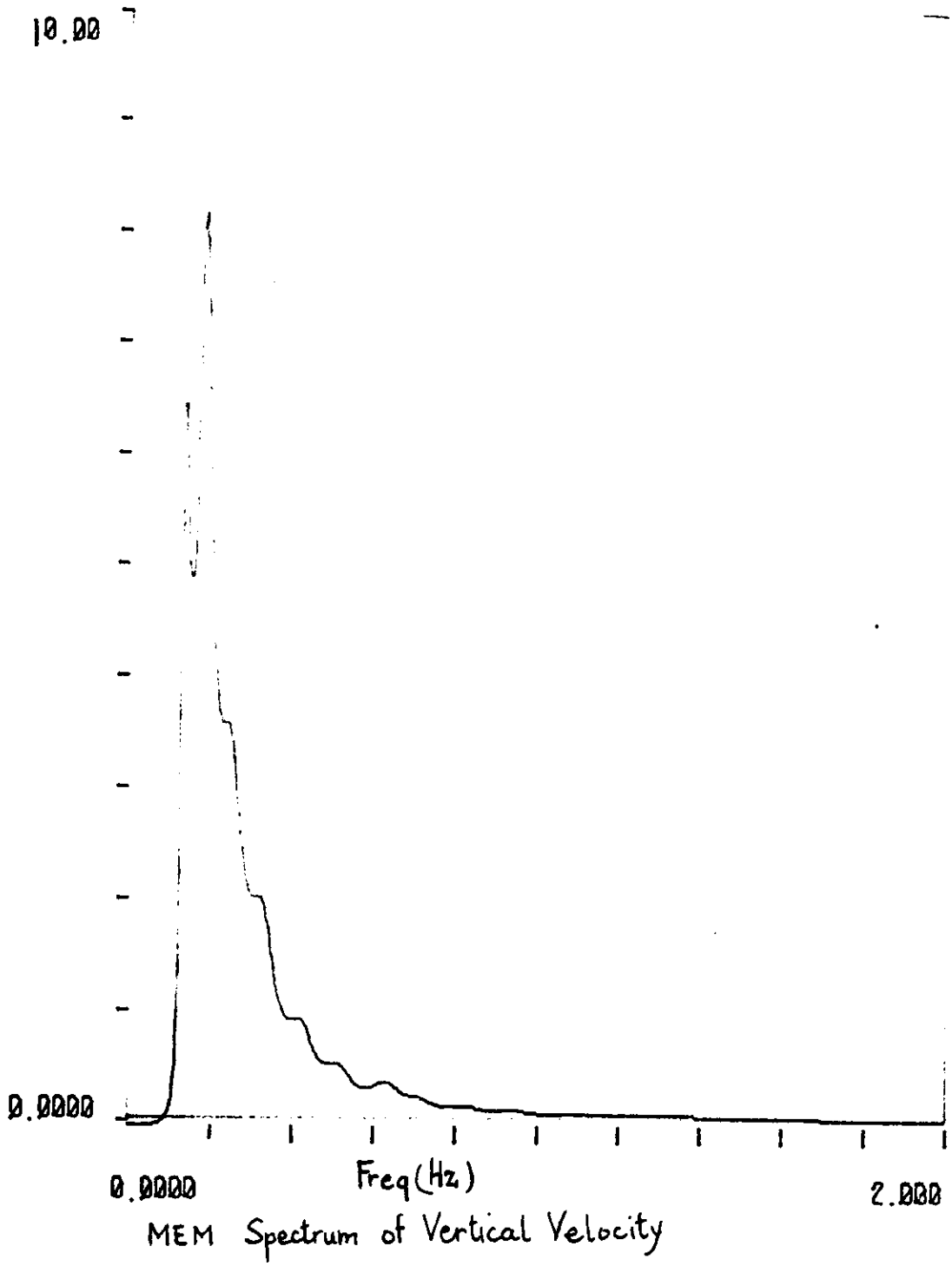
10.00
0.0000
0.0000
Freq(Hz)
2.000
MEM Spectrum of Vertical Velocity

FIGURE 11

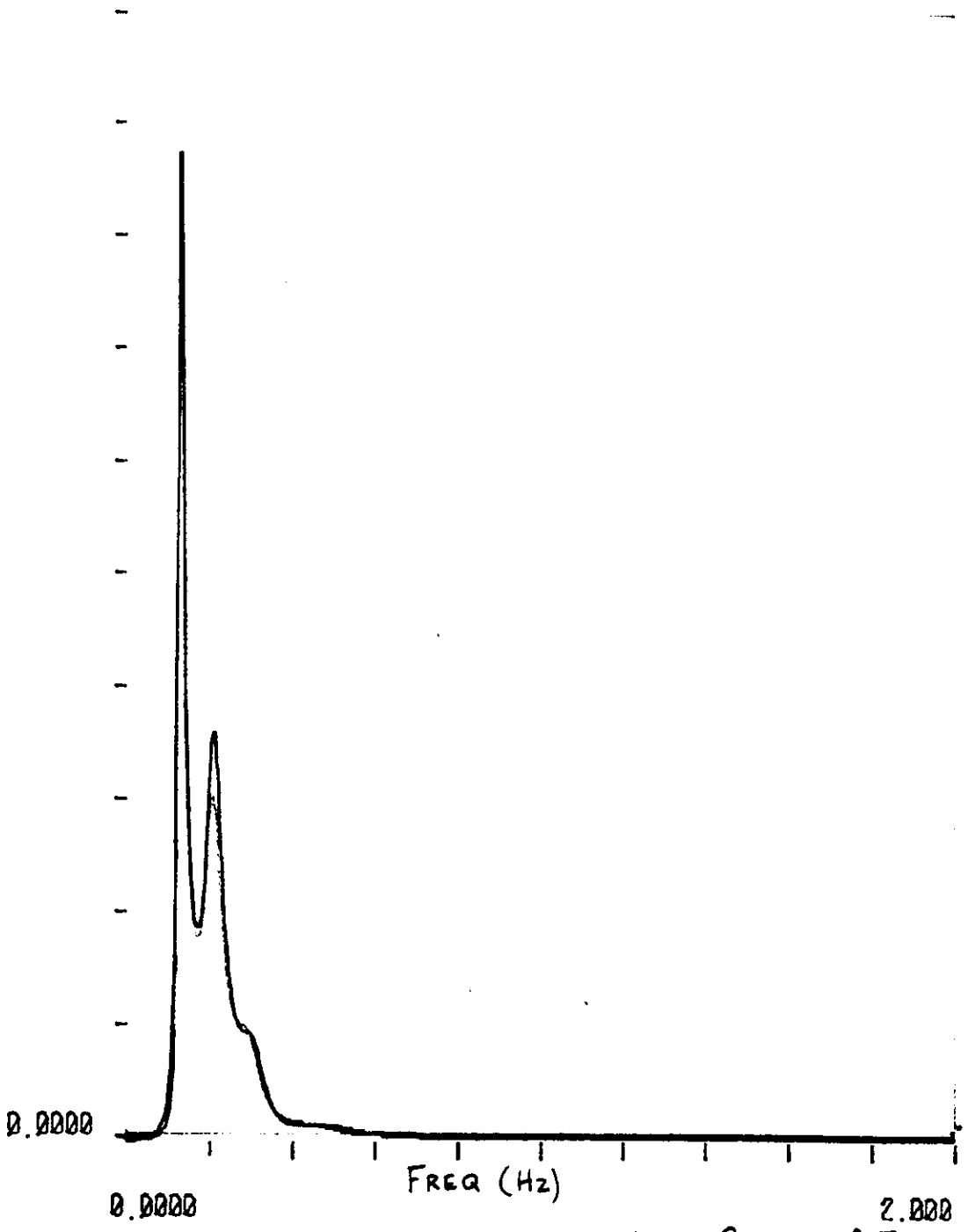

Comparison of Linear and Stretched Linear Spectra of Forces

FIGURE 12

accentuates the dynamic response of offshore structures. Figure 12 shows this point.

4.4 Horizontal Wave Propagation

The proposed impulse response is obtained by numerical Inverse Fourier Transform. The number of samples N required for a good frequency resolution even at the cutoff frequency is determined by the following equation:

$$N \geq 16\, \alpha\, R$$

where $R = F_s/2F_c$ and $\alpha = Dx/L_c$; L_c is the wave length corresponding to the cutoff F_c; F_s is the sampling frequency. This equation expresses that the maximum phase difference must be less than $\pi/4$. This $\Delta\varphi_{max}$ occurs at the cutoff frequency because the phase monotonically increases with frequency. It is a requirement that the worst phase resolution between two frequency samples be less than 1/8th of a wave length. One, first, has to choose:

1) Dx, the horizontal distance of propagation
2) F_c, the cutoff frequency
3) R, the sampling rate $R = F_s/2F_c$

Thus, the parameter becomes determined because is equal to:

$$\alpha = 2\pi\, Dx\, F_c^2/g$$

The transfer function is:

$$H = |H| \exp(-j\varphi) = \exp\left\{- \operatorname{sign}(f) \frac{Dx}{g} (2\pi f)^2 \right\}$$

The impulse response is obtained by an Inverse Fourier Transform or analytically by:

$$t>0 \quad H_{hor}(t,Dx) = \sqrt{\frac{g}{2\pi Dx}} \left[\left(S\left(2\sqrt{\alpha} - \frac{F_c t}{\sqrt{\alpha}}\right) + S\left(\frac{F_c t}{\sqrt{\alpha}}\right) \right) \sin\frac{\pi}{2\alpha}(F_c t)^2 + \left(C\left(2\sqrt{\alpha} - \frac{F_c t}{\sqrt{\alpha}}\right) + C\left(\frac{F_c t}{\sqrt{\alpha}}\right) \right) \cos\frac{\pi}{2\alpha}(F_c t)^2 \right]$$

where $\alpha = 2\pi Dx F_c^{\,2}/g$, and the Fresnel Integrals S(y) and C(y) are defined by:

$$S(y) = \int_0^y \sin\frac{\pi}{2} u^2 \, du \qquad \text{and} \qquad C(y) = \int_0^y \cos\frac{\pi}{2} u^2 \, du$$

Here, one has to remember that the impulse response is a non-causal function of time. If one selects the impulse response according to these relations, the error is negligible: the relative errors on phase and magnitude between the theoretical and the FIR impulse response is of the order of 10^{-6} at the cutoff frequency.

In Figure 13, the impulse response is shown: it has been obtained from the numerical Inverse Fourier Transform of the theoretical transfer function and not from the analytical equation of the impulse response function. From Figures 14 and 15, the results of the numerical convolution for a moderate sea state are presented. They demonstrate

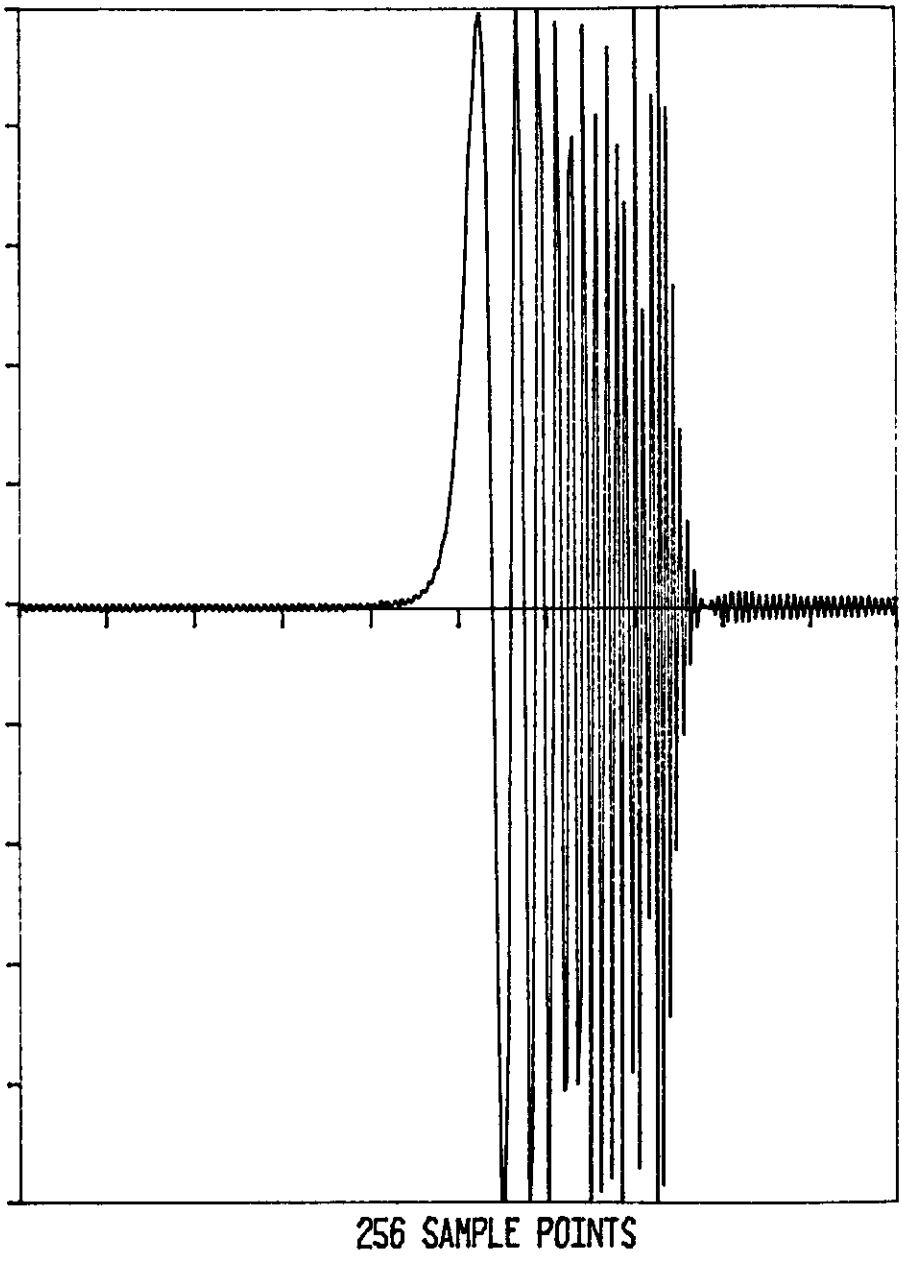

IMPULSE RESPONSE FUNCTION

FIGURE 13

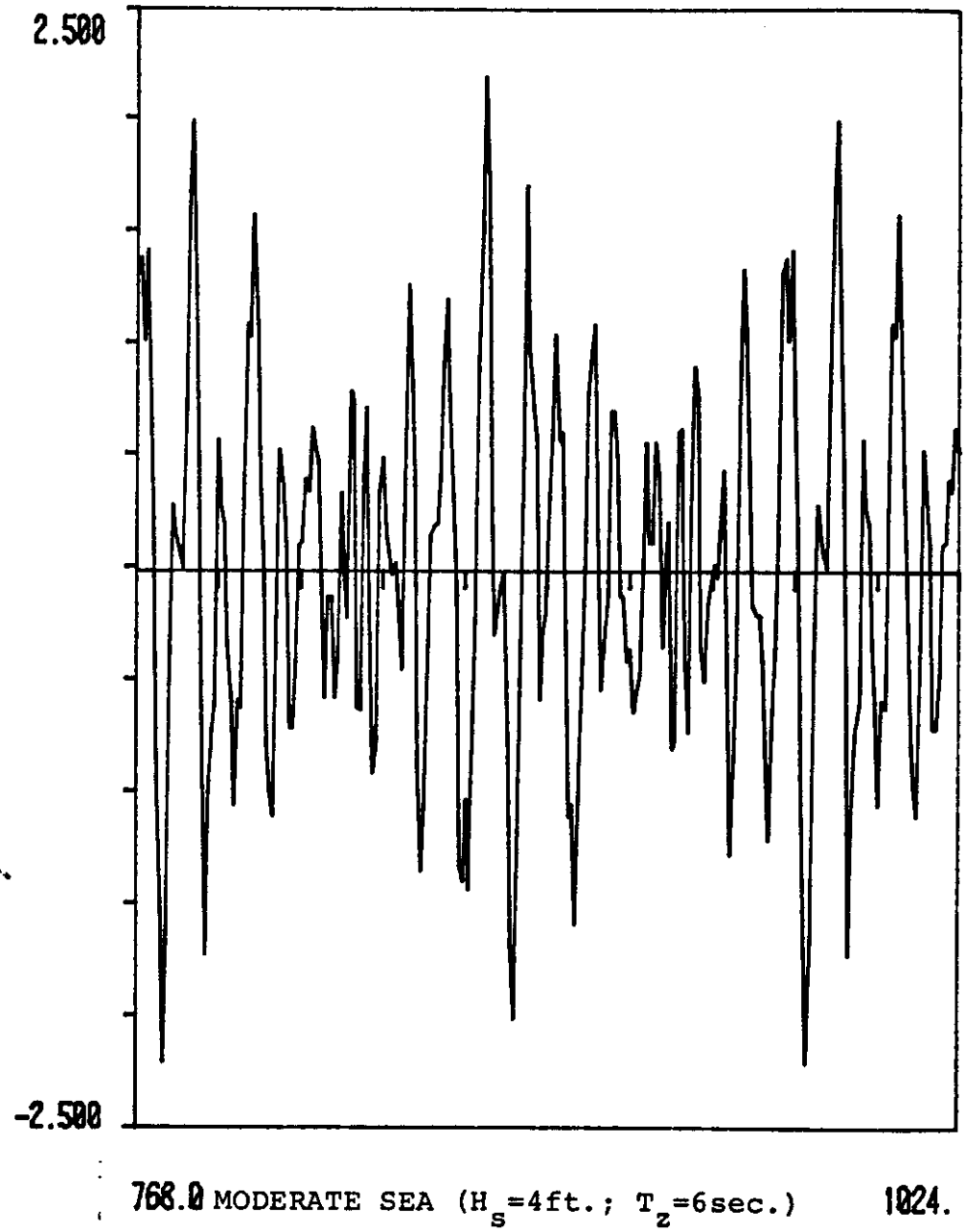

INPUT TO THE CONVOLUTION

(VERTICAL VELOCITIES AT THE ORIGIN OF COORDINATES)

FIGURE 14

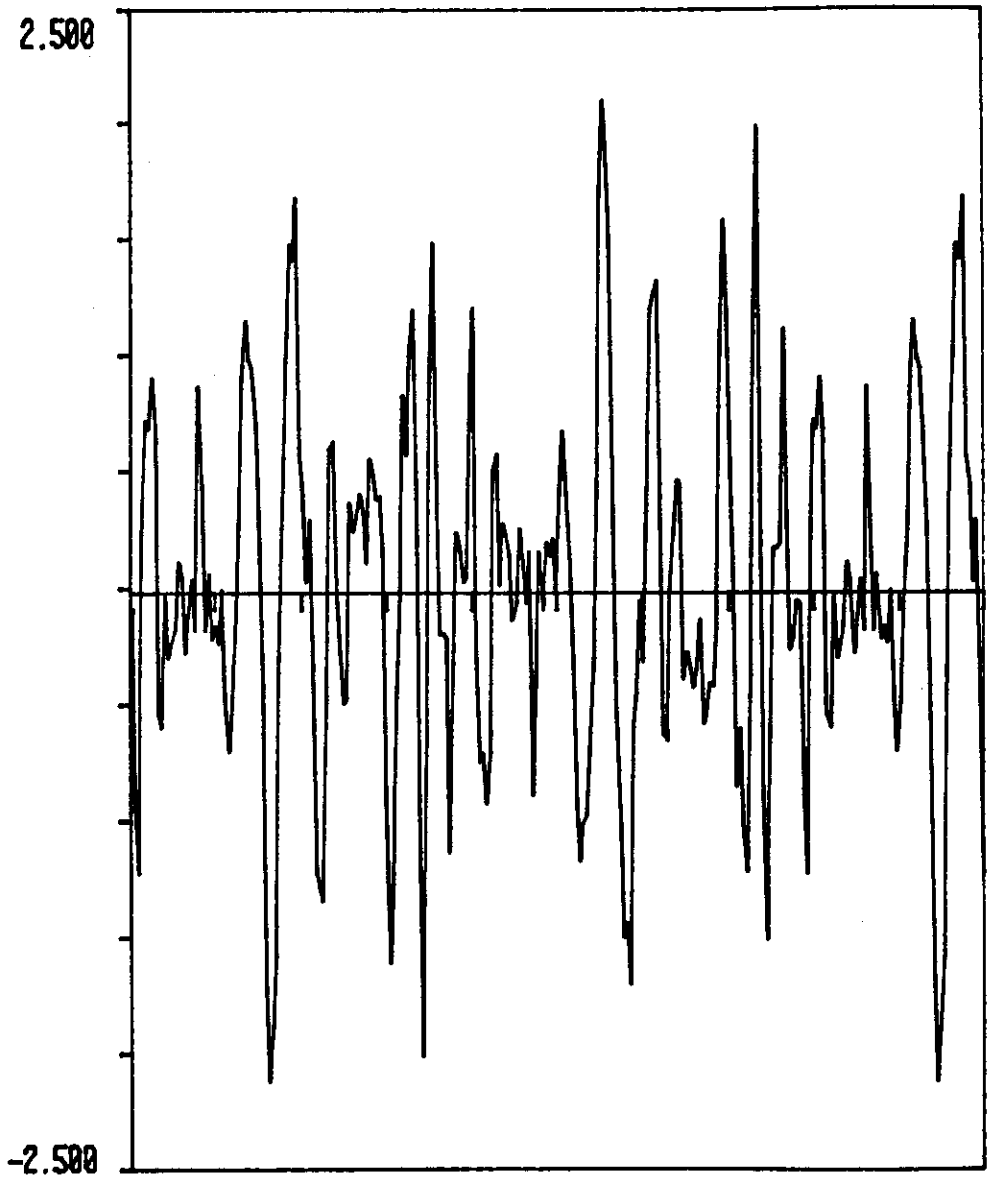

SIMULATION AT 100 METERS HORIZONTALLY

COMPARED TO THE THEORETICAL KINEMATICS

FIGURE 15

both the accuracy and the numerical efficiency of the convolution method.

4.5 Wave Spreading Problem

The wave spreading problem concerns itself with including the directionality of ocean spectra into the simulation of wave kinematics[5].

The directional velocity spectrum $S_{\dot{x}}(f, \theta_i)$ can be expressed from the Bretschneider sea amplitude spectrum $S_x(f)$ and a directional spreading function $G(\theta_i)$ assumed to be independent of the frequency f. Therefore, the spectrum for any direction θ_i keeps the same shape as the target wave velocity spectrum $S_{\dot{x}}(f)$ without the effect of directionality. Only the scale of the spectrum, not its shape varies. This is not important for the ARMA wave kinematics simulation because the scale of the spectrum is normalized at its peak frequency. Thus, the same ARMA coefficients $\{a_n\}_N$ and $\{b_m\}_M$ are used for any direction θ_i. The scale of the output of the ARMA simulation is normalized by the following factor depending on the spectral value at peak frequency: $\sqrt{S_{\dot{x}}(f, \theta_i)}$

The Bretschneider velocity spectrum is given by:

$$S_{\dot{x}}(f) = S_{\dot{x}}(F_1)\, e^{3/4\left(\frac{F_1}{f}\right)^3} \exp\left(-\frac{3}{4}\left(\frac{F_1}{f}\right)^4\right)$$

Assuming that the directional spreading function is independent of the frequency, the directional spectrum $S_{\dot{x}}(f, \theta_i)$ is given by:

$$S_{\dot{x}}(f,\theta_i) = S_{\dot{x}}(F_1,\theta_1)\, e^{3/4\left(\frac{F_1}{f}\right)^3} \exp\left(-\frac{3}{4}\left(\frac{F_1}{f}\right)^4\right)$$

The non-dimensional graph of the directional spectrum is the same for all directions:

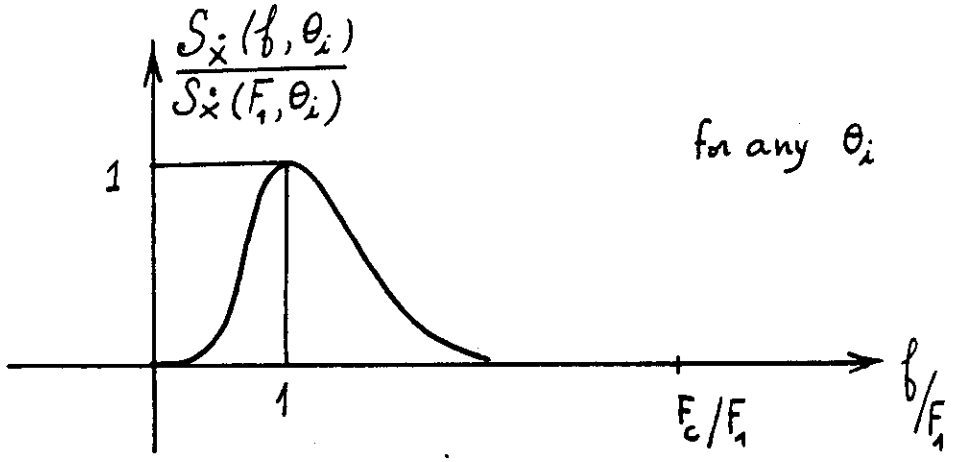

However for each direction θ_1, the wave kinematics and amplitudes are assumed to be uncorrelated with one another. This means that for each different direction, a different Gaussian white noise time history W_i must be used as input

to the ARMA wave kinematics simulations.

Suppose that N plane wave directions are considered for wave spreading and that all the Gaussian white noises W_i (i=1,...,N) are uncorrelated. Assume for example that the waves are propagating in the direction of the right half-space.

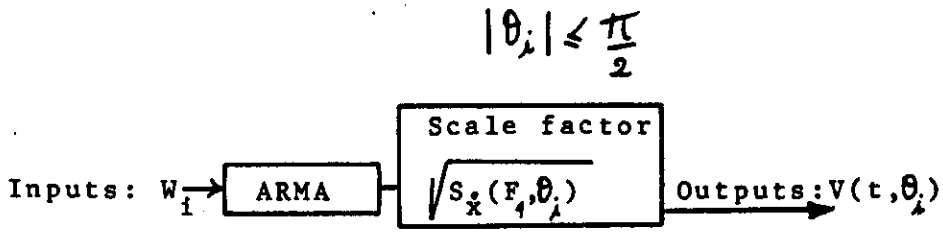

where i=1,...,N and the directions θ_i vary between $\pi/2$ and $-\pi/2$. The outputs are wave vertical velocities at the origin of coordinates for each direction θ_i.

The horizontal propagation of wave kinematics upon the mean water surface (z=o) requires careful attention. The appropriate system of coordinates is cylindrical (r,θ,z). The ARMA simulation takes place for the wave kinematics at $(r=o,\theta,z=o)$ the origin, where all different plane wave components are superposed. At another point $(r,\theta,z=0)$, each plane wave is subject to a phase shift, so the horizontal propagation transfer function depends on the frequency and the projected distance of the point considered on the direction of wave propagation k.

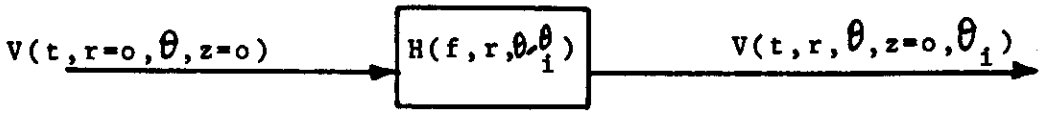

where i=1,...,N. Since this is true for each wave direction, the superposition principle implies that the total velocity at the point $(r,\theta,z=o)$ is the sum of all the uncorrelated directional components because the Gaussian white noise used as inputs for each direction are themselves uncorrelated.

$$V(t,r,\theta,z=o)=\sum_{\theta_i} V(t,r,\theta,z=o,\theta_i)$$

The input/output system for the horizontal wave spreading is as follows for each direction θ_i:

1) Inputs: $V(t,r=o,\theta,z=o)$, the vertical velocity at the origin for a random wave propagating in the direction θ_i.

2) System: $H(f,r,\theta-\theta_i)$, the transfer function yielding any wave amplitude or kinematics at a point located at $(r,\theta,z=o)$ assuming deepwater linear waves. This function is the same as the one used in the unidirectional case (Chapter 3):

$$H(f,r,\theta,\theta_i)= \exp(-j(2\pi f)^2 \text{sign}(f) r\cos(\theta-\theta_i)/g)$$

where $r\cos(\theta-\theta_i)$ is the projected distance of the point (r,θ,z) on the phase wave direction θ_i. There is no problem in implementing the convolution-sum in the time-domain. One has still to choose the three parameters α,R, and N that obey the equation $N \geq 16\,\alpha R$.

3) Outputs: $V(t,r=o,\theta,z=o,\theta_i)$, the vertical velocity at the point $(r,\theta,z=o)$ for a random wave propagating in the θ_j direction. Note that $V(t,r,\theta,z=o)$, the total wave particle vertical velocity at the point $(r,\theta,z=o)$ takes all the directions into consideration.

$$V(t,r,\theta,z=o) = \sum_{\theta_i} V(t,r,\theta,z=o,\theta_i)$$

One must be careful in calculating the components of the horizontal wave kinematics. These are obtained at each grid-point by performing a Hilbert Transform of the vertical velocities. This horizontal velocity $U(t,r,\theta,z=o)$ is projected like a vector on the orthogonal coordinate system (X,Y,Z).

$$U(t,r,\theta) = V(t,r,\theta) * h_{hill}(t)$$

and

$$\begin{cases} U_x = U(t,r,\theta)\cos\theta \\ U_y = U(t,r,\theta)\sin\theta \end{cases}$$

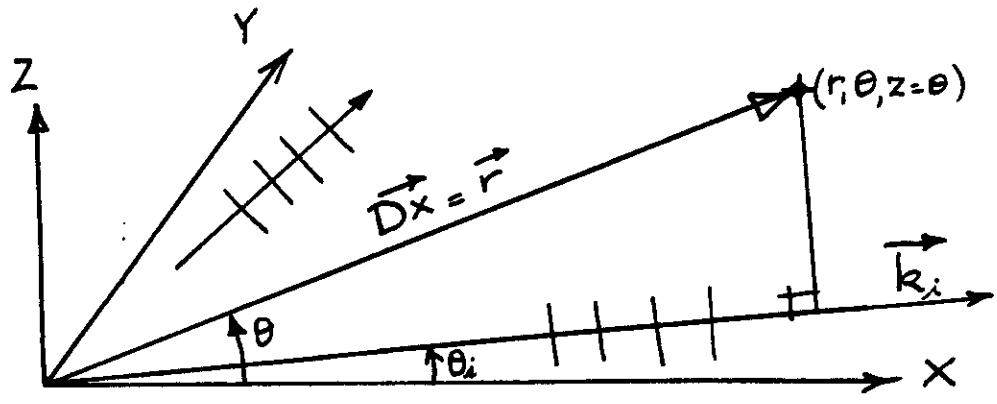

For the vertical propagation, the same techniques previously described can be used. The directional wave kinematics at m.w.l. are used as input to the vertical propagation transfer function instead of the unidirectional wave kinematics. One can, therefore, use the stretched linear approximation for finite amplitudes that affects the impulse response g(t,Dz+η) and compound simultaneously both the effects of wave spreading for horizontal propagation and the effects of finite amplitudes for vertical propagation. This separates and rationalizes the difficulties in simulating time histories of wave kinematics throughout the water column. Such a method remains numerically more efficient than "summing sines" and accuracy is adequately provided.

4.6 Hilbert Transforms and Differentiations

Hilbert transforms are widely used in digital signal processing. It is defined by two sets of equations:

$$H_{hilb}(f) = -j \, sign(f)$$

where $j^2=-1$ and sign(f) is the function defining the sign (positive or negative) of the frequency f.

$$H_{hilb}(t) = \begin{cases} 2\sin(t\pi/2)/t\pi & t\neq 0 \\ 0 & t=0 \end{cases}$$

A finite impulse response (FIR) digital filter design is obtained by the following standard technique: windowing of the frequency transfer function defining $H_{hilb}(f)$, frequency sampling of $H_{hilb}(f)$, and an equiripple approximation of the ideal characteritics of the filter (L.R.Rabiner and R.W.Schafer). For the results presented in Figures 16 to 18, the order of the Hilbert transform corresponding to both sea states is found to be 29.

The differentiation uses a central difference scheme:

$$D(z) = z - z^{-1}/2Dt$$

Here, acuracy increases with higher sampling frequencies. Therefore, the ratio $R= F_s/2F_c$ is chosen to be equal to or higher. Figures 19 to 21 present the results of differentiation.

4.7 Intermediate Depths and Shallow Waters

The difference between deep water and shallow water is defined in terms of the ratio of depth D to the cutoff wave length L_c corresponding to the cutoff frequency F_c.

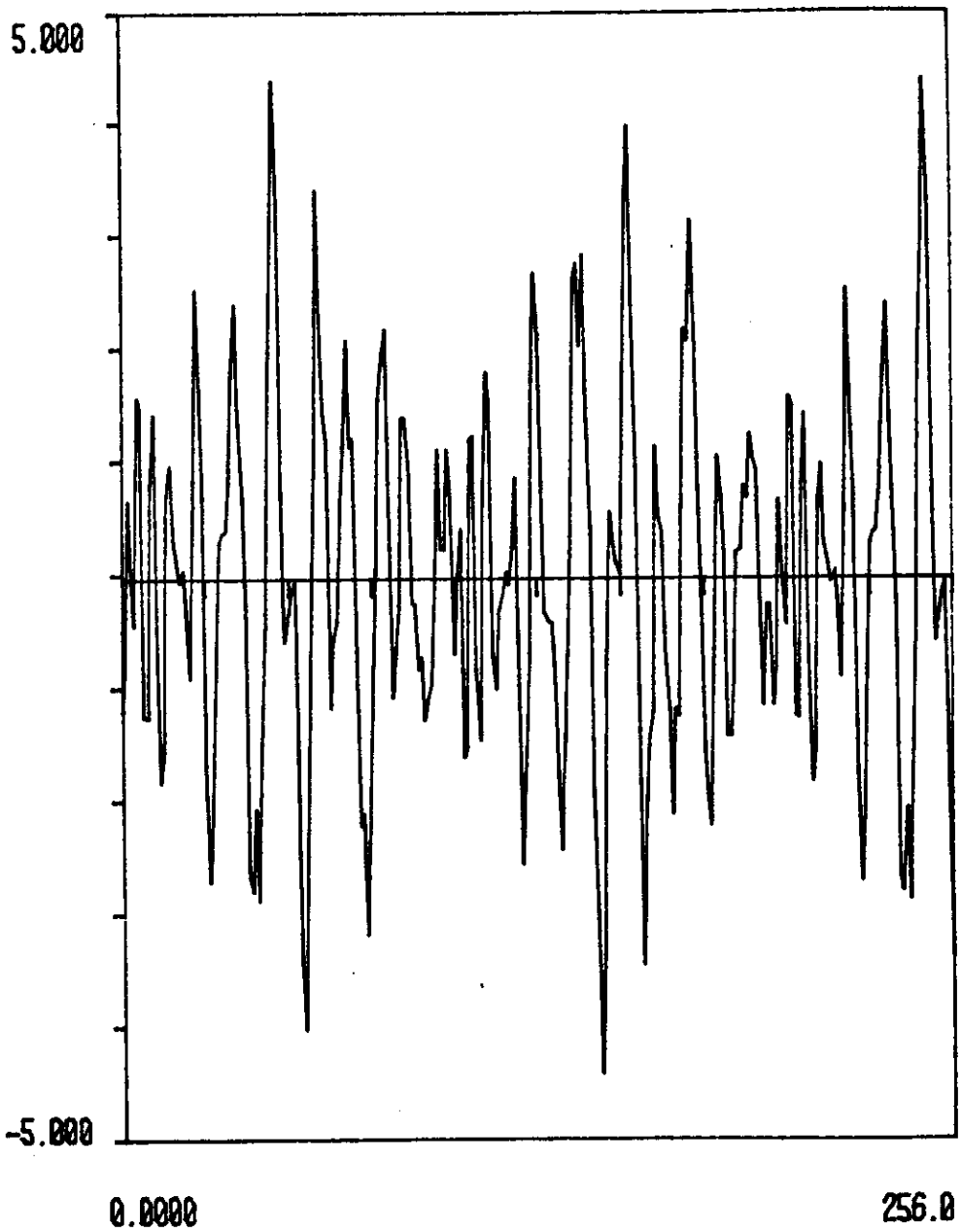

VERTICAL VELOCITY USED AS INPUT TO THE HILBERT FILTER

FIGURE 16

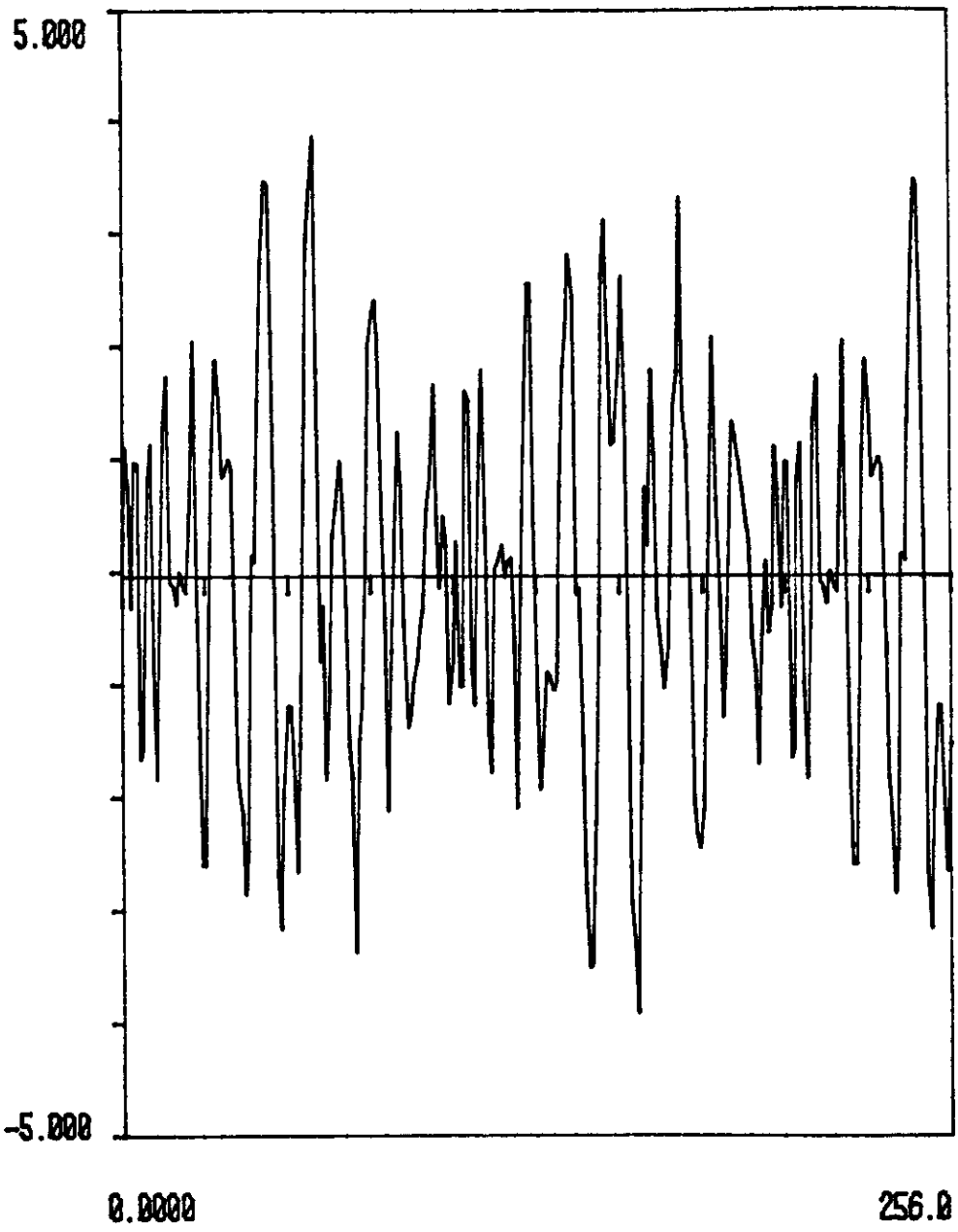

HORIZONTAL VELOCITY CALCULATED BY
HILBERT FILTER FROM VERTICAL VELOCITY AS INPUT

FIGURE 17

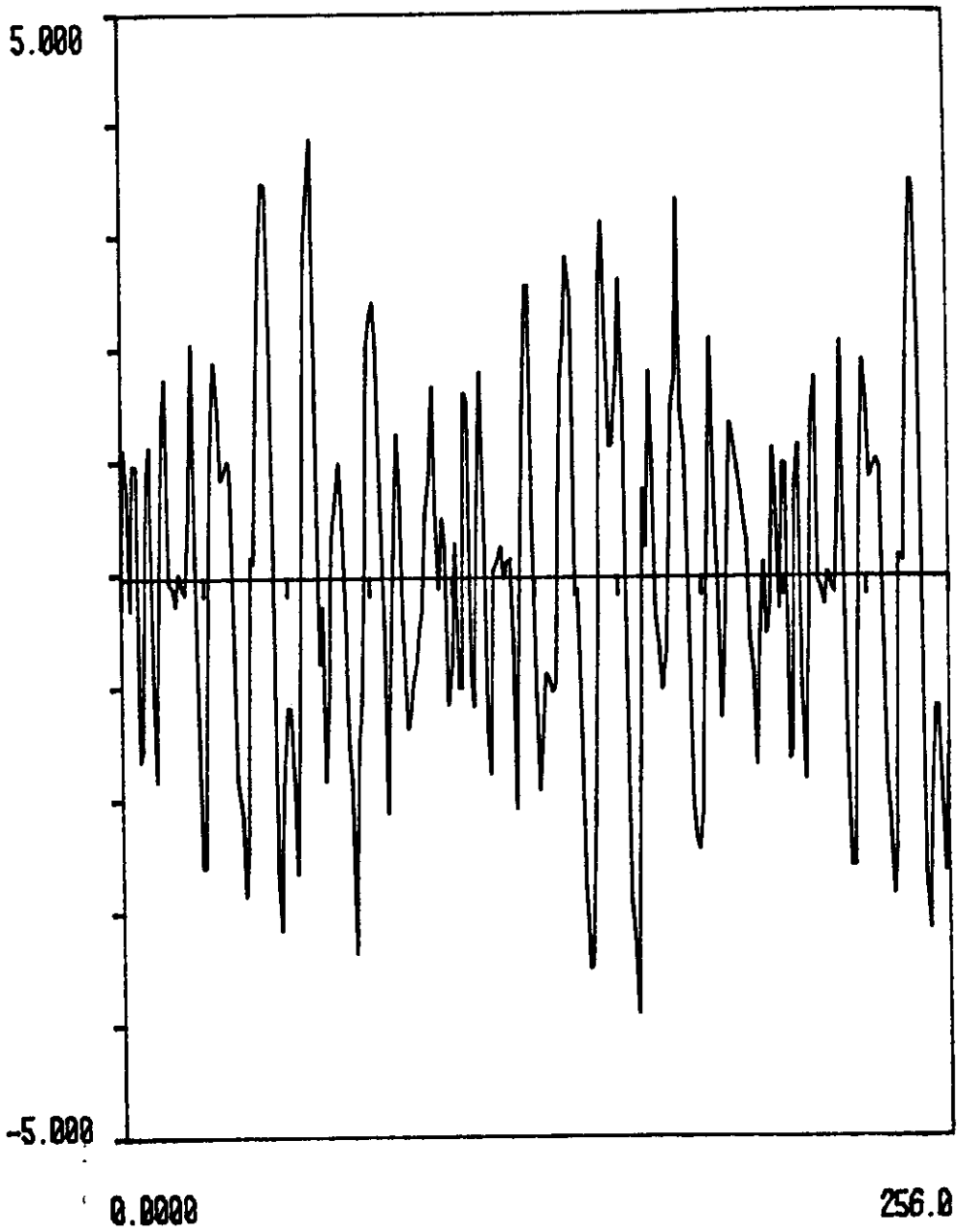

THEORETICAL HORIZONTAL VELOCITY (90 DEGREE SHIFT)

FIGURE 18

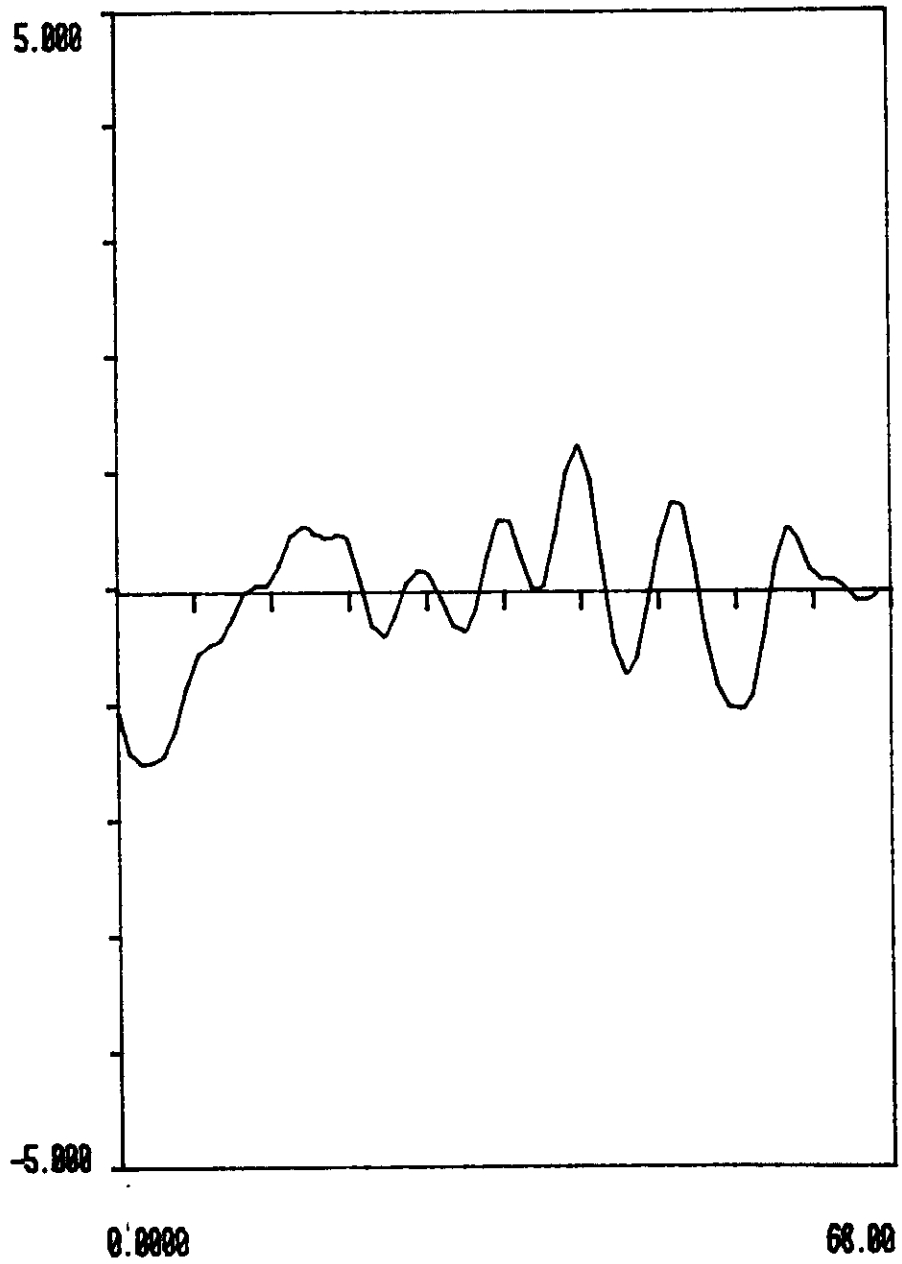

VELOCITY INPUT TO THE DIFFERENTIATOR

FIGURE 19

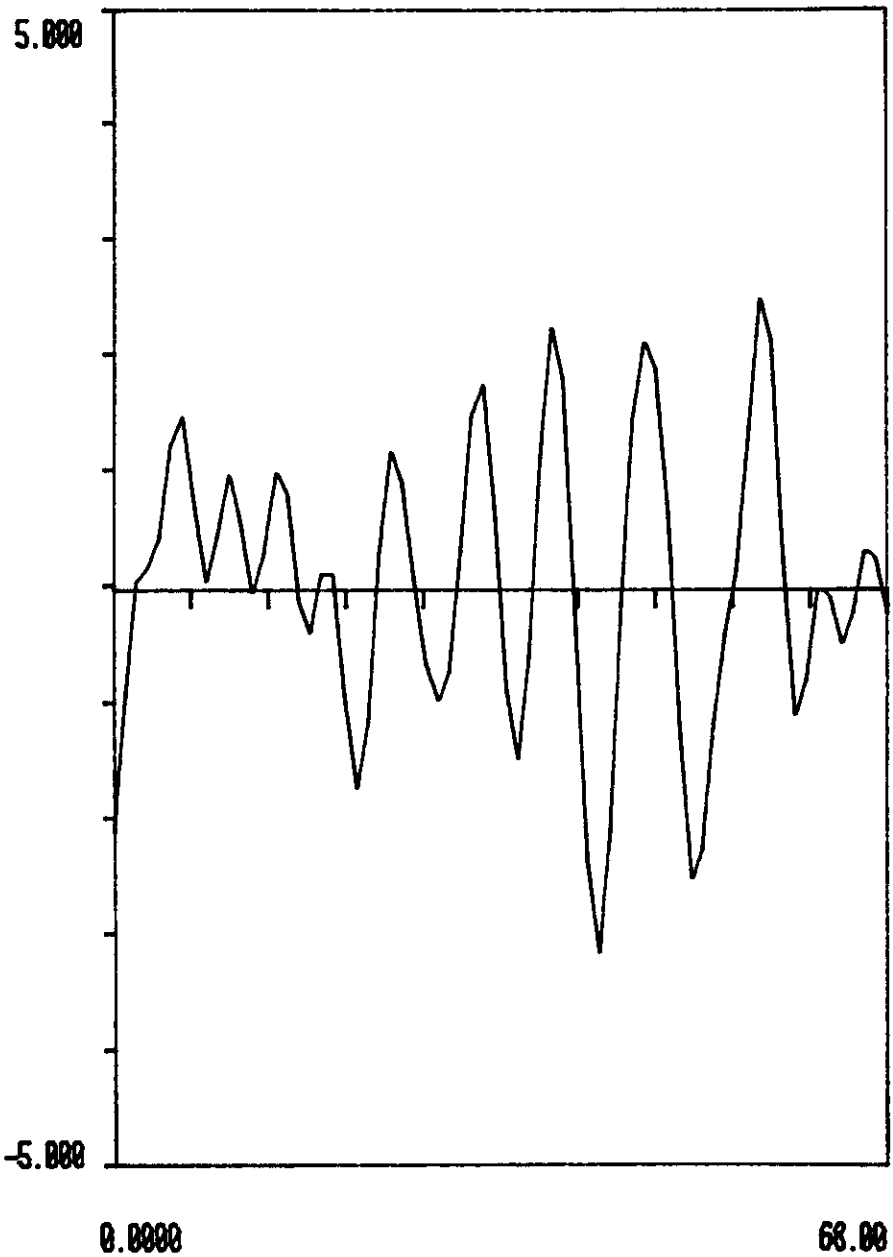

ACCELERATION OBTAINED FROM VELOCITY
USING A CENTRAL DIFFERENCE DIFFERENTIATOR

FIGURE 20

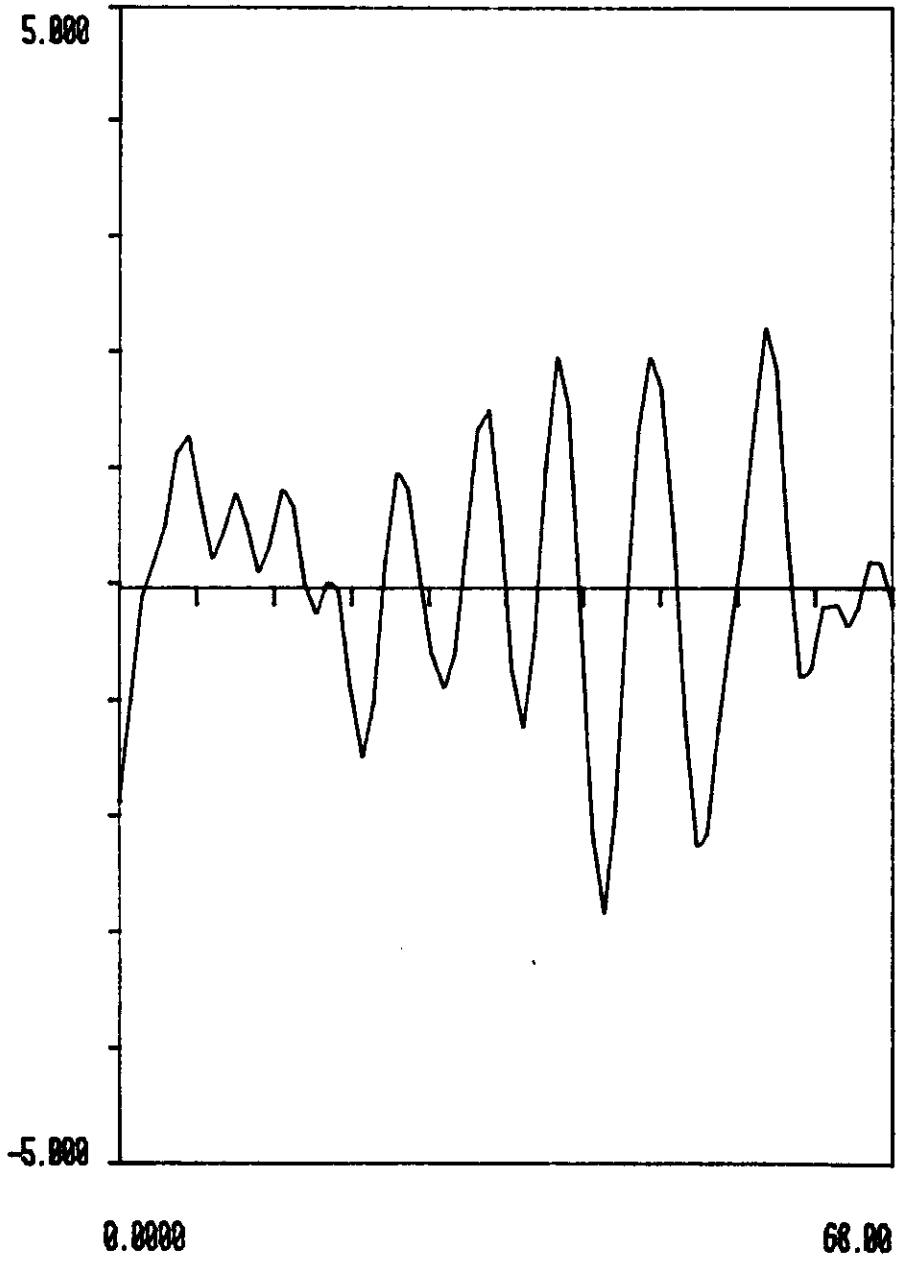

THEORETICAL ACCELERATION (68 SAMPLES, DT=.25)

FIGURE 21

Shallow water: $D/L_c < 1/20$

Intermediate depths: $1/20\ D/L_c < 1/2$

Deep waters: $D/L_c > 1/2$

For shallow waters, there is no dispersion and therefore, the waves propagate horizontally without any phase change. The solution for horizontal wave propagation is trivial and the vertical decay is linear and independent of the frequency. Thus both the vertical and horizontal propagation problems are easily solved.

For intermediate depths, the dispersion relation does not have a parabolic shape[22]. The non-dimensional graph of this dispersion curve is:

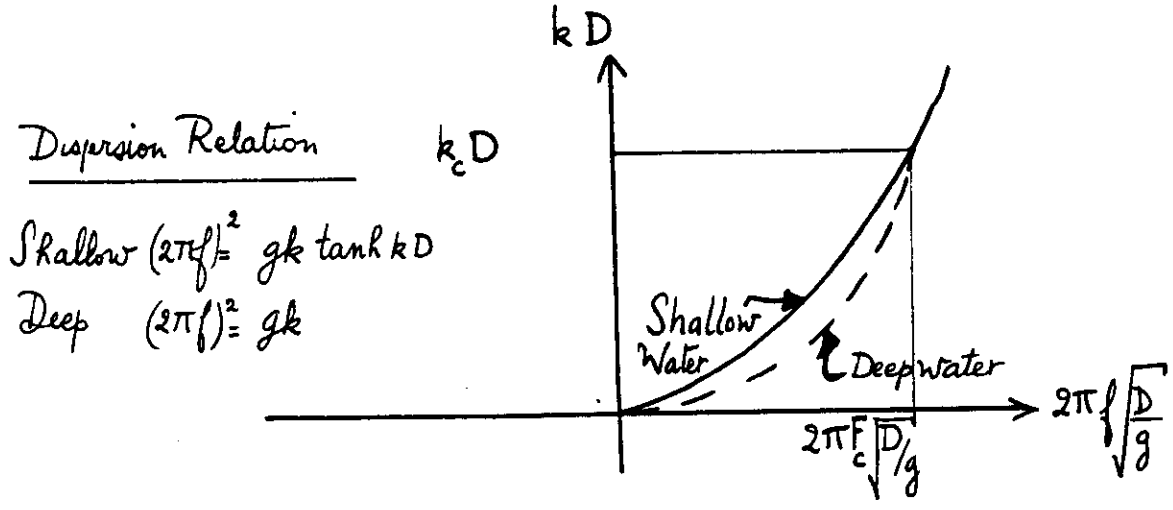

where F_c is the cutoff frequency; k_c and L_c are the cutoff wave number and the cutoff wave length; D is the water depth; g is the gravity field. By substituting the intermediate water limit $D/L_c < 1/2$ into the dispersion

relation, one obtains the following values for F_c and k_c:

$$F_c = \sqrt{g \tanh(\pi)/4\pi D^2} \quad \text{and} \quad k_c = \pi/D$$

The ARMA simulation of wave kinematics in intermediate depth water is divided into four problems.

1) ARMA simulation of horizontal wave kinematics.

The target velocity spectrum is deduced from the wave amplitude spectrum: $S_u(f) = gk\, S_x(f)$. A time history of horizontal wave kinematics is generated as shown.

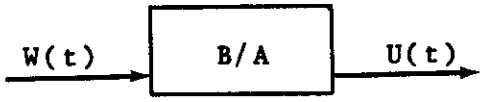

where W is Gaussian white noise and U the horizontal velocity and U(t) is given by the following expression.

$$U(t) = -\sum_{n=1}^{N} a_n U(t-nDt) + \sum_{m=0}^{M} b_m W(t-mDt)$$

where the a's and b's are the ARMA parameters and Dt is the sampling time.

2) At the mean-water-line, the following filter describes the transfer function between the horizontal and vertical wave kinematics.

$$H(f) = |H(f)|\, e^{-j\varphi} = \begin{cases} \text{phase} & \frac{\pi}{2}\, \text{sign}(f) \\ \text{magnitude} & \tanh(|k|D) \end{cases}$$

It has an even magnitude and an odd phase, the corresponding impulse response is thus real. This filter is designed by using the state-of-the-art in Finite Impulse Response (FIR) filter design. In the case of finite-duration approximations, the standard technique of windowing, frequency sampling, and equiripple approximation can be applied in approximating the ideal characteristics of this equation.

3) The horizontal propagation problem is solved by designing a FIR digital filter with the following ideal characteristics:

$$H(f,Dx) = |H|\, e^{-j\varphi} = \begin{cases} \text{phase} & = kDx\, W(f) \\ \text{magnitude} & = W(f) \end{cases}$$

The frequency resolution and accuracy depend on the maximum acceptable phase difference $\Delta\varphi_{max}$ at the cutoff frequency.

$$\Delta\varphi_{max} = \Delta k\, Dx \Big/_{@f=F_c} = \frac{2\pi\Delta f}{C_g(k_c)} Dx = \frac{2\pi}{C_g(k_c)} Dx F_c \frac{R}{N} \leq \frac{\pi}{4}$$

The group velocity C_g is given by the following equation:

$$C_{g(k)} = \frac{1}{2}\sqrt{\frac{g}{k}\tanh kD}\left(1 + \frac{2kD}{\sinh(2kD)}\right)$$

By its definition, the group velocity C_g is used to change wave number characteristics to wave frequency characteristics because $d\Omega = C_g dk$ and this phase resolution $\Delta\varphi_{max}$ is set to be less than $\pi/4$ as the following graph illustrates:

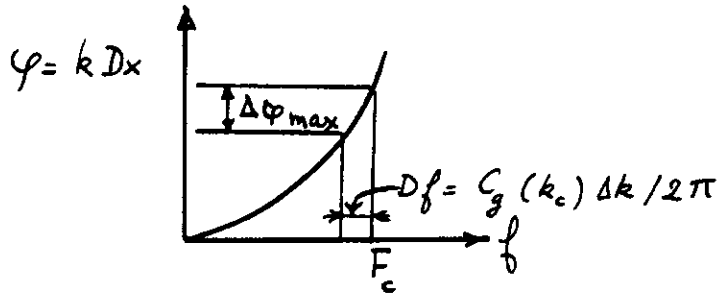

As in the deepwater case, the three following parameters are used: N (the number of samples for the impulse response), R (the ratio of the sampling frequency F_s to the double of the cutoff frequency F_c, $R = F_s/2F_c$, and $\alpha = F_c Dx/2C_g$ (where this wave group velocity C_g is calculated at the cutoff frequency). With all these, the condition reduces to:

$$N \geq 16\,\alpha\,R$$

4) The vertical propagation problem is solved by designing the two following filters[22]:

a) the transfer function between horizontal wave velocities on the m.w.l. and some grid-point at a vertical distance of Dz.

$$G_u(f,Dz) = \frac{\cosh k(D-Dz)}{\cosh kD}$$

where f, the frequency, is given by the dispersion relation.

b) for vertical wave velocities the transfer function is instead

$$G_v(f,Dz) = \frac{\sinh k(D-Dz)}{\sinh kD}$$

These filters all have a smooth shape that look like a bell-shape when drawn as a function of frequency. The standard techniques of windowing, frequency sampling and FIR filter design can be used to approximate these ideal characteristics[16].

4.8 Statistics of ARMA Wave Forces - Comparison to Real Data and to the Crandall and Moe Model

The statistics of the wave forces acting on a 1m diameter vertical cylinder of unit length at the mean waterline are presented as histograms. The first histogram is computed from the time history of wave forces using 100 minutes of ARMA simulated waves representing a sea state with T_z= 9.94 sec and H_s = 7m. The second histogram presents the extremes of Morison-type wave loading, from the ARMA wave force data at the m.w.l. There are about 600 peaks in the total record. These peaks correspond to local maxima of the wave force time history. Between two zero-upcrossings, there may be more than one peak because the wave force is not necessarily a narrow band process.

Although not narrow band, the wave kinematics are Gaussian because the input of the linear ARMA model is Gaussian white noise. The Morison-type force should deviate from the Gaussian probability distribution for large force values because these are caused by the drag force which is nonlinear. Figure 22 is the histogram of Morison wave loading per unit length. It shows very well the non-Gaussian behavior for wave forces several standard deviations in size. These results are in good qualitative

agreement with wave forces measured on a vertical pile in towing tank experiments carried out at M.I.T. by B. Dunwoody, for a 40 knot sea state corresponding to T_z=9.94 sec, H_s=7 m (U=37.3 knots).

For the extreme wave loads, very long time histories are needed in order to have a histogram of peak forces with good reliability. Instead of 600 peaks, 10,000 peaks would be desirable. Such a study was not within the scope of this thesis. Nonetheless with the 600 peaks, a histogram is computed and Figure 23 shows that in the range of $1x10^3$kgf/meter to $4x10^3$kgf/meter where most of our data is located, an exponential trend can be observed for the probability distribution of extreme wave loadings. On a logarithmic ordinate axis, the exponential probability distribution is a straight line. Crandall and Moe have studied the extremes of Morison-type wave loading on a single pile (J. Mech. Design, 100, 100-104, 1978) and model the statistics of peak wave forces for stationary Gaussian random waves. The probability distribution for large forces is asymptotically given by an exponential formula.

$$p(\hat{f}) = \frac{1}{2k_D\sigma_u^2} \exp\left\{\frac{-(\hat{f}-f_0/2)}{2k_D\sigma_u^2}\right\} ; \quad f>f_0$$

where f is the Morison-type force per unit length

$$f = k_D\, u|u| + k_D\, A_h \;;\; k_D = \rho\, C_D\, D/2 \text{ and } k_M = \rho\, C_M \frac{\pi D^2}{4}$$

$$f_o = \frac{\sigma_a^2 \; k_M^2}{2\sigma_u^2 \; k_D}$$

and where the associated variances σ_a^2 and σ_u^2 are defined as follows.

The mean square velocity σ_u^2 at the MWL is given by:

$$\sigma_u^2 = (2\pi)^2 M_2 = (2\pi F_o \frac{H_s}{4})^2 \sqrt{\frac{5\pi}{4}}\, \text{erfc}\left(\sqrt{\frac{5}{4}} \frac{F_o^2}{F_c^2}\right)$$

$$\sigma_u^2 = \int_o^{F_c} S_{\dot{x}}(\omega)\, d\omega = 1.24 \; m^2/s^2$$

and the root mean square velocity $\sigma_u = 1.11$ m/s.

As to σ_a^2, the mean square acceleration at the m.w.l.

$$\sigma_a^2 = (2\pi)^4 M_4 = (2\pi F_o)^4 \frac{H_s^2}{16} \frac{5}{4} E_1\left(\frac{5}{4} \frac{F_o^4}{F_c^4}\right)$$

$$\sigma_a^2 = \int_o^{F_c} S_{\ddot{x}}\, d\omega = 1.64 \; m^2/sec^4$$

σ_a = root mean square acceleration = 1.28 m/sec^2

The exponential probability distribution starts from f_o

$$\hat{f} > f_o = 1.09\; 10^3 \text{ kgf/m}$$

The slope of the straight line (exponential decay) is given

by

$$\frac{1}{2k_D \sigma_u^2} = 1.13$$

The comparison of Crandall and Moe's probability density function with the ARMA m.w.l. peak force simulation yields a very good fit for the ARMA simulation (Figure 23).

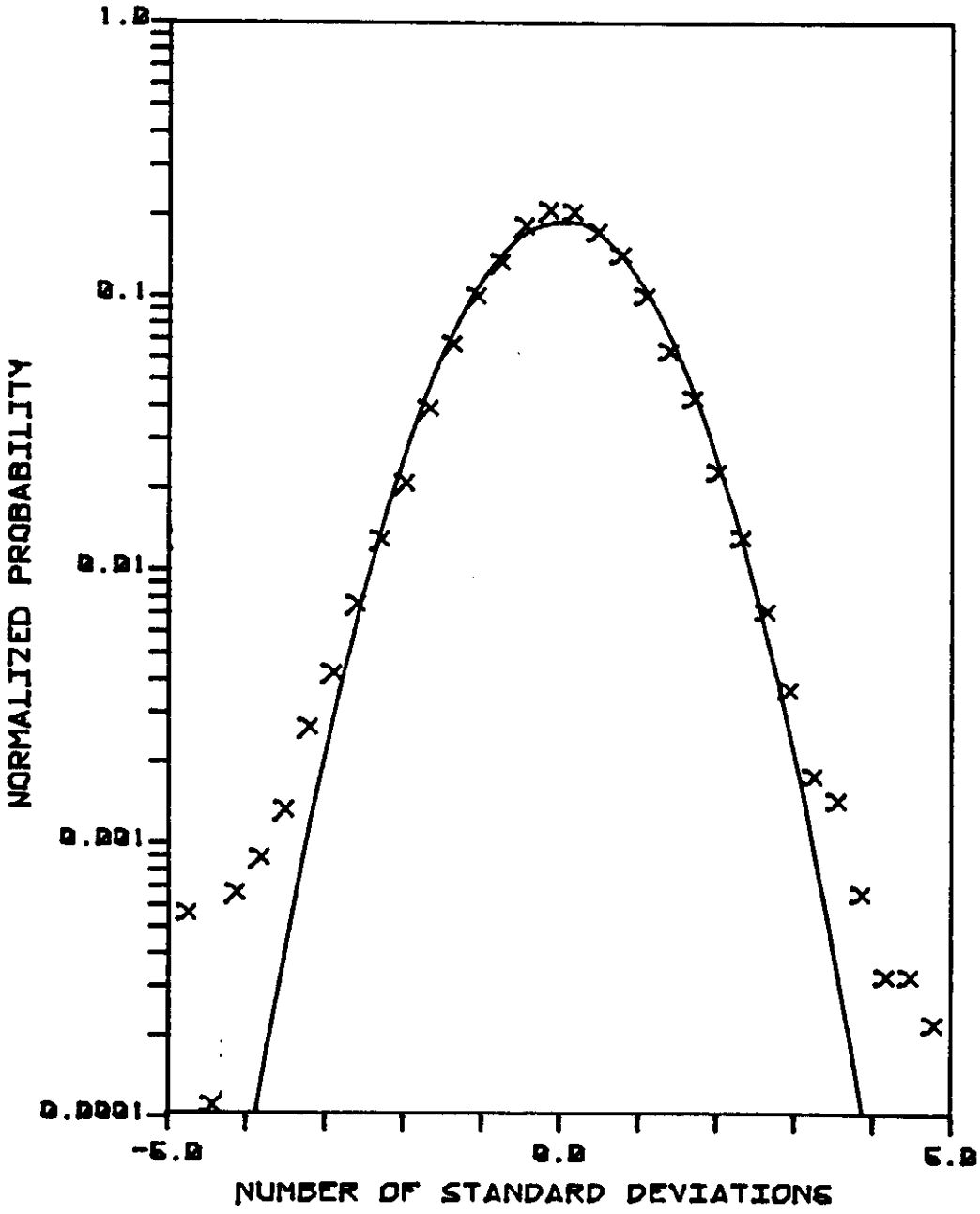

WAVE FORCES HISTOGRAM
AT MWL Figure 22

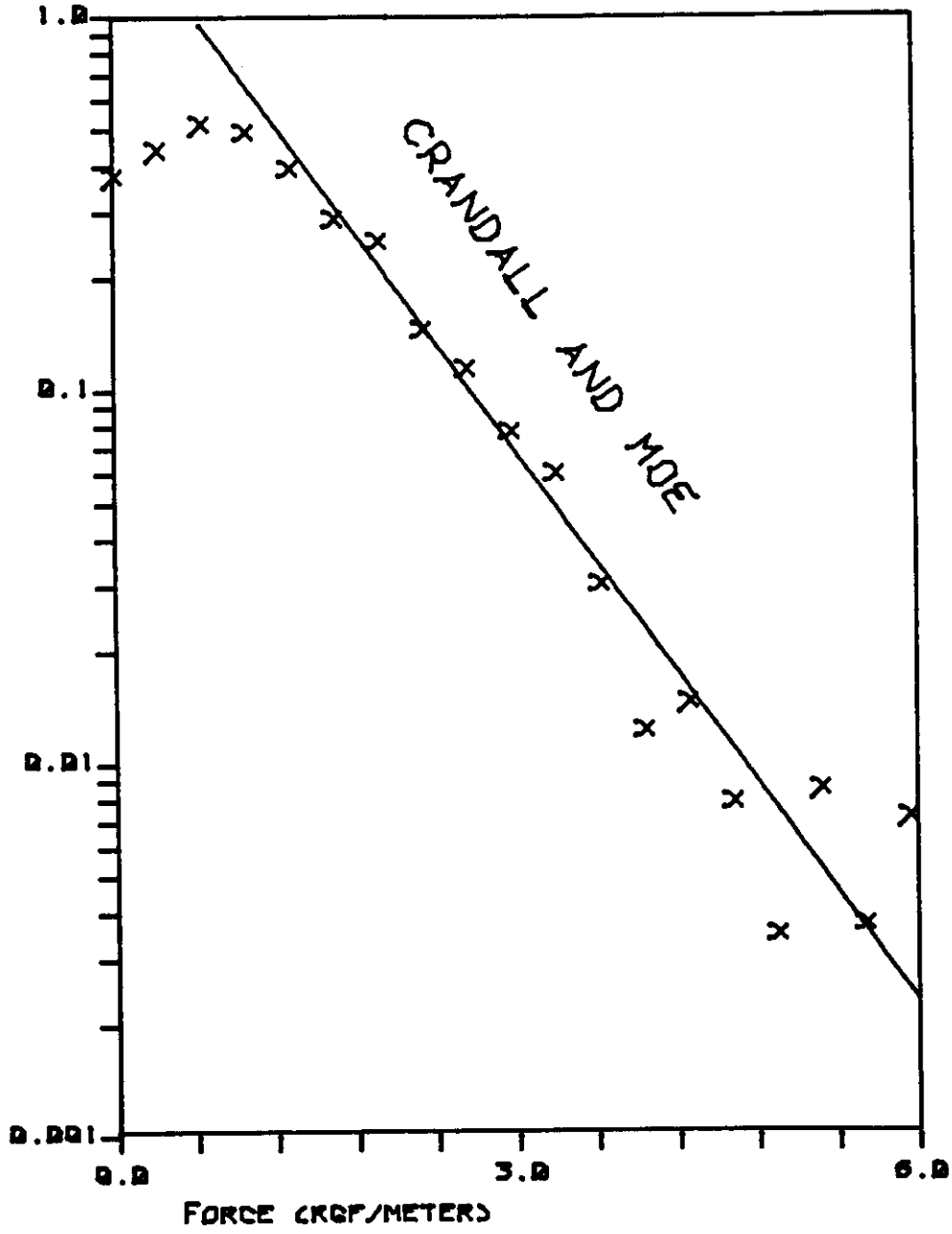

HISTOGRAM OF PEAK WAVE FORCES
FOR LINEAR WAVE AT MWL Figure 23

CHAPTER 5

CONCLUSIONS

The following conclusions may be made based on the results presented in Chapter 4:

1) A procedure is presented and demonstrated for the numerical simulation of wave kinematics at any place on an offshore structure (assuming negligible diffraction of the waves) and at any time. For each desired wave spectrum, a small number of ARMA coefficents are required to simulate random wave particle kinematics from Gaussian white noise as input. The method for computing these coefficients is described. Instead of a sum of sinusoids, the wave particle velocities are used in a simple linear prediction algorithm to generate time histories with the desired spectral properties. Once wave kinematics are simulated at any grid-point and at any time, it is a simple step then to compute wave forces in deep or shallow waters.

2) The wave kinematics are propagated horizontally and vertically by convolving the ARMA time history at the origin of coordinates. The impulse responses that are used, are derived from linear wave theory. Their analytic equations and the way the convolution-sums are implemented provide an accurate and efficient method for calculating wave

kinematics throughout the water column to each node of a finite element model of an offshore structure.

3) For the purpose of wave force calculations, the non-linear finite amplitude effects are incorporated into the vertical propagation model. Actually, the stretched linear wave kinematics, an approximation for finite amplitude effects, is considered and a simple time-dependent impulse response is used to compute stretched linear wave kinematics by a convolution over the mean water line wave kinematics.

4) For the wave spreading problem, the spectral directionality is incorporated into the ARMA simulation of wave kinematics and the horizontal propagation impulse response takes into consideration precisely this wave directionality effect. At any point on the mean water surface, the wave kinematics from different directions are superposed because uncorrelated Gaussian white noise sources are used to simulate the ARMA wave kinematics for each direction.

5) In the case of shallow waters or intermediate depths, the same methodology as in the case of deepwater water is used: only the dispersion relation is different. The correct procedure is described, and an example calculation demonstrates the deepwater procedure.

6) The strong points of this method are its accuracy,

its numerical efficiency, the inclusion of wave finite amplitude effects and the means for accounting for the effects of wave spreading. In contrast to the discrete spikes which result when one sums sinusoids, the ARMA spectrum is smooth and continuous, properly modelling the non-linearities which depend on the difference frequencies as is the case of slowly varying drift forces. When compared to the state-of-the-art, this method is more efficient in terms of calculations, memory storage, and input/output memory transfer because it is based on a series of recursive algorithms. Moreover, by dividing the wave propagation problem into a horizontal one and a vertical one, the wave spreading and the directionality problem is easily solved. The finite amplitude non-linearities are modelled by implementing the stretched linear approximation. For both deepwater and shallow waters, this methodology yields a numerically efficient random wave force time history simulation, modelling wave dispersion, spreading, and finite amplitudes.

The ARMA spectral analysis method can be used for other applications whenever a spectrum exists for the description of the phenomenon. Earthquakes are recorded in terms of an acceleration spectrum and winds have been modelled by a velocity spectrum. In both cases, a numerical time simulation of a given spectrum can be generated by using an

ARMA model.

The sum of sinusoids or the ARMA method have a problem in common: neither method can guarantee that simulated time series are physically realizable. This is a topic for future research and analysis: to prevent freak synthesized events that could not happen in nature.

Another topic for future research is the effort to optimize the ARMA method and the numerical time domain convolution sums in order to render the numerical method even more efficient. Finally, although the total procedure for random wave force calculation was used in the case of a single pile, it can now be extended to simulate the dynamic response of a large deepwater offshore platform.

APPENDIX 1

Characteristics of the Velocity Spectrum

The wave amplitude spectrum is the better known unidirectional frequency function employed to describe random ocean waves. The Bretschneider and Pierson-Moskowitz spectra- which are essentially of the same form- are the most commonly used at present. The JONSWAP spectrum, which is an extension of the Pierson-Moskowitz spectrum to account for a much sharper spectral peak, is more recent and involves additional parameters.

This appendix does not describe how wave spectra are measured from wave recordings. Nonetheless, from precisely these wave records, the significant wave height Hs, the zero-crossing period T_z are derived. In the case of the Bretschneider spectrum, the peak frequency F_o of the wave energy spectrum is deduced from the zero-crossing period T_z by the following relation[22]:

$$F_o = .710/T_z \qquad (A.1)$$

Supposing that these sea parameters are known for the area where the offshore structure will be placed, this appendix presents some of the characteristics of the Bretschneider velocity spectrum.

The dimensionless form of the target velocity spectrum is deduced from the wave amplitude spectrum. For conformity, all the spectra are presented here in terms of the frequency f in Hz. The wave amplitude spectrum has the general form:

$$S_x(f) = \exp(-B/f^4)\ A/f^5 \qquad (A.2)$$

where $A = 5H_s^2 F_o^4/16$ (A.3) and $B = 5F_o^4/4$ (A.4)

Then the dimensionless wave energy spectral shape will be:

$$S_{\dot{x}}(f)/S_{\dot{x}}(F_o) = e^{+5/4}\left(\frac{F_o}{f}\right)^5 \exp\left(-\frac{5}{4}\left(\frac{F_o}{f}\right)^4\right)$$

where F_o is the peak frequency and $S_{\dot{x}}(F_o) = e^{-\frac{5}{4}} 5H_s^2/16F_o$ (A.6)

The wave velocity spectrum is derived from the previous spectrum:

$$S_{\dot{x}}(f) = (2\pi f)^2 S_x(f) \qquad (A.7)$$

All the relations that are given here, provide some error measurement on two wave parameters, i.e. the zeroth moment M_o and the second moment M_2 of the wave energy spectrum. The dimensionless wave velocity spectrum is:

$$S_{\dot{x}}(f)/S_{\dot{x}}(f_1) = e^{3/4}\left(\frac{f}{f_1}\right)^3 \exp\left(-\frac{3}{4}\left(\frac{f}{f_1}\right)^4\right) \qquad (A.8)$$

where F_1, the maximum peak of the velocity spectrum, is proportional to F_o:

$$F_1 = F_o \sqrt[4]{5/3} \tag{A.9}$$

$$S_{\dot{x}}(F_1) = e^{-3/4} \frac{3}{4} \pi^2 H_s^2 F_1 \tag{A.10}$$

The moments of the Bretschneider wave energy spectrum are defined as follows:

$$M_o = \int_o^{F_c} df\, S_x = \frac{A}{4B} \exp\left(-B/F_c^4\right) \tag{A.11}$$

$$M_2 = \int_o^{F_c} df\, f^2 S_x = \sqrt{\frac{\pi}{B}} \frac{A}{4} \left(1 - \text{erf}\left(\sqrt{B}/F_c^2\right)\right)$$

$$M_4 = \frac{A}{4} E_1\left(\frac{3}{4}\left(\frac{F_1}{F_c}\right)^4\right)$$

where F_c is the cutoff frequency. Now, these moments can be expressed alternatively in terms of either (H_s, F_o) or $(S_{\dot{x}}(F_1), F_1)$ when a cutoff frequency is selected: for example, $F_c/F_1 = 3$ is the cutoff with 20 dB down from the peak F_o on the wave amplitude spectrum, ($6F_1$, 20 DB down from the peak F_1 on the wave velocity spectrum).

$$M_o = \frac{H_s^2}{16} \exp\left(-\frac{3}{4}\left(\frac{F_1}{F_c}\right)^4\right) = \frac{S_{\dot{x}}(F_1)}{12\pi^2 F_1} \exp\left\{\frac{3}{4}\left(1-\left(\frac{F_1}{F_c}\right)^4\right)\right\} \quad (A.13)$$

$$M_2 = \frac{\sqrt{3\pi}}{32} H_s^2 F_1^2 \operatorname{erf}\left(\sqrt{\frac{3}{2}}\left(\frac{F_1}{F_c}\right)^2\right) = S_{\dot{x}}(F_1) F_1 \; e^{3/4} \operatorname{erf}\left(\sqrt{\frac{3}{2}}\left(\frac{F_1}{F_c}\right)^2\right) \Big/ 8\sqrt{3\pi} \quad (A.14)$$

Thus, the relative errors on M_o and M_2 can be expressed in terms of either the (H_s, F_1) pair or the $(S\dot{x}(F_1), F_1)$ pair.

$$\Delta F_o / F_o = \Delta F_1 / F_1 = 0 \quad (A.15)$$

$$\Delta M_o / M_o = 2\,\Delta H_s / H_s \quad (A.16) \text{ and } \Delta M_2 / M_2 = 2\Delta H_s / H_s \quad (A.17)$$

By normalizing the ARMA spectrum at its peak frequency F_1 to its value $S_{\dot{x}}(F_1)$, the relative errors on F_1 and on F_o are set equal to zero, thus the error measured on the ARMA spectrum's estimate of the second moment M_2 is thus the result of an error on the significant wave height H_s.

The theoretical value of M_2 is known and is given by formula (A.14), the ARMA estimate of M_2, M_2 computed from the ARMA velocity spectrum is proportional to the area under the velocity spectrum:

$$\hat{M}_2 = \frac{1}{4\pi^2} \int_o^{F_c} df\, S_{\dot{x}} = \frac{1}{4\pi^2} \oint \frac{B(z)}{A(z)} \frac{B(z^{-1})}{A(z^{-1})} \frac{dz}{z} \quad (A.18)$$

The relative error on M_2 will be given by:

$$\Delta M_2/M_2 = \Delta M_0/M_0 = \frac{2\Delta H_s}{H_s} \qquad (A.19)$$

As one varies the order of the ARMA filter, i.e. its number of poles and zeros, that there is no criterion that yet permits one to unequivocally determine the optimum ARMA spectrum. Therefore, this suggests that at least one should obtain an ARMA estimate that matches not only the general shape of the given spectrum but also its two moments (M_0,M_2) and two parameters (H_s,F_0).

Normalization of the ARMA spectrum.

The ARMA spectrum should be normalized at its peak frequency F_1 assuming that its shape fits the given spectrum from 0 to F_c. The maximum F_1 is a solution to the two following equations:

$$\left.\begin{array}{ll} \text{Extremum} & \\ dS_{\dot{x}}/df = 0 & \sum_{l=1}^{N} l\left(\frac{\alpha_l}{\alpha_0} - \frac{\beta_l}{\beta_0}\right) \sin 2\pi \hat{F} \Delta T l = 0 \\ \text{Maximum} & \\ d^2S_{\dot{x}}/df^2 < 0 & \sum_{l=1}^{N} l^2\left(\frac{\alpha_l}{\alpha_0} - \frac{\beta_l}{\beta_0}\right) \cos 2\pi \hat{F} \Delta T l \leq 0 \end{array}\right\} \hat{F} = F_1 \qquad (A.20)\ (A.21)$$

where

$$\alpha_l = \sum_{k=0}^{N-l} a_k a_{k+l} \qquad 0 \leq l \leq N \qquad (A.22)$$

and

$$\beta_l = \begin{cases} 0 & M < l \leq N \\ \sum_{k=0}^{M-l} b_k b_{k+l} & 0 \leq l \leq M \end{cases} \qquad (A.23)$$

BIBLIOGRAPHY

1. Baggeroer, A.B., "Maximum Likelihood Estimation of Cross Spectra," Lincoln Laboratory, MIT, Lexington, MA., 1974.

2. Baggeroer, A.B., "Sonar Signal Processing," Chapter 6 on Applications of Digital Signal Processing, ed. A.V. Oppenheim, Prentice Hall, Englewood Cliffs, N.J., 1978.

3. Baggeroer, A.B., "Recent Signal Processing Advances in Spectral and Frequency Wavenumber Function Estimation and Their Application to Offshore Structures," Proceedings, BOSS '79, Paper 80, p. 457.

4. Borgman, L.E., "Techniques for Computer Simulation of Ocean Waves," Topics in Ocean Physics, LXXX Corso, Soc. Italiana di Fisica, Bologna, Italy, 1982.

5. Borgman, L.E. and Yfantis, E., "Directional Spectral Density of Forces on Fixed Platforms," Proceedings of the Conference on Directional Wave Spectra Applications, ASCE/Berkeley, California, September 14-16, 1981.

6. Bretschneider, C., "Wave Variability and Wave Spectra for Wind Generated Gravity Waves," Beach Erosion Board, Tech. Mem. No. 118, U.S. Army Corps of Engineers, August 1959.

7. Burke, B.G. and Tighe, James T., "A Time Series Model for Dynamic Behavior of Offshore Structures", Proceedings of the 1971 Offshore Technology Conference, Paper No. 14.3

8. Durbin, J., "The Fitting of Time Series Models", Review of the Institute of International Statistics, Vol. 28, pp. 233-243, 1960.

9. Gersch, Will, "Estimation of the Autoregressive Parameters of a Mixed Autoregressiev Moving-Average Time Series", IEEE Transactions on Automatic Control, October 1970.

10. Holm, Sverre and Hoven, Jens M., "Estimation of Scalar Ocean Wave Spectra by the Maximum Entropy Method", IEEE Journal of Oceanic Engineering, Vol. OE-4, No. 3, July 1979, pp. 76-83.

11. Johnsen, S.J. and Andersen, N., "On Power Estimation in Maximum Spectral Analysis", Geophysics, Vol. 43, No. 4, (June 1978), pp. 681-690.

12. Maddox, Roger N., "Fatigue Analysis for Deepwater Fixed-Bottom Platforms", Proceedings of the 1974 Offshore Technology Conference, Paper No. 2051.

13. Milgram, J., "Waves and Wave Forces," Proceedings of BOSS '76.

14. Moe, G., "Static and Dynamic Analysis of Fixed Offshore Towers Subjected to Wave Loadings," Ph.D. Thesis, M.I.T., Department of Ocean Engineering, 1975.

15. Mullis, C.T. and Roberts, R.A., "The Use of Second-Order Information in the Approximation of Discrete-Time Linear Systems", IEEE Trans. Acoust., Speech, Signal Processing, Vol. ASSP-24, June 1976, pp. 226-238.

16. Oppenheim, Alan Vv. and Schafer, Ronald W., Digital Signal Processing, Prentice Hall, Englewood Cliffs, New Jersey, 1975.

17. Overvik, T. and Houmb, O.G., "On The Statistical Modelling of Ocean Waves by Parametric Methods", Seminar on Ocean Waves, Paris, 1979.

18. Overvik, T., Mo, K. and Fines, S., "On the Estimation of Wind Wave Spectra by Parametric Methods", Coastal Eng., pp. 97-109, May 1981.

19. Overvik, T., and Houmb, O.G., "Some Applications of Maximum Entropy Spectral Estimation to Ocean Waves and Linear Systems Response in Waves", Applied Ocean Research, Vol. 3, No. 4, pp. 154-162, 1981.

20. Rabiner, Lawrence R. and Schafer, R.W., "On The Behavior of Minimax FIR Digital Helbert Transformers", Bell Syst. Tech. J., Vol. 53, No. 2, pp. 361-388, Feb. 1974.

21. Rabiner, Lawrence R., Schafer, Ronald W., and Roder, Charles M., "The Chirp Z Transform Algorithm and Its Application", The Bell System Technical Journal, pp. 1249-1293, May/June 1969.

22. Sarpkaya, Turgut and Isaacson, Michael, Mechanics of Wave Forces on Offshore Structure, Van Nostrand Reinhold, New York, 1981.

23. Scharf, Louis L. and Luby, James C., "Statistical Design of Autoregressive-Mooring Average Digital Filters", IEEE Trans. on Acoustics, Speech, and Signal Processing, Vol. ASSP-27, No. 3, June 1979,, pp. 240-247.

24. Spanos, P.T.D.V., and Hausen, J.E., "Linear Prediction Theory for Digital Simulation of Sea Waves", Journal of Energy Resources Technoloogy, American Society of Mechanical Engineers, Vol. 103, pp. 243-249.

25. Spanos, P.T.D., "ARMA Algorithm for Ocean Spectral Analysis", Engineering Mechanics Research Laboratory, Univ. of Texas at Austin, Report No. 1137, June 1982.

26. Sunder, Shyam S., Angelides, D.C. and Connor, J.J., "A Stochastic Model for the Simulation of Non-Stationary Sea," Proceedings BOSS '79.

27. Sunder, Shyam S. and Connor, J.J., "Sensitivity Analysis for Steel Jacket Offshore Platforms," Proceedings of the Brazil Offshore '79 Conference held in Rio de Janeiro, Pentech Press, London, 1980.

28. Sunder, Shyam S., "On the Standard Processing of Strong Motions Earthquake Signals," M.I.T., Department of Civil Engineering, Research Report R80-38, Order No. 683, September 1980.

29. Triantafyllou, M. and Chryssostomidis, C., "Offshore Structures Design," M.I.T., Department of Ocean Engineering, Class Notes, May 1980.

30. Triantafyllou, M., Athans, M., and Bodson, M., "Real Time Estimation of Ship Motions Using Kalman Filtering Techniques," IEEE Journal of Oceanic Engineering, Vol. OE-8, No. 1, January 1983.

31. Vandiver, J.K., "Prediction of the Damping Controlled Response of Offshore Structures to Random Wave Excitations," Soc. of Petroleum Engineers Journal, Vol. 20, No. 1, February 1980.

32. Vandiver, J.K., "Detection of Structural Failure on Fixed Platforms by Measurement of Dynamic Response," Journal of Petroleum Technology, Vol. XXIX, March 1977.

33. Vandiver, J.K., "The Estimation of Natural Frequencies and Damping Ratios of Offshore Structures," Proceedings of the Offshore Technology Conference, Houston, Texas, May 1980.

34. Wiegel, R.L., "Waves and Wave Spectra and Design Estimates," Conference on Deep-Sea Oil Production Structures, University of California, Berkeley, January 1978.